Analytical Cellular Pathology

Molecular Regulation of Cancer Cell Migration, Invasion, and Metastasis

Lead Guest Editor: Lubna H. Tahtamouni
Guest Editors: Christian Rolfo, Mamoun Ahram, and Jennifer E. Koblinski

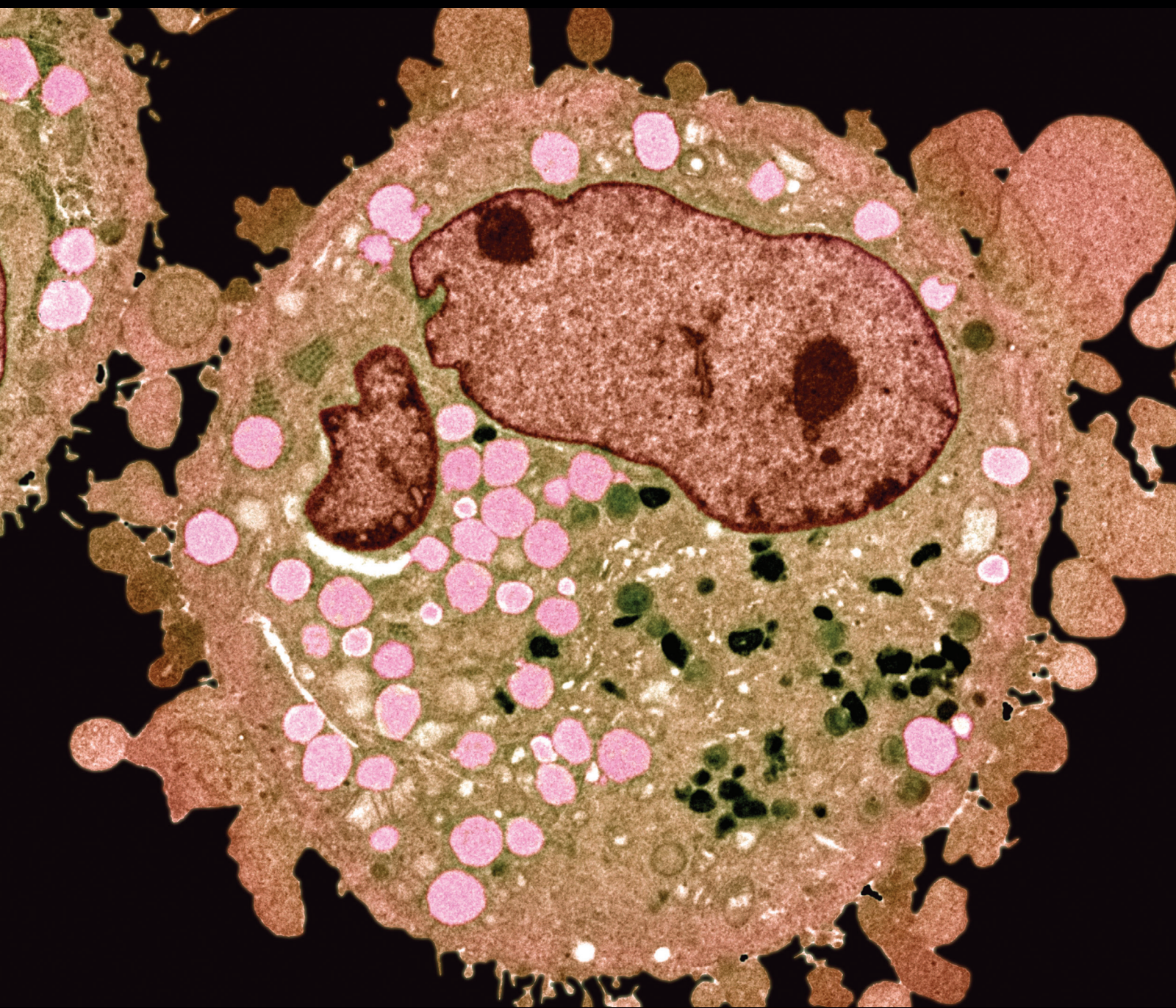

Molecular Regulation of Cancer Cell Migration, Invasion, and Metastasis

Analytical Cellular Pathology

Molecular Regulation of Cancer Cell Migration, Invasion, and Metastasis

Lead Guest Editor: Lubna H. Tahtamouni
Guest Editors: Christian Rolfo, Mamoun Ahram, and Jennifer E. Koblinski

Editorial Board

Contents

Hindawi
Analytical Cellular Pathology
Volume 2019, Article ID 1356508, 2 pages
https://doi.org/10.1155/2019/1356508

Editorial

Molecular Regulation of Cancer Cell Migration, Invasion, and Metastasis

Lubna Tahtamouni,[1] **Mamoun Ahram**,[2] **Jennifer Koblinski**,[3] **and Christian Rolfo**[4]

[1]*Hashemite University, Zarqa, Jordan*
[2]*University of Jordan, Amman, Jordan*
[3]*Virginia Commonwealth University, Richmond, USA*
[4]*University of Maryland School of Medicine, Baltimore, MD, USA*

Correspondence should be addressed to Lubna Tahtamouni; lubnatahtamuni@hu.edu.jo

Received 25 February 2019; Accepted 26 February 2019; Published 14 May 2019

Cancer metastasis represents an advanced stage of malignancy and is the leading cause of cancer-related deaths. Metastasis is a multistep process that includes migration and invasion of cancer cells, hallmarks of malignancy. These processes require the involvement of a wide array of cellular mechanisms led by cytoskeleton dynamics as well as molecular alterations such as expression of adhesion and proteolytic enzymes. Cell migration in itself is a highly integrated process that includes development of cytoplasmic protrusions, attachment, and traction. Additional secondary changes associated with cell migration and invasion include production of reactive oxygen species (ROS), development of chemoresistant cancer stem cells, introduction of mutations in DNA damage repair genes, and contribution of microRNAs (miRNAs). Cell release of exosomes and their participation in modulating cell behavior are a new and exciting observation. In this special issue on Molecular Regulation of Cancer Cell Migration, Invasion, and Metastasis, we have invited a few papers that address such issues.

One of the papers investigated the binding partner of AG73, a synthetic laminin α1 chain peptide, in breast cancer cells that mediate cancer progression. The findings demonstrated an intrinsic interaction between AG73 and syndecans that mediates tumor cell adhesion and invasion. One of the papers investigated the expression of syndecans, Sdc1 in particular, in tumor cells and stroma of invasive lobular and ductal breast carcinoma. Sdc1 was expressed in the epithelium of 90% carcinoma of both histological types. It was also most frequently expressed in tumor-associated stroma. In metastatic epithelium, Sdc1 was negatively correlated with patient's age and statuses of estrogen receptors (ERs) and progesterone receptors (PRs) in the primary tumors, while stroma of metastases demonstrated a positive correlation with focus number in primary tumors and a negative association with PRs in primary tumors. One of the papers found a role of syndecan-2 in colorectal cancer cell migration. This finding can help understand the biology of tumors and suggests that syndecan-2 may be used as a target to therapy and diagnosis.

One of the papers of this special issue assessed the expression level of Epac1 and PDE4 in rectal carcinoma. It was found that their expression is increased in rectal carcinoma tissue; however, no significant association between these proteins and degree of differentiation, histological type, and lymph node metastasis was reported. The fifth paper investigated the anticancer potential of metformin against glioblastoma multiforme cancer. The results showed a significant decrease in survival, motility, and invasion as well as an increase in cell adhesion in metformin-treated cancer cells.

One of the papers assessed the role of long noncoding RNA LOXL1-AS1 on human medulloblastoma cell proliferation and metastasis. The paper reported overexpression of Lcn RNA LOX1-AS1 in medulloblastoma tissues as well as in advanced stages. The proliferation and metastasis of

medulloblastoma by this noncoding RNA was mediated by activation of the P13K-AKT pathway. The latter study opens the door for the exciting roles of noncoding RNA in regulating cancer cell behavior.

Conflicts of Interest

The lead and guest editors of the special issue "Molecular Regulation of Cancer Cell Migration, Invasion, and Metastasis" declare that there are no conflicts of interest regarding the publication of this special issue.

Lubna Tahtamouni
Mamoun Ahram
Jennifer Koblinski
Christian Rolfo

Hindawi
Analytical Cellular Pathology
Volume 2019, Article ID 9192516, 10 pages
https://doi.org/10.1155/2019/9192516

Research Article

The Laminin-α1 Chain-Derived Peptide, AG73, Binds to Syndecans on MDA-231 Breast Cancer Cells and Alters Filopodium Formation

Madhavi Puchalapalli,[1] Liang Mu,[2] Chevaunne Edwards,[1] Benjamin Kaplan-Singer,[3] Pearl Eni,[2] Kiran Belani,[3] David Finkelstein,[2] Arpan Patel,[2] Megan Sayyad,[1] and Jennifer E. Koblinski[1]

[1]*Department of Pathology, Virginia Commonwealth University, School of Medicine, Massey Cancer Institute, Richmond, VA, USA*
[2]*Department of Pathology, Women's Cancer Research Program, Feinberg School of Medicine, Robert H. Lurie Comprehensive Cancer Institute, Northwestern University, Chicago, IL, USA*
[3]*Craniofacial Developmental Biology and Regeneration Branch, National Institute of Dental and Craniofacial Research, National Institutes of Health, Department of Health and Human Services, Bethesda, MD, USA*

Correspondence should be addressed to Jennifer E. Koblinski; jennifer.koblinski@vcuhealth.org

Received 7 April 2018; Accepted 17 February 2019; Published 30 April 2019

Academic Editor: Silvia Cantara

Breast cancer is one of the most common forms of cancer affecting women in the United States, second only to skin cancers. Although treatments have been developed to combat primary breast cancer, metastasis remains a leading cause of death. An early step of metastasis is cancer cell invasion through the basement membrane. However, this process is not yet well understood. AG73, a synthetic laminin-α1 chain peptide, plays an important role in cell adhesion and has previously been linked to migration, invasion, and metastasis. Thus, we aimed to identify the binding partner of AG73 on breast cancer cells that could mediate cancer progression. We performed adhesion assays using MCF10A, T47D, SUM1315, and MDA-231 breast cell lines and found that AG73 binds to syndecans (Sdcs) 1, 2, and 4. This interaction was inhibited when we silenced Sdcs 1 and/or 4 in MDA-231 cells, indicating the importance of these receptors in this relationship. Through actin staining, we found that silencing of Sdc 1, 2, and 4 expression in MDA-231 cells exhibits a decrease in the length and number of filopodia bound to AG73. Expression of mouse Sdcs 1, 2, and 4 in MDA-231 cells provides rescue in filopodia, and overexpression of Sdcs 1 and 2 leads to increased filopodium length and number. Our findings demonstrate an intrinsic interaction between AG73 in the tumor environment and the Sdcs on breast cancer cells in supporting tumor cell adhesion and invasion through filopodia, an important step in cancer metastasis.

1. Introduction

Laminin-111 (LM-111) is involved in both normal and neoplastic breast biology and enhances adhesion, migration, and metastasis of tumor cells. This basement membrane glycoprotein is cleaved in the breast tumor environment, suggesting bioactive fragments may be released into the tumor environment [1–7]. Supporting this idea, synthetic peptides of LM-111 can alter the behavior of tumor cells. AG73 is a synthetic peptide based on the LM-α1 chain (RKRLQVQLSIRT, residues 2719-2731) that affects many physiological events. The role of AG73 in metastasis has been documented in melanoma, adenoid cystic, oral squamous cell, and ovarian carcinoma [8–14], and we previously reported that AG73 increases breast cancer metastasis to the bone [14]. Further, HT1080 human fibrosarcoma, B16F10 mouse melanoma, and SW480 human colon adenocarcinoma cells are known to adhere to AG73 [15]. However, a scrambled sequence of AG73 (LQQRRSVLRTKI) does not promote cell adhesion. Furthermore, AG73 can be conjugated

to polysaccharides (chitosan and alginate) and hyaluronate hydrogels and promote cell viability, neurite extension, capillary-like networks with endothelial cells, and acinar-like structures with salivary gland cells [16–19]. AG73 also inhibits the ability of cells to spread on LM-111 [15], indicating it likely has physiological relevance.

The receptors for AG73 may also play an important role in tumor growth and metastasis. In the absence of an added peptide, a subpopulation of B16F10 cells, which were adhesion selected to AG73 over 30 times, has effects on tumor cells including increased invasion in vitro, subcutaneous tumor growth, and metastatic colony growth in the lungs and the liver [10]. These results suggest that AG73 receptors and their signaling pathway(s) are important in the metastasis of these cells, and thus, we focused on the receptors in the breast cancer cells that bind to AG73. AG73 specifically binds to cell surface proteoglycans, including syndecans (Sdcs) 1, 2, and 4 in nonbreast cells [12, 20–24]. The Sdcs are a family consisting of four transmembrane heparan sulfate proteoglycans that interact with integrins, growth factors, and chemokine receptors. Although they are not the primary receptors for the extracellular matrix (ECM), growth factors, or chemokines, they synergize with these molecules' prototypic receptors through simultaneous ligand engagement [25–27]. These receptors play critical regulatory roles in a variety of physiological and pathophysiological functions including wound healing, inflammation, neural patterning, tumor growth, and angiogenesis [28, 29]. Thus, we hypothesized that AG73 binds to breast cancer cells through the Sdcs. Here, we demonstrate that AG73-induced filopodium formation in breast cancer cells is mediated through Sdcs 1, 2, and 4. These data identify the receptors for a sequence in LM-111 that may play a role in the malignant phenotype of breast cancer. This is the first study to our knowledge to identify Sdcs as a binding partner for the laminin peptide, AG73, in breast cancer cells.

2. Materials and Methods

2.1. Cell Culture. The human breast carcinoma cell line MDA-MB-231 (MDA-231) was grown in DMEM/F-12 (Invitrogen) supplemented with 5% FBS (Gemini), 2 mM L-glutamine, 1 mM sodium pyruvate, 0.02 mM nonessential amino acids, puromycin (1 μg/ml), and fungizone (2.5 μl/ml) (Invitrogen). The MDA-231 cells expressing Green Fluorescent Protein (GFP) were a gift from Dr. D. Welch (The University of Kansas Medical Center). Human MCF7 and T47D breast carcinoma cells were grown in DMEM (Invitrogen) supplemented with 10% FBS (Gemini), 4.5 g/l D-glucose, (+) L-glut, and (-) sodium pyruvate (Invitrogen). Human SUM1315 breast carcinoma cells were grown in Ham's F-12 (Invitrogen), 5% FBS (Gemini), 5 μg/ml insulin, 10 ng/ml EGF, and 10 mM HEPES (Sigma-Aldrich). Human MCF10A normal breast epithelial cells were grown in DMEM/F-12 (Invitrogen) supplemented with 5% horse serum (Invitrogen), 20 ng/ml EGF, 10 μg/ml insulin, and 0.5 μg/ml hydrocortisone (Sigma-Aldrich). All cell media contained 100 U/ml penicillin and 100 μg/ml streptomycin (Invitrogen). Additionally, all cells were maintained at 37°C in a 5% CO_2/95% humidified air atmosphere and were routinely checked for mycoplasma.

2.2. Adhesion Assays. Adhesion assays were performed as described [30, 31]. Briefly, 96-well plates were coated with AG73 and scrambled (2 μg/ml), laminin (10 μg/ml), rec-LG-4 and mutant rec-LG4 [20] (AG73 site mutated RKR-AAA; 11 μg/ml, a kind gift from Drs. Kentaro Hozumi and Yoshihiko Yamada), or basement membrane extract (10 μg/ml, BME/Matrigel, Trevigen/Bio-Techne) overnight in PBS at 4°C. (The scrambled peptide is a random sequence scramble of the AG73 amino acid sequence.) Wells were blocked with 3% heat-denatured BSA (10 min at 85°C) for 1 hr at 37°C. Cells were untreated or treated for 30 min with either PBS; 5 mM EDTA; 10 mg/ml heparin; heparan sulfate; chondroitin sulfates A, B, and C; hyaluronic acid (Sigma-Aldrich); 10-fold molar excess of AG73; or scrambled peptide, prior to 30 min adhesion. Heparin, heparan sulfate, and chondroitin sulfate B were used at 1-200 μg/ml in the dose-response experiment with the IC_{50} calculated using Prism (GraphPad Software). The cells (30,000 cells/50 μl/well of DMEM-0.1% BSA) were then added with the treatment to the blocked wells and incubated at 37°C for 30 min. The medium with unattached cells was removed from the wells. The adherent cells were stained for 10 min with 0.2% crystal violet in 20% methanol and washed twice with water. The cells were lysed with 10% SDS (50 μl/well), and the optical density (600 nm) was measured. Each sample was performed in triplicate, and the experiment was repeated at least three times.

2.3. Silencing of Sdc Expression and Rescue. MDA-231 cells were infected with a lentivirus from Open Biosystems containing GFP. NS1 control is the nonsilencing (NS) shRNAmir sequence in the lentivirus vector GINZEO; Sdc 1 KD, the Sdc 1-silencing shRNAmir sequence in the lentivirus vector GINZEO; NS2 control, the nonsilencing (NS) shRNAmir sequence in the lentivirus vector GIPZ; Sdc 2 KD, the Sdc 2-silencing shRNAmir sequence in the lentivirus vector GIPZ; and Sdc 4 KD, the Sdc 4-silencing shRNAmir sequence in the lentivirus vector GIPZ. All cells were selected two times by flow cytometry for the top 5% of the GFP expression. These cells are not a cloned population but a heterogeneous population of cells that stably express the shRNAmir. Stable expression was determined by flow cytometry. To assure the results were not due to off-target effects of the shRNAmir, rescue experiments were carried out in the human cell lines using mouse Sdcs 1, 2, and 4 (OriGene) which are not targeted by the human shRNAmir. Specific targeting to human Sdc family members while expressing a mouse homolog has been demonstrated [32]. Mouse Sdc does rescue the knockdown of human Sdc. The mouse Sdc cDNA was cloned into the pBABE retrovirus (a kind gift from Dr. B. Parker, Northwestern University) which expresses the mCherry fluorescent protein. The cells were selected two times by flow cytometry for the top 5% of the mCherry fluorescent expression. Controls were the KD or NS cells infected with the pBABE retrovirus containing only the mCherry fluorescent protein and termed

empty vector (EV) since there was no cDNA for Sdc. Stable expression was determined by flow cytometry.

2.4. Flow Cytometry. Cells were harvested with Versene (Invitrogen, 0.48 mM EDTA) for 10 min at 37°C with gentle agitation. Cells were washed in PBS and resuspended in cold buffer containing 1% FCS. A total of 2×10^5 cells per sample was used. Following centrifugation, cells were resuspended in Hanks' balanced salt solution/2% BSA and incubated for 30 min at 4°C with titrated antibodies (20 μg/ml mouse anti-Sdc 1 (B-A38, AbD Serotec), rabbit anti-Sdc 2 (R&D Systems), rabbit anti-Sdc 3 (midi), and rabbit anti-Sdc 4 (Zymed)); cells were then washed 2x with PBS, incubated with secondary antibody for 30 min at 4°C (1 : 100 dilution of donkey anti-mouse or rabbit-Cy5 (Jackson ImmunoResearch)), washed again 2x with PBS, and resuspended in 100 μl of PBS. The samples were analyzed using a Beckman Coulter FC500 flow cytometer. Human Sdc expression was analyzed comparing the relative amount of human Sdc-stained cells with the IgG controls, and then KD cells were compared to NS-infected cells. Isotype-matched antibodies were used as negative controls.

2.5. Real-Time Quantitative PCR Analyses. Total RNA was isolated from breast cancer cells using RNAqueous-4PCR (Invitrogen) according to the manufacturer's instructions. RNA samples were then quantified using a NanoDrop (NanoDrop Technologies), and equal RNA concentrations were used for reverse-transcriptase PCR. First-strand cDNA synthesis and amplification were performed using a qScript cDNA SuperMix (Quanta BioSciences). Real-time PCR was carried out using a 7900HT Fast Real-Time PCR System (Applied Biosystems). cDNA templates were combined with a SYBR Green PCR Master Mix (Applied Biosystems). Primer sequences were obtained from PrimerBank, which contains primers that can be used for qPCR under stringent and allele-invariant amplification conditions [33]. The information can be accessed at https://pga.mgh.harvard.edu/primerbank/. The specific Sdc primers used were as follows: Sdc 1 forward: 5′-CTC TGA CAA CTT CTC CGG CTC-3′, Sdc 1 reverse: 5′-TCT GGC AGG ACT ACA GCC TC-3′; Sdc 2 forward: 5′-GCT CTG CCC CTA AAC TTC TGC-3′, Sdc 2 reverse: 5′-CTC TGC TGT GGT TTT GCT CCT-3′; Sdc 3 forward: 5′-CCC AGC TCC CTA GCT CTC TC-3′, Sdc 3 reverse: 5′-GCT GTC TCA ATG CCC GAC T-3′; Sdc 4 forward: 5′-GCT CTT CGT AGG CGG AGT-3′, Sdc 4 reverse: 5′-CCT CAT CGT CTG GTA GGG CT-3′; and GAPDH forward: 5′-TGG TGA AGC AGG CGT CGG AGG-3′, GADPH reverse: 5′-CGT CAA AGG TGG AGG AGT GGG TGT C-3′. Samples were amplified by an initial denaturation at 95°C for 2 min, followed by 40 cycles at 95°C for 10 sec and at 62°C for 30 sec. A melting curve was generated at the end of every run to ensure product uniformity. Gene expression was normalized to GAPDH. All reactions were run in triplicate, and each experiment was repeated at least three times.

2.6. Solid Phase. Solid-phase assays were performed as described [34]. Peptides were coated on 96-well plates (dried onto the well overnight, 100 μg/ml in H_2O); the wells were blocked (3% heat-denatured BSA) for 1 hr at 37°C and then incubated with MDA-231 cell lysate (2 mg/ml) in 3% BSA overnight at 4°C. For heparin inhibition, 20 mg/ml of heparin was added to the cell lysate before binding to the plate. For trypsin inhibition, cells were treated with trypsin (Invitrogen) for 10 min before lysing the cells. Binding was detected using anti-Sdc antibodies (0.2 μg/ml, mouse anti-Sdc 1 (B-A38, AbD Serotec); rabbit anti-Sdcs 2, 3 (midi), and 4 (Zymed/Thermo Fisher Scientific)) followed by goat anti-mouse or rabbit-HRP-conjugated secondary antibodies (1 : 5000 dilution in 3%BSA-PBS). The signal was detected at 450 nm after incubation with TMB solution followed by 1 M H_2SO_4. For protein analysis, MDA-231 cell membranes were biotinylated (62) and membrane factions were isolated for enrichment of proteoglycans as described (82). Six-well plates were coated with peptide, and the biotinylated MDA-231 cell membrane was incubated with either AG73 or scrambled peptide. The bound material was scraped from the dish and electrophoresed on a 4-12% Bis-Tris gel. Bound material was transferred to PVDF and incubated with streptavidin-horseradish peroxidase, and reactive proteins were detected using a SuperSignal® West Dura Extended Duration Substrate (Pierce). Chemiluminescence was detected using a Fujifilm LAS-1000 Luminescent Image Analyzer "intelligent dark box" (Fujifilm Medical Systems USA Inc., Stamford, CT) using exposure times at subsaturation levels.

2.7. Actin Staining. AG73 or a scrambled peptide was dried onto coverslips overnight (100 μg/ml in H_2O). The coverslips were washed and blocked with 3% heat-denatured BSA. MDA-231 cells were collected using EDTA and counted and attached for 2 hours in serum-free media to the blocked and coated coverslips. The cells were fixed for 20 min in 4% paraformaldehyde (Electron Microscopy Sciences, Hatfield, PA) in PBS. After washing, the cells were permeabilized with 0.1% Triton X-100 (Sigma-Aldrich) in PBS for 5 min and washed, and then actin filaments were detected by staining with a 1 : 40 dilution of Alexa Fluor 647 fluorescent-labeled phalloidin (Invitrogen) in 1% BSA. The cells were then washed, fixed, and mounted upside down on slides with a SlowFade Antifade Reagent (Invitrogen) and observed with a LSM 510 Zeiss confocal microscope (Carl Zeiss MicroImaging Inc., Thornwood, NY). The filopodia were quantified using ImageJ analysis software.

3. Results and Discussion

3.1. AG73 Binds to Sdcs on Breast Cancer Cells. AG73 mediates the adhesion of many different cell types, while a scrambled sequence of AG73 does not promote cell adhesion or have other biological activities [9, 30, 31]. To determine whether breast carcinoma cell lines bind to and interact with AG73, adhesion assays were performed as previously described [30, 31]. MDA-231 breast carcinoma cells bound to LM-111, AG73, and recombinant LM-LG4 (a

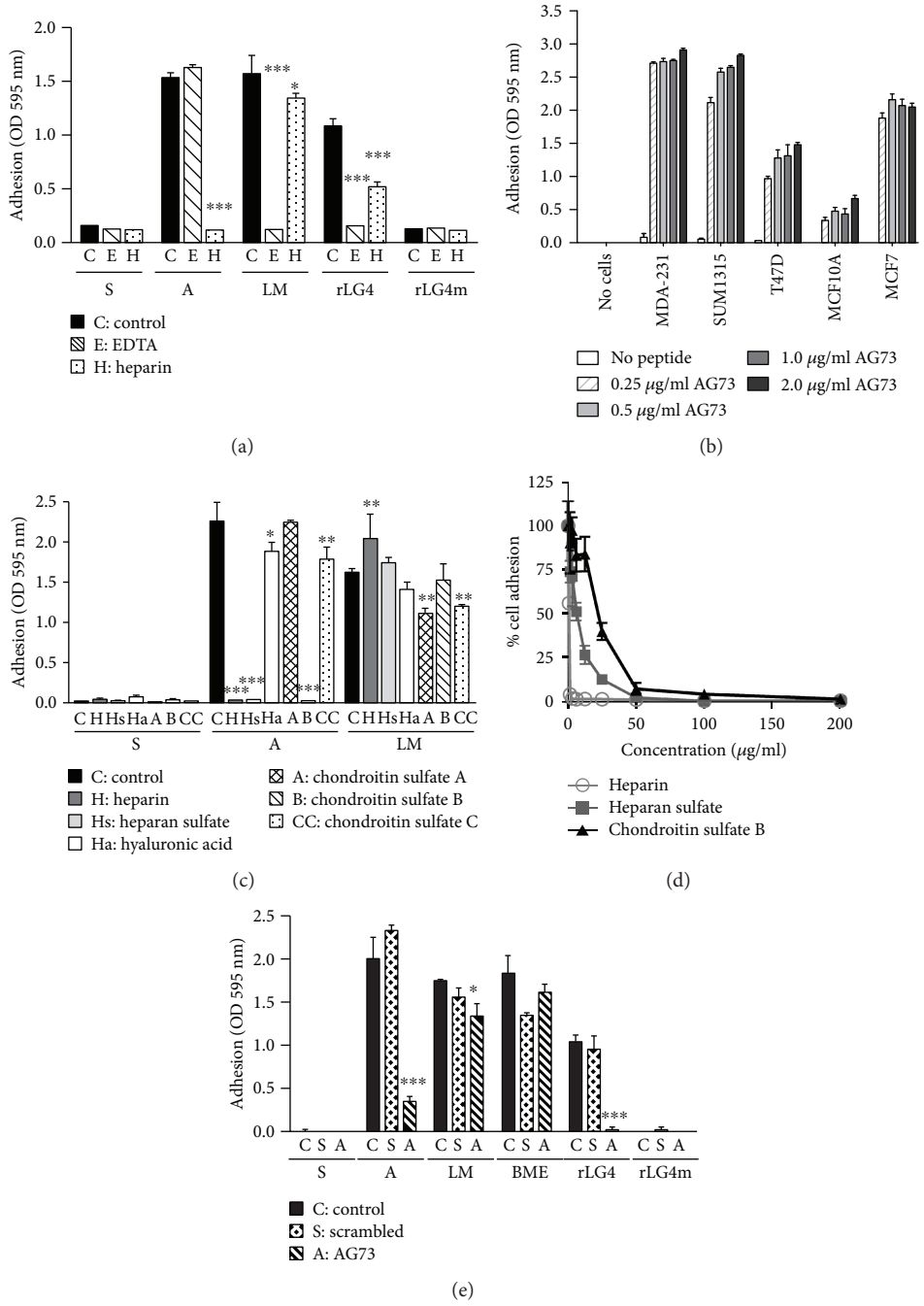

Figure 1: Breast cancer cell adhesion to AG73 is likely through a proteoglycan. (a) Adhesion to AG73 (A) and recombinant LG4 (rLG4) is inhibited by heparin (H, hatched; 10 mg/ml), while adhesion to LM-111 (LM) is inhibited by EDTA (E, diagonal; 5 mM) compared to PBS-treated cells (C, control, solid). The cells do not bind to the scrambled (S) peptide or rLG4 mutant (rLG4m, AG73 site mutated RKR-AAA). (b) Many different breast cancer cells (MDA-231, SUM1315, T47D, and MCF7) as well as normal breast cell lines (MCF10A) bind to AG73. (c) Heparin (H), heparan sulfate (Hs), and chondroitin sulfate B (B) significantly inhibited adhesion of MDA-231 cells to AG73 compared to PBS-treated cells (C, control). Hyaluronic acid (Ha), chondroitin sulfate A (A), and chondroitin sulfate C (CC) had no effect on adhesion to AG73 but did affect adhesion to LM-111 (LM). $^{*}p < 0.05$, $^{**}p < 0.01$, and $^{***}p < 0.001$. One-way ANOVA with Bonferroni posttest. (d) Serial dilutions of heparin, heparan sulfate, and chondroitin sulfate B inhibit adherence of cell binding. The IC_{50} followed the order heparin (0.8 μg/ml), heparan sulfate (6.6 μg/ml), and chondroitin sulfate B (22.4 μg/ml);. (e) MDA-231 cell adhesion to LM-111 (LM), AG73, and rLG4 is inhibited by a 10-fold molar access of AG73 but not the scrambled (S) peptide. Adhesion to basement membrane extract (BME, Matrigel) was unaffected by AG73 or scrambled peptide. Cells were treated with either PBS (C, solid), 10-fold molar excess of AG73 (diagonal), or scrambled peptide (S, hatched) prior to adhesion. Bars: mean adhesion ± SEM.

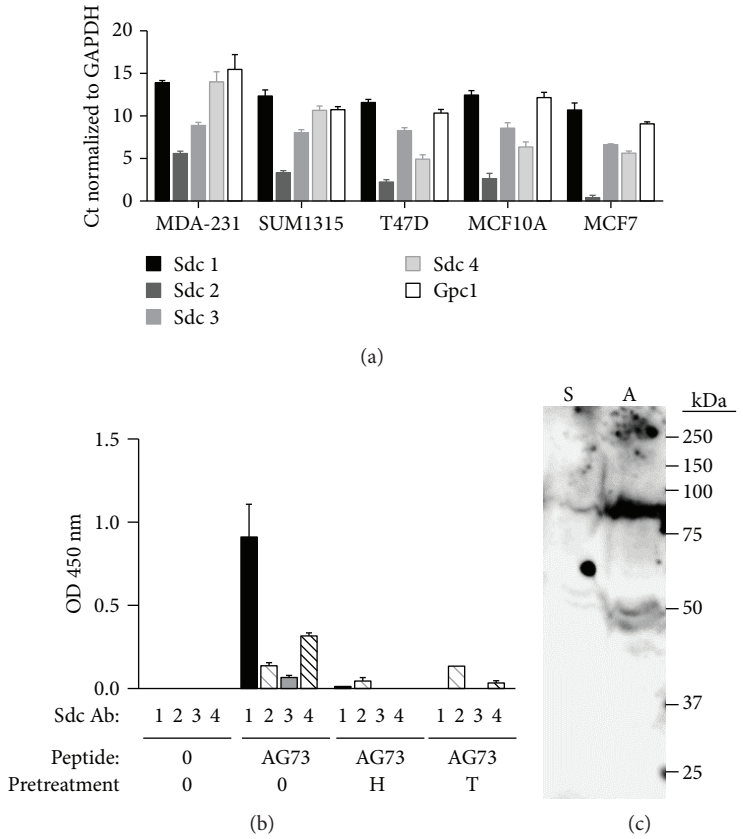

Figure 2: Sdcs 1-4 as well as glypican (Gpc)1 are expressed in MDA-231 cells. (a) qPCR was used to detect the message levels of each Sdc and glypican 1 (Gpc1) in breast cancer cell lines. Bars: mean Ct values are normalized to GAPDH ± SEM. All reactions were run in triplicate and repeated three times, and gene expression was normalized to the housekeeping gene GAPDH. (b) Sdcs 1 and 4 bind to AG73. For this solid-phase assay, wells were uncoated (0) or coated with AG73. Cells were pretreated with either heparin (H) or trypsin (T) before they were lysed. Controls were left untreated (0). The MDA-231 cell lysate binds to AG73 but not to the scrambled peptide (data not shown). The wells were then incubated with antibodies to Sdcs and detected using a secondary-HRP conjugate. Heparin and trypsin pretreatment inhibited Sdcs 1 and 4 binding to AG73. Bars: mean OD 450 nm ± SEM. (c) AG73 binds a >250, 90, and 50 kDa biotinylated protein from the surface of MDA-231 cells. Biotinylated MDA-231 cell membrane was incubated with AG73 (A) or scrambled peptide (S) as in (b). Proteoglycan bands usually appear as a smear due to the heparan sulfate and chondroitin sulfate glycosaminoglycan chains.

recombinant protein from the laminin globular domain 4 at the C terminus of the LM-α1 chain where the AG73 sequence is located (rec-LG4) [20]), but not to either the scrambled peptide or the rec-LG4-mutant (mutated AG73 site; RKR-AAA [20]) (Figure 1(a)). We found that a variety of different breast cell lines bound to AG73 including MCF10A, T47D, SUM1315, and MDA-231 (Figure 1(b)).

To evaluate if cell binding was through proteoglycans or integrins, the effects of heparin and EDTA on MDA-231 cell adhesion to these peptides were examined. Heparin completely inhibited the binding of the MDA-231 cells to AG73, while EDTA had no effect (Figure 1(a)). These results suggest that the MDA-231 cells interact with AG73 through membrane-associated heparan sulfate proteoglycans but not through integrins. In addition, heparin and EDTA inhibited binding to LM-111 and rec-LG4 suggesting that cells bind to these molecules through proteoglycans and integrins (Figure 1(a)). Cell binding to LM-111 through both proteoglycans and integrin $\alpha 6\beta 1$ is well established [35], and binding to the rec-LG4 is mediated through both Sdcs and integrin $\alpha 2\beta 1$ in fibroblasts [20].

Additional experiments were performed to further characterize the proteoglycan receptor binding of AG73 to MDA-231 breast cancer cells. Since proteoglycans contain heparan sulfate and chondroitin sulfate side chains, these glycosaminoglycans (GAG) and others were tested for their ability to inhibit the MDA-231 cell attachment to AG73. Adhesion of MDA-231 cells to AG73 could be significantly ($p < 0.001$) blocked by heparin, heparan sulfate, and chondroitin sulfate B, but not by hyaluronic acid, chondroitin sulfate A, or chondroitin sulfate C (Figure 1(c)). Serial dilutions of heparin, heparan sulfate, and chondroitin sulfate B demonstrated that the concentration required to inhibit adherence by 50% followed the order of heparin (IC_{50}, 0.8 μg/ml), heparan sulfate (IC_{50}, 6.6 μg/ml), and chondroitin sulfate B (IC_{50}, 22.4 μg/ml) (Figure 1(d)). These results suggest that the charge of the glycosaminoglycan is important for preventing the AG73-receptor contact because heparin has the most negative charge and chondroitin sulfate B the

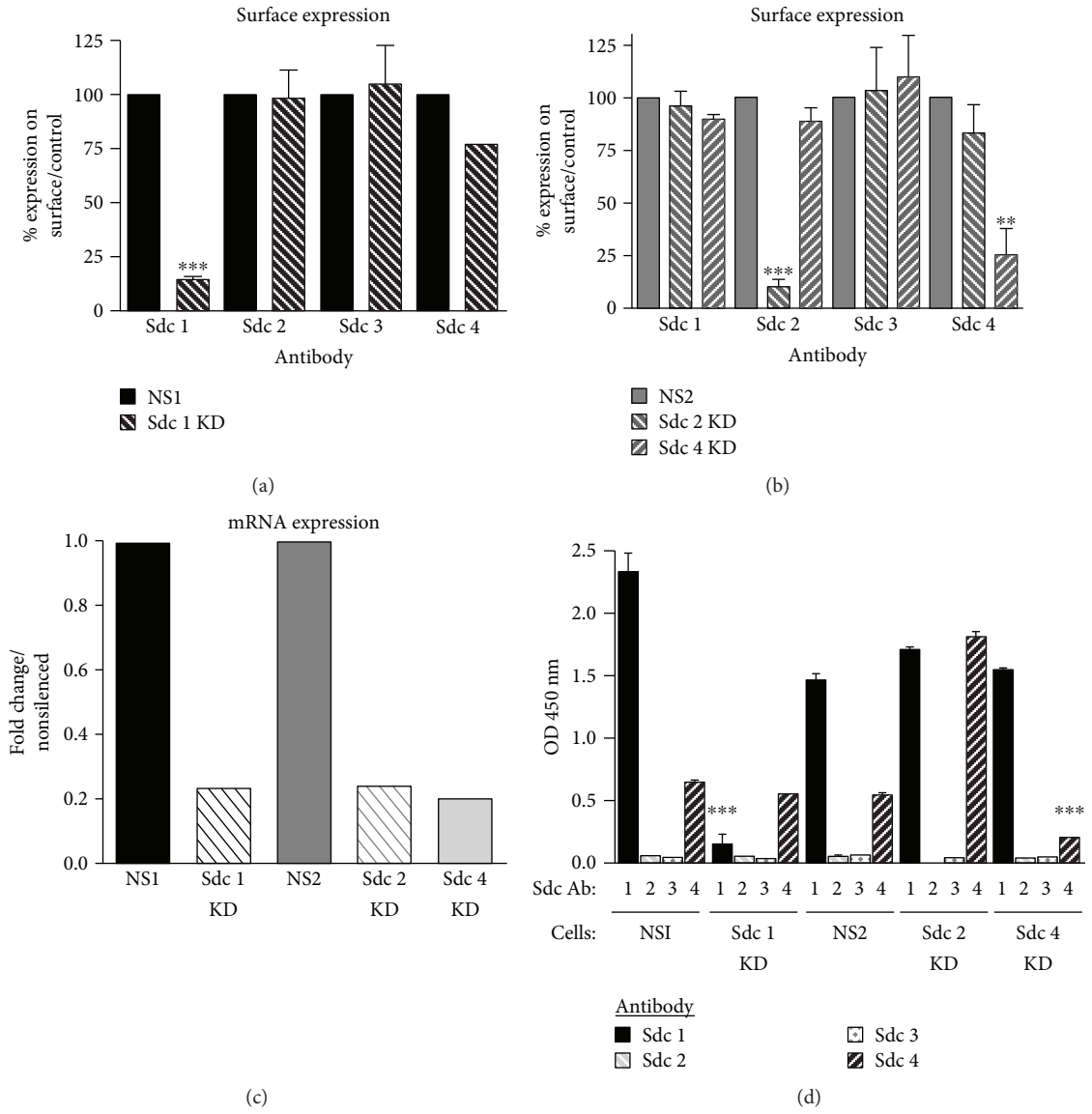

Figure 3: Expression of Sdcs 1, 2, and 4 is decreased by 75% at the protein (a, b) and message (c) levels in MDA-231 cells. (a, b) Flow cytometry measuring surface expression of Sdcs in MDA-231: (a) only Sdc 1 expression is decreased at the cell surface when the Sdc 1 expression is silenced in the MDA-231 cells. (b) In Sdc 2 KD cells, only the Sdc 2 surface expression is decreased, and in Sdc 4 KD cells, only the Sdc 4 surface expression is decreased. The decreased expression of these Sdcs is specific. (c) qPCR was used to detect the message levels of each Sdc. The fold change is plotted in comparison to the control. (d) Solid-phase assays were performed with the Sdc KD cells as described in Figure 2(b). Sdcs 1 and 4 bind to AG73 in control cells (NS1 and NS2) as well as the Sdc 2 KD cell lysate. No binding to AG73 was detected in the Sdc 1 and 4 KD cell lysate. Silencing of Sdcs 1 or 4 expression inhibited binding of these receptors to AG73, and thus, binding of the Sdc 1 and 4 antibodies was significantly decreased. Bars: mean OD 450 nm ± SEM. MDA-231-Sdc 1 KD cells compared to MDA-231-NS1 cells. MDA-231-Sdc 2 and 4 KD cells compared to MDA-231-NS2 cells. $^{***}p < 0.001$. One-way ANOVA with Bonferroni posttest.

least. In addition, these results indicate that heparan sulfate may be the GAG involved in binding AG73 since it had a greater affinity for AG73 than chondroitin sulfate B. Previous studies have also demonstrated that cell binding to AG73 can be inhibited by heparin and that these peptides bind to several different types of proteoglycans, e.g., AG73 binds to Sdcs 1 and 4 on both human salivary gland cells and human dermal fibroblasts and to a chondroitin-heparan sulfate proteoglycan on B16F10 melanoma cells [22, 30]. A tenfold molar access of AG73 was unable to inhibit breast cancer cell adhesion to the basement membrane extract (BME) that contains LM-111, entactin, collagen IV, and heparan sulfate proteoglycans [36] (Figure 1(e)). However, AG73 could inhibit the ability of the breast cancer cells to adhere to LM-111 (Figure 1(e)), indicating it likely has physiological relevance in the direct binding of cells to LM-111.

Hozumi et al. [20] have shown that the AG73 sequence is essential for binding of the proteoglycan receptors Sdcs 1, 2, and 4 to rec-LG4 on fibroblasts; however, other

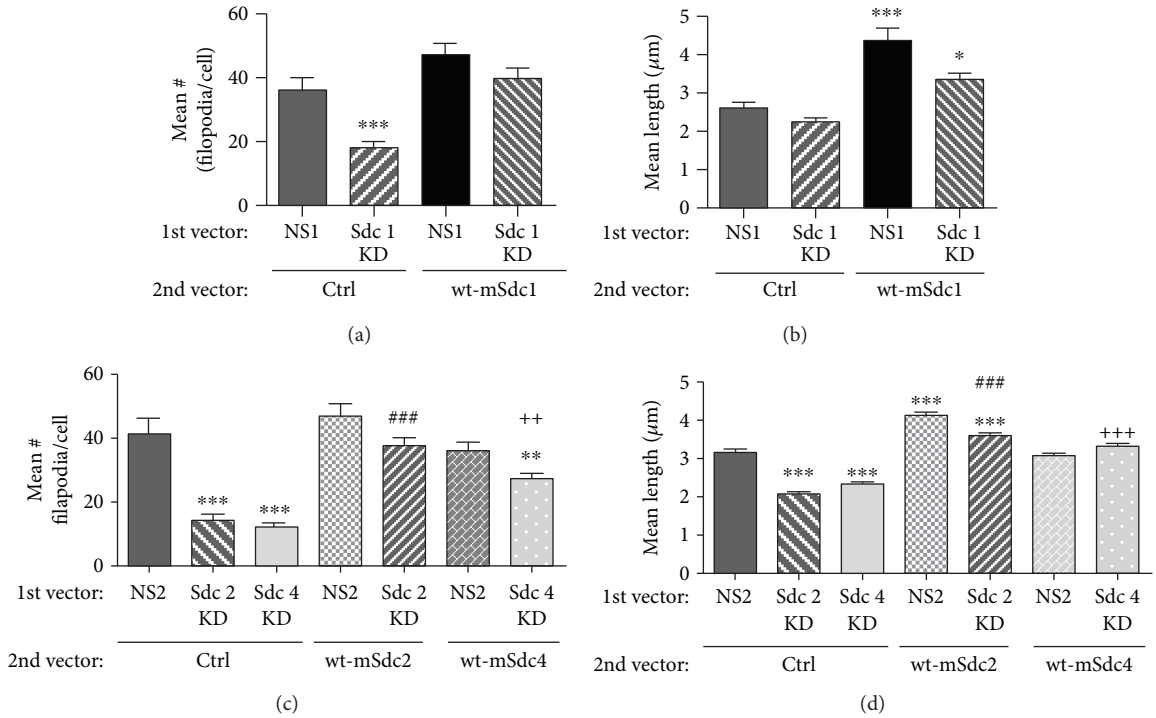

Figure 4: Silencing the expression of Sdcs 1, 2, and 4 decreased filopodium formation in MDA-231 breast cancer cells. (a) Silencing of the Sdc 1 expression decreased the number of filopodia/cells, and wild-type-mouse Sdc 1 (wt-mSdc1) could rescue this significant decrease. (b) The silencing of the Sdc 1 expression had no effect on the length of filopodia; however, overexpression of wt-mSdc1 (NS1-wt-mSdc1) as well as the rescue of the Sdc 1 knockdown increased the length of the filopodia. (c, d) Silencing of the Sdc 2 and 4 expression decreased the number of filopodia/cells (c) and the length of the filopodia (d). Expression of wt-mSdc2 or wt-mSdc4, respectively, could rescue these decreases. Overexpression of Sdc 2 (NS2-wt-mSdc2) but not Sdc 4 (NS2-wt-mSdc4) increased the length of the filopodia. Images in Supplemental Figure 1. $^{***}p < 0.001$ and $^{**}p < 0.01$ comparing NS2 to all other conditions; $^{\#\#\#}p < 0.001$ comparing Sdc 2 KD to Sdc 2 KD rescued with wt-mSdc2; $^{++}p < 0.01$ or $^{+++}p < 0.001$ comparing Sdc 4 KD to Sdc 4 KD rescued with wt-mSdc2. One-way ANOVA with Bonferroni posttest.

proteoglycans like glypican-1 do not bind to rec-LG4 or AG73. Thus, to explore if the Sdcs could be the proteoglycan receptor binding AG73 in breast cancer cells, expression of the Sdcs in MDA-231 cells was examined by qPCR. MDA-231 breast cancer cells as well as other breast cancer cell lines, e.g., MCF7, T47D, and SUM1315, express all four Sdcs, i.e., 1-4 (Figure 2(a)). Therefore, binding of the Sdcs to AG73 was investigated using a solid-phase assay as previously described [34]. Sdcs 1 and 4 bound to AG73 (Figure 2(b)) but did not bind to the scrambled peptide (data not shown), and this binding was inhibited by heparin and pretreatment of MDA-231 cells with trypsin, which cleaves proteoglycans from the cell surface [37, 38] (Figure 2(b)). CD44 or glypican-1 (other proteoglycan receptors) binding to either AG73 or the scrambled peptide was not detected (data not shown). To further characterize the receptor for AG73, the biotinylated MDA-231 cell membrane was incubated with either AG73 or scrambled peptide as in the solid-phase assay. Electrophoreses and blotting of the bound material revealed that AG73 binds components at >250, 90, and 50 kDa (Figure 2(c)). These molecular weights are consistent with those observed for the Sdc receptors [39, 40]. These data suggest that the likely candidates for the AG73 cell surface receptor on breast cancer cells are the Sdcs.

Knockdown (KD) of Sdcs 1, 2, and 4 in the MDA-231 breast cancer cell line was generated using a shRNAmir. Sdc expression was successfully decreased by 75% both at the protein (Figures 3(a) and 3(b)) and message (Figure 3(c)) levels. Each knockdown was confirmed to be specific. The silencing of one family member did not affect the expression of the other family members (Figures 3(a) and 3(b)). In the solid-phase assay, knockdown of Sdc(s) 1 and/or 4 was found to inhibit binding to AG73 (Figure 3(d)), suggesting that these receptors are important in AG73-mediated cell activities. Sdcs 1, 2, and 4 have been shown to be a binding partner to AG73 in nonbreast cells including salivary gland cells, fibroblasts, and melanoma cells [12, 20–24]. Our results indicate that AG73 binds to Sdcs 1 and 4 in breast cancer cells. Sdcs 1 and 4 are expressed in the basolateral border of epithelial cells and myoepithelium in normal breast tissue [41]. In clinical samples of breast tumors, staining for Sdcs 1 and 4 is found in both the stroma and the tumor cells [41–43]. In addition, high Sdc 1 expression is associated with triple-negative and Her2+ breast tumors, which are highly metastatic subtypes, and it is a negative predictor of disease-free and overall survival [41–44]. These studies indicate that the Sdcs may play a role in breast cancer progression and metastasis. We have previously shown that AG73 increases breast cancer metastasis to the bone [14]. Taken together,

our findings suggest that the interaction between AG73 and the Sdcs facilitates breast cancer metastasis.

3.2. AG73 Affects Filopodium Formation in Breast Cancer Cells through Sdcs 1, 2, and 4. Filopodia play key roles in cancer cell migration, invasion, and metastasis [45]. We previously demonstrated that AG73 increases the formation of filament spikes in breast cancer cells, which resemble filopodia, whereas a scrambled peptide does not cause these morphological changes [14]. These increased filopodia are also seen in fibroblasts bound to AG73 [31]. Silencing of the expression of Sdcs 1, 2, or 4 significantly decreased the length and number of filopodia on MDA-231 breast cancer cells bound to AG73 (Figure 4 and Supplemental Figure 1). Expression of mouse Sdcs 1, 2, or 4, in the silenced cells, could rescue this decrease in filopodium length and number. Furthermore, overexpression of Sdcs 1 and 2 significantly increased the length of filopodia on the cells (Figure 4 and Supplemental Figure 1). These data demonstrate that AG73 binds to Sdcs 1, 2, and 4 on breast cancer cells and mediates filopodium formation through these Sdcs. Although we could not detect Sdc 2 in the solid-phase assay possibly due to limitations with antibody recognition in this assay, we did however still observe its effects on filopodium formation. A previous study also reported a synergistic relationship between AG73, Sdcs, and integrins in promoting cell adhesion and spreading, thus supporting our findings reported here [16]. The increase in filopodia we observed in our study emphasizes a possible link between AG73, Sdcs, and cancer as others have shown that expression of filopodium regulatory proteins in cancer patients correlates with poor prognosis and low survival [45]. In addition, a meta-analysis of filopodium gene expression in breast cancer patients revealed a link between filopodium-inducing genes and high rates of breast cancer metastasis [46]. Overall, our findings demonstrate a critical function resulting from the interaction between AG73 and the Sdcs in driving filopodium formation in breast cancer cells.

4. Conclusions

Breast cancer metastasis affects 20-30% of patients and remains to be fully understood [47]. In order to metastasize, disseminated breast cancer cells must cooperate with their environment to bypass the basement membrane and enter into circulation to transit to distant sites. In this study, we focused on this early step in cancer progression and thus investigated the interaction between breast cancer cells and AG73, a laminin peptide found in the basement membrane. We focused on receptors for AG73 and determined that the heparan sulfate proteoglycan receptors, Sdcs 1, 2, and 4, expressed on various breast cancer cells, facilitate this interaction by binding to AG73. We believe this to be the first report describing a direct binding relationship between AG73 and the Sdcs in breast cancer cells. Further, we found that the binding of AG73 to Sdcs 1, 2, and 4 promotes filopodium formation in breast cancer cells such as the MDA-231 cell line. Increased filopodia in breast cancer cells have been associated with tumor invasion and metastasis [45, 46]. Taken together, our findings demonstrate a previously unreported link between AG73 and Sdcs 1, 2, and 4 on breast cancer cells, highlighting the unique interplay between cancer cells and the tumor environment in mediating cancer progression.

Data Availability

The data used to support the findings of this study are included within the article and supplementary figure.

Conflicts of Interest

There are no conflicts of interest to report.

Authors' Contributions

Madhavi Puchalapalli and Liang Mu contributed equally to the study.

Acknowledgments

We thank Drs. Kentaro Hozumi and Yoshihiko Yamada for the recombinant LG4 and LG4 mutant and for their expert advice. This work was financially supported by funding from the NCI K22CA116258-02 and the Lynn Sage Cancer Research Foundation and the Zell Foundation, Chicago, IL. Imaging work was performed at the Northwestern University Center for Advanced Microscopy generously supported by NCI CCSG P30 CA060553 awarded to the Robert H. Lurie Comprehensive Cancer Center.

Supplementary Materials

Supplemental Figure 1: silencing the expression of Sdcs 1, 2, and 4 decreased filopodium formation in MDA-231 breast cancer cells and wtSdc (WT) can rescue filopodium formation. Representative images are included in the quantification shown in Figure 4. Cells infected with the nonsilencing (NS) shRNAmir as well as the empty vector (EV) were used as the control. This EV was the same vector (pBABE) that was used for the wtSdc expression. *(Supplementary Materials)*

References

[1] E. Ioachim, A. Charchanti, E. Briasoulis et al., "Immunohistochemical expression of extracellular matrix components tenascin, fibronectin, collagen type IV and laminin in breast cancer: their prognostic value and role in tumour invasion and progression," *European Journal of Cancer*, vol. 38, no. 18, pp. 2362–2370, 2002.

[2] W. Q. Zheng, L. M. Looi, and P. L. Cheah, "Correlation between laminin and cathepsin D expressions in breast carcinoma," *Tumori Journal*, vol. 88, no. 4, pp. 296–299, 2002.

[3] E. Ioachim, S. Kamina, M. Kontostolis, and N. J. Agnantis, "Immunohistochemical expression of cathepsin D in correlation with extracellular matrix component, steroid receptor status and proliferative indices in breast cancer," *Virchows Archiv*, vol. 431, no. 5, pp. 311–316, 1997.

[4] R. Albrechtsen, M. Nielsen, U. Wewer, E. Engvall, and E. Ruoslahti, "Basement membrane changes in breast cancer detected by immunohistochemical staining for laminin," *Cancer Research*, vol. 41, 12, Part 1, pp. 5076–5081, 1981.

[5] M. J. Bissell, A. Rizki, and I. S. Mian, "Tissue architecture: the ultimate regulator of breast epithelial function," *Current Opinion in Cell Biology*, vol. 15, no. 6, pp. 753–762, 2003.

[6] T. Gudjonsson, L. Ronnov-Jessen, R. Villadsen, F. Rank, M. J. Bissell, and O. W. Petersen, "Normal and tumor-derived myoepithelial cells differ in their ability to interact with luminal breast epithelial cells for polarity and basement membrane deposition," *Journal of Cell Science*, vol. 115, Part 1, pp. 39–50, 2002.

[7] Y. Kikkawa, K. Hozumi, F. Katagiri, M. Nomizu, H. K. Kleinman, and J. E. Koblinski, "Laminin-111-derived peptides and cancer," *Cell Adhesion & Migration*, vol. 7, no. 1, pp. 150–159, 2013.

[8] C. F. Nascimento, A. S. de Siqueira, J. J. V. Pinheiro, V. M. Freitas, and R. G. Jaeger, "Laminin-111 derived peptides AG73 and C16 regulate invadopodia activity of a human adenoid cystic carcinoma cell line," *Experimental Cell Research*, vol. 317, no. 18, pp. 2562–2572, 2011.

[9] W. H. Kim, M. Nomizu, S. Y. Song et al., "Laminin-α1-chain sequence Leu-Gln-Val-Gln-Leu-Ser-Ile-Arg (LQVQLSIR) enhances murine melanoma cell metastases," *International Journal of Cancer*, vol. 77, no. 4, pp. 632–639, 1998.

[10] S. Y. Song, M. Nomizu, Y. Yamada, and H. K. Kleinman, "Liver metastasis formation by laminin-1 peptide (LQVQLSIR)-adhesion selected B16-F10 melanoma cells," *International Journal of Cancer*, vol. 71, no. 3, pp. 436–441, 1997.

[11] Y. Yoshida, K. Hosokawa, A. Dantes, F. Kotsuji, H. K. Kleinman, and A. Amsterdam, "Role of laminin in ovarian cancer tumor growth and metastasis via regulation of Mdm2 and Bcl-2 expression," *International Journal of Oncology*, vol. 18, no. 5, pp. 913–921, 2001.

[12] N. Suzuki, N. Ichikawa, S. Kasai et al., "Syndecan binding sites in the laminin α1 chain G domain," *Biochemistry*, vol. 42, no. 43, pp. 12625–12633, 2003.

[13] A. S. Siqueira, L. N. Gama-de-Souza, M. V. C. Arnaud, J. J. V. Pinheiro, and R. G. Jaeger, "Laminin-derived peptide AG73 regulates migration, invasion, and protease activity of human oral squamous cell carcinoma cells through syndecan-1 and β1 integrin," *Tumour Biology*, vol. 31, no. 1, pp. 46–58, 2010.

[14] J. A. Engbring, R. Hossain, S. J. VanOsdol et al., "The laminin α-1 chain derived peptide, AG73, increases fibronectin levels in breast and melanoma cancer cells," *Clinical & Experimental Metastasis*, vol. 25, no. 3, pp. 241–252, 2008.

[15] M. Nomizu, W. H. Kim, K. Yamamura et al., "Identification of cell binding sites in the laminin α1 chain carboxyl-terminal globular domain by systematic screening of synthetic peptides," *Journal of Biological Chemistry*, vol. 270, no. 35, pp. 20583–20590, 1995.

[16] K. Hozumi, T. Akizuki, Y. Yamada et al., "Cell adhesive peptide screening of the mouse laminin α1 chain G domain," *Archives of Biochemistry and Biophysics*, vol. 503, no. 2, pp. 213–222, 2010.

[17] M. Mochizuki, D. Philp, K. Hozumi et al., "Angiogenic activity of syndecan-binding laminin peptide AG73 (RKRLQVQLSIRT)," *Archives of Biochemistry and Biophysics*, vol. 459, no. 2, pp. 249–255, 2007.

[18] Y. Yamada, K. Hozumi, A. Aso et al., "Laminin active peptide/agarose matrices as multifunctional biomaterials for tissue engineering," *Biomaterials*, vol. 33, no. 16, pp. 4118–4125, 2012.

[19] Y. Yamada, K. Hozumi, F. Katagiri, Y. Kikkawa, and M. Nomizu, "Laminin-111-derived peptide-hyaluronate hydrogels as a synthetic basement membrane," *Biomaterials*, vol. 34, no. 28, pp. 6539–6547, 2013.

[20] K. Hozumi, N. Suzuki, P. K. Nielsen, M. Nomizu, and Y. Yamada, "Laminin α1 chain LG4 module promotes cell attachment through syndecans and cell spreading through integrin $\alpha 2\beta 1$," *Journal of Biological Chemistry*, vol. 281, no. 43, pp. 32929–32940, 2006.

[21] M. P. Hoffman, J. A. Engbring, P. K. Nielsen et al., "Cell type-specific differences in glycosaminoglycans modulate the biological activity of a heparin-binding peptide (RKRLQVQLSIRT) from the G domain of the laminin α1 chain," *Journal of Biological Chemistry*, vol. 276, no. 25, pp. 22077–22085, 2001.

[22] J. A. Engbring, M. P. Hoffman, A. J. Karmand, and H. K. Kleinman, "The B16F10 cell receptor for a metastasis-promoting site on laminin-1 is a heparan sulfate/chondroitin sulfate-containing proteoglycan," *Cancer Research*, vol. 62, no. 12, pp. 3549–3554, 2002.

[23] L. N. Gama-de-Souza, E. Cyreno-Oliveira, V. M. Freitas et al., "Adhesion and protease activity in cell lines from human salivary gland tumors are regulated by the laminin-derived peptide AG73, syndecan-1 and β1 integrin," *Matrix Biology*, vol. 27, no. 5, pp. 402–419, 2008.

[24] K. Hozumi, K. Kobayashi, F. Katagiri, Y. Kikkawa, Y. Kadoya, and M. Nomizu, "Syndecan- and integrin-binding peptides synergistically accelerate cell adhesion," *FEBS Letters*, vol. 584, no. 15, pp. 3381–3385, 2010.

[25] M. D. Bass, M. R. Morgan, and M. J. Humphries, "Syndecans shed their reputation as inert molecules," *Science Signaling*, vol. 2, no. 64, article pe18, 2009.

[26] C. C. Lopes, L. Toma, M. A. S. Pinhal et al., "EJ-*ras* oncogene transfection of endothelial cells upregulates the expression of syndecan-4 and downregulates heparan sulfate sulfotransferases and epimerase," *Biochimie*, vol. 88, no. 10, pp. 1493–1504, 2006.

[27] E. Tkachenko, J. M. Rhodes, and M. Simons, "Syndecans: new kids on the signaling block," *Circulation Research*, vol. 96, no. 5, pp. 488–500, 2005.

[28] A. N. Alexopoulou, H. A. B. Multhaupt, and J. R. Couchman, "Syndecans in wound healing, inflammation and vascular biology," *The International Journal of Biochemistry & Cell Biology*, vol. 39, no. 3, pp. 505–528, 2007.

[29] M. R. Morgan, M. J. Humphries, and M. D. Bass, "Synergistic control of cell adhesion by integrins and syndecans," *Nature Reviews Molecular Cell Biology*, vol. 8, no. 12, pp. 957–969, 2007.

[30] M. P. Hoffman, M. Nomizu, E. Roque et al., "Laminin-1 and laminin-2 G-domain synthetic peptides bind syndecan-1 and are involved in acinar formation of a human submandibular gland cell line," *Journal of Biological Chemistry*, vol. 273, no. 44, pp. 28633–28641, 1998.

[31] N. Suzuki, H. Nakatsuka, M. Mochizuki et al., "Biological activities of homologous loop regions in the laminin α chain G domains," *Journal of Biological Chemistry*, vol. 278, no. 46, pp. 45697–45705, 2003.

[32] D. L. M. Beauvais and A. C. Rapraeger, "Syndecans in tumor cell adhesion and signaling," *Reproductive Biology and Endocrinology*, vol. 2, no. 1, p. 3, 2004.

[33] X. Wang, A. Spandidos, H. Wang, and B. Seed, "PrimerBank: a PCR primer database for quantitative gene expression analysis, 2012 update," *Nucleic Acids Research*, vol. 40, no. D1, pp. D1144–D1149, 2011.

[34] M. L. Ponce, M. Nomizu, and H. K. Kleinman, "An angiogenic laminin site and its antagonist bind through the $\alpha v\beta 3$ and $\alpha 5\beta 1$ integrins," *The FASEB Journal*, vol. 15, no. 8, pp. 1389–1397, 2001.

[35] P. Ekblom, P. Lonai, and J. F. Talts, "Expression and biological role of laminin-1," *Matrix Biology*, vol. 22, no. 1, pp. 35–47, 2003.

[36] G. Benton, I. Arnaoutova, J. George, H. K. Kleinman, and J. Koblinski, "Matrigel: from discovery and ECM mimicry to assays and models for cancer research," *Advanced Drug Delivery Reviews*, vol. 79-80, pp. 3–18, 2014.

[37] K. J. Bame, "Release of heparan sulfate glycosaminoglycans from proteoglycans in Chinese hamster ovary cells does not require proteolysis of the core protein," *Journal of Biological Chemistry*, vol. 268, no. 27, pp. 19956–19964, 1993.

[38] D. Heinegård and V. C. Hascall, "Aggregation of cartilage proteoglycans III. Characteristics of the proteins isolated from trypsin digests of aggregates," *Journal of Biological Chemistry*, vol. 249, no. 13, pp. 4250–4256, 1974.

[39] F. Granés, R. García, R. P. Casaroli-Marano et al., "Syndecan-2 induces filopodia by active cdc42Hs," *Experimental Cell Research*, vol. 248, no. 2, pp. 439–456, 1999.

[40] C. Mundhenke, K. Meyer, S. Drew, and A. Friedl, "Heparan sulfate proteoglycans as regulators of fibroblast growth factor-2 receptor binding in breast carcinomas," *The American Journal of Pathology*, vol. 160, no. 1, pp. 185–194, 2002.

[41] F. Baba, K. Swartz, R. van Buren et al., "Syndecan-1 and syndecan-4 are overexpressed in an estrogen receptor-negative, highly proliferative breast carcinoma subtype," *Breast Cancer Research and Treatment*, vol. 98, no. 1, pp. 91–98, 2006.

[42] M. Barbareschi, P. Maisonneuve, D. Aldovini et al., "High syndecan-1 expression in breast carcinoma is related to an aggressive phenotype and to poorer prognosis," *Cancer*, vol. 98, no. 3, pp. 474–483, 2003.

[43] M. Leivonen, J. Lundin, S. Nordling, K. von Boguslawski, and C. Haglund, "Prognostic value of syndecan-1 expression in breast cancer," *Oncology*, vol. 67, no. 1, pp. 11–18, 2004.

[44] T. L. Nguyen, W. E. Grizzle, K. Zhang, O. Hameed, G. P. Siegal, and S. Wei, "Syndecan-1 overexpression is associated with nonluminal subtypes and poor prognosis in advanced breast cancer," *American Journal of Clinical Pathology*, vol. 140, no. 4, pp. 468–474, 2013.

[45] G. Jacquemet, I. Paatero, A. F. Carisey et al., "FiloQuant reveals increased filopodia density during breast cancer progression," *The Journal of Cell Biology*, vol. 216, no. 10, pp. 3387–3403, 2017.

[46] A. Arjonen, R. Kaukonen, and J. Ivaska, "Filopodia and adhesion in cancer cell motility," *Cell Adhesion & Migration*, vol. 5, no. 5, pp. 421–430, 2014.

[47] American Cancer Society, *Breast Cancer Facts & Figures 2015-2016*, American Cancer Society, Inc., Atlanta, GA, USA, 2015.

Hindawi
Analytical Cellular Pathology
Volume 2019, Article ID 7145198, 5 pages
https://doi.org/10.1155/2019/7145198

Research Article

PDE4 and Epac1 Synergistically Promote Rectal Carcinoma via the cAMP Pathway

Xiangyu Kong,[1] Ganghao Ai,[1] Dai Wang,[2] Renzhen Chen,[2] Dongbei Guo,[2] Youliang Yao,[2] Kai Wang,[2] Guiye Liang,[2] Fengjie Qi,[3] Wenzhi Liu,[1] and Yongxing Zhang[2]

[1]*Department of Gastrointestinal Surgery, Affiliated Zhongshan Hospital of Dalian University, Dalian, 116001 Liaoning, China*
[2]*State Key Laboratory of Molecular Vaccinology and Molecular Diagnostics, School of Public Health, Xiamen University, Xiamen, 361102 Fujian, China*
[3]*Department of Pathology, The third Affiliated Hospital of Shenzhen University, Shenzhen, Guangdong 518001, China*

Correspondence should be addressed to Wenzhi Liu; liuwenzhi1965@163.com and Yongxing Zhang; z63y94x@xmu.edu.cn

Received 6 February 2018; Revised 9 September 2018; Accepted 27 September 2018; Published 23 January 2019

Guest Editor: Lubna H. Tahtamouni

Objective. To assess the expression levels of exchange protein 1 directly activated by cAMP (Epac1) and phosphodiesterase 4 (PDE4) in rectal carcinoma, and their associations with clinicopathological indexes. In addition, the associations of PDE4 and Epac1 with A-kinase anchor protein 95, connexin 43, cyclin D1, and cyclin E1 were evaluated. *Methods*. The PV-9000 two-step immunohistochemistry method was used to determine protein expression in 44 rectal carcinoma tissue samples and 16 paracarcinoma tissue specimens. *Results*. The positive rate of PDE4 protein expression in rectal carcinoma tissues was higher than that of paracarcinoma tissues (59.09% vs. 12.5%, $P < 0.05$). Similar findings were obtained for Epac1 (55% vs. 6.25%, $P < 0.05$). No significant associations of PDE4 and Epac1 with degree of differentiation, histological type, and lymph node metastasis were found in rectal carcinoma ($P > 0.05$). Correlations between PDE4 and Epac1, PDE4 and Cx43, PDE4 and cyclin E1, and Epac1 and Cx43 were observed (all $P < 0.05$). There was no correlation between the other protein pairs examined ($P > 0.05$). *Conclusion*. PDE4 and Epac1 expression levels are increased in rectal carcinoma tissues, suggesting that the two proteins may be involved in the development of this malignancy. Meanwhile, correlations between PDE4 and Epac1, PDE4 and Cx43, PDE4 and cyclin E1, and Epac1 and Cx43 suggested synergistic effects of these proteins in promoting rectal carcinoma.

1. Introduction

Signal transduction is a necessary process for cells to achieve normal physiological processes. The PDE4 enzyme specifically hydrolyzes cAMP and reduces cAMP levels in the cell, to allow cAMP-dependent proteins to modulate cell signal transduction [1]. PKA, which is a downstream of cAMP signal pathway, is an important protein kinase. AKAP95 is a PKA-anchored protein that anchors PKA RII subunits; the anchored PKA can catalytically target protein phosphorylation, ensuring and expanding signal transduction by the cAMP pathway [2, 3]. Cyclin D and cyclin E proteins can promote cell proliferation at the G1 phase in mammalians, while AKAP95 as an intermediary can help cyclin D/E and PKA RII subunits from the cyclin D/E-AKAP95-PKA complex [4]. The novel exchange protein directly activated by cAMP (Epac) is a multifunctional molecule that participates in a variety of cellular processes [5]. The Epac protein includes two subtypes, i.e., Epac1 and Epac2, both of which are expressed in many tissues and organs [6, 7]. Different organs and distinct developmental stages also show differences [8]. We have previously reported the combinatory relationship between AKAP95 and Cx43 in the cell cycle [9]. Studies mentioned that Epac can regulate Cx43 to promote gap junction formation and intercellular communication [10].

The above findings suggest that PDE4, Epac, AKAP95, Cx43, and cyclin D/E have some associations. The immunohistochemical method was used to assess the protein expression of PDE4 and Epac1 in 44 samples of rectal carcinoma

alongside 16 paracarcinoma tissue samples. The associations of various proteins were analyzed.

2. Materials and Methods

2.1. Tumor Sources. Tissue samples from 44 cases with definite pathological diagnosis of invasive rectal carcinoma were collected from the First Affiliated Hospital of Liaoning Medical University. Patient age ranged between 39 and 79 years, averaging 60 ± 8; there were 28 males and 16 females. A total of 38, 4, and 2 patients had tubular or papillary adenocarcinoma, mucinous adenocarcinoma, and signet-ring cell carcinoma, respectively. Cancer cells were highly, moderately, and poorly differentiated in 4, 36, and 4 patients, respectively. A total of 23 patients had lymph node metastasis; 15 presented no lymph node metastasis, while the lymph node metastasis status was unclear for the remaining 6 individuals. In addition, paracarcinoma tissues were obtained from normal rectal tissues at least 3 cm away from cancerous tissues, in 16 of the 44 patients. Pathological examination was also performed on the paracarcinoma tissues to confirm the absence of cancer cells. The study protocol was approved by the Medical Ethics Committee of the School of Public Health in Xiamen University, China.

2.2. Reagents and Methods. All specimens were fixed in 10% neutral formaldehyde, paraffin embedded, and sliced into continuous sections of 4 μm. The PV-9000 two-step immunohistochemical staining kit (Zhongshan Jinqiao Biotechnology Company, Beijing, China) was used for protein expression analysis, according to the manufacturer's instructions. The assay involved DAB staining and hematoxylin counterstaining. Rabbit anti-human Epac1 antibodies were purchased from Abcam (Cambridge, UK), whereas mouse anti-human PDE4 monoclonal antibodies were from Santa Cruz (Dallas, Texas, USA). PBS was used as the negative control sample.

2.3. Criteria for Judging Positive Expression. A brown–yellow stain was considered positive expression of the protein, while the absence of brown–yellow staining indicated no protein expression. Ten different high-power fields were randomly evaluated per section, with 200 tumor cells counted per field. The ratio of positive to total cells was used as a metric to assess positive protein expression: "–," <10% brown; "±," ≥10% and <25%; "+," ≥25% and <50%; "++," ≥50% and <75%; and "+++," ≥75%. For data analysis, "–" and "±" were considered negative expression and "+," "++," and "+++" indicated positive expression.

3. Statistical Analysis

Positive rates of protein expression were assessed by the χ^2 test and were assessed by Spearman's rank correlation analysis. $P < 0.05$ was considered statistically significant, and data were analyzed with the SPSS13.0 software.

Table 1: PDE4 and Epac1 protein levels in rectal cancer tissues.

Protein	Features	Rectal cancer	Paracarcinoma tissues	χ^2	P
Epac1	Positive	24	1	11.260	0.01
	Negative	20	15		
PDE4	Positive	26	2	10.233	0.01
	Negative	18	14		

Note: in rectal cancer and paracarcinoma tissues, PDE4 and Epac1 levels showed a statistically significant difference.

4. Results

4.1. PDE4 and Epac1 Protein Levels in Rectal Carcinoma Tissues. We previously assessed rectal carcinoma tissues and found higher positive rates of AKAP95, cyclin E1, and cyclin D1 compared with paracarcinoma tissues. Meanwhile, the positive rate of Cx43 was lower than that of paracarcinoma tissues. These findings suggested that AKAP95, cyclin D1, and cyclin E1 may promote cancer, while the Cx43 protein suppresses cancer development [11].

In this study, PDE4 and Epac1 protein levels were further assessed in rectal cancer samples. PDE4 and Epac1 protein levels in 44 rectal cancer and 16 paracarcinoma tissue samples were assessed (Table 1). The positive expression rate for PDE4 in rectal cancer was 59.09% (26/44), which was higher than that of paracarcinoma tissue specimens (12.5%, 2/16, $P < 0.05$). The positive expression rate for Epac1 in rectal cancer was 55.00% (24/44), which was also higher than that of paracarcinoma tissue samples (6.25%, 1/16, $P < 0.05$). The PDE4 and Epac1 proteins were expressed in the cytoplasm of rectal carcinoma tissues and with expression obtained in nuclei (Figure 1).

There were no associations of PDE4 and Epac1 with degree of differentiation, histological type, and lymph node metastasis in rectal carcinoma ($P > 0.05$).

4.2. Associations of PDE4, Epac1, AKAP95, Cx43, Cyclin E1, and Cyclin D1 in Rectal Carcinoma Tissues. The associations of PDE4 and Epac1 with AKAP95, Cx43, cyclin E1, and cyclin D1 in 44 rectal carcinoma samples were assessed. The results indicated correlations between PDE4 and Epac1 (Table 2), PDE4 and cyclin E1 (Table 3), PDE4 and Cx43 (Table 4), and Epac1 and Cx43 (Table 5) ($P < 0.05$). No significant associations were obtained for the remaining protein pairs (data not shown).

5. Discussion

The Epac protein is mainly involved in cell adhesion, ?communication, secretion, and differentiation [5]. As a multifunctional signaling molecule, it has multiple unique regulatory functions, in the immune, respiratory, nervous, cardiovascular, and endocrine systems [12, 13]. Epac1 exists in all organisms, and the Epac2 protein is found only in gland tissues and the nervous system [14]. It was recently reported that the Epac inhibitor ESI-09 suppresses the proliferation of pancreatic tumor cells [15]; meanwhile, Epac1 is highly

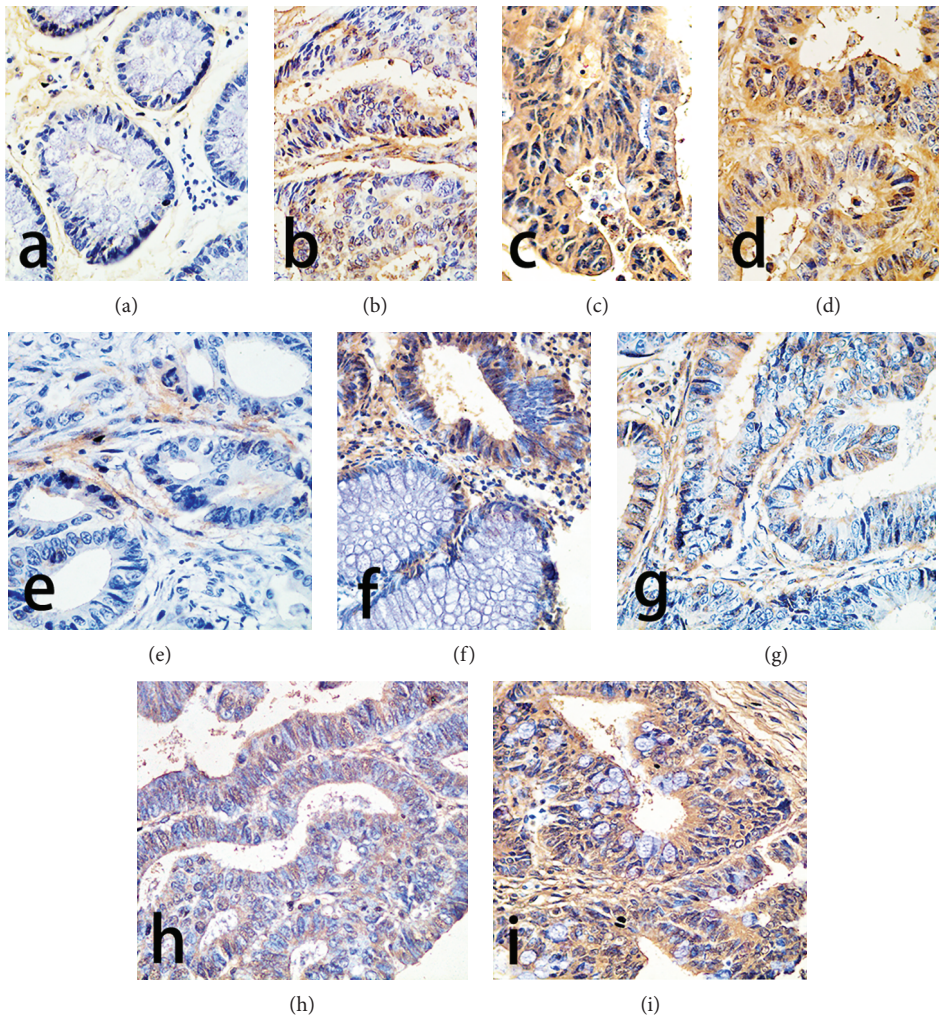

Figure 1: Epac1 and PDE4 expression in rectal carcinoma tissues (×400). The subfigures (a), (b), (c), and (d) indicated the protein expression of Epac1 in rectal cancer tissues. (a) No expression. (b) Moderately expression. (c, d) High expression levels, expression in the cytoplasm and in the nucleus. The subfigures (e), (f), (g), (h), and (i) indicated the protein expression of PDE4 in rectal cancer tissues. (e) No expression. (f) The top of the picture is moderately expression, and the bottom is no expression. (g) Low expression levels. (h) Moderately expression. (i) High expression levels, mainly in the cytoplasm, with low amounts in the nucleus.

Table 2: Correlation between PDE4 and Epac1 protein levels in rectal cancer.

Epac1	PDE4					r_s	P
	–	+–	+	++	+++		
–	5	1	1	1	0		
+–	3	4	5	0	0		
+	2	0	5	3	1	0.419	0.005
++	0	1	3	5	0		
+++	1	1	2	0	0		

Note: r_s is the spearman rank correlation coefficient.

Table 3: Correlation between PDE4 and cyclin E1 protein levels in rectal cancer.

Cyclin E1	PDE4					r_s	P
	–	+–	+	++	+++		
–	5	1	3	1	0		
+–	0	2	3	3	0		
+	5	2	3	0	0	0.300	0.048
++	1	0	6	2	1		
+++	0	2	1	3	0		

Note: r_s is the spearman rank correlation coefficient.

expressed in gastric cancer cells [16]. This study also demonstrated high Epac1 expression levels in rectal cancer tissue samples, which may indicate that this protein promotes ?cancer in the digestive system.

PDE is an enzyme involved in cAMP hydrolysis. PDE4 is a member of the PDE family of proteins; it specifically hydrolyzes cAMP, to enable inactivation by 5′-AMP formation, which ends the downstream signal transduction [17]. PDE4

Table 4: Correlation between PDE4 and Cx43 protein levels in rectal cancer.

PDE4	Cx43					r_s	P
	−	+−	+	++	+++		
−	6	3	2	0	0		
+−	1	5	1	0	0		
+	2	7	7	0	0	0.367	0.014
++	2	2	2	2	1		
+++	0	1	0	0	0		

Note: r_s is the spearman rank correlation coefficient.

Table 5: Correlation between Epac1 and Cx43 protein levels in rectal cancer.

Epac1	Cx43					r_s	P
	−	+−	+	++	+++		
−	5	2	1	0	0		
+−	4	3	5	0	0		
+	1	7	2	1	0	0.360	0.016
++	1	3	3	1	1		
+++	0	3	1	0	0		

Note: r_s is the spearman rank correlation coefficient.

is associated with the occurrence of multiple tumors and highly expressed in a variety of tumor tissues [18]. PDE4 showed high expression levels in rectal cancer tissues, which may suggest that it promotes rectal cancer as well, corroborating previous reports.

Meanwhile, PDE4 can bind and activate the downstream Epac protein, which is the downstream target of cAMP. Epac binds to cAMP with high affinity and activates the Ras superfamily small GTPases Rap1 and Rap2, indicating the existence of the PDE4/cAMP/Epac1 signaling pathway [18]. As shown above, correlations were found between PDE4 and Epac1, PDE4 and Cx43, and Epac1 and Cx43 ($P < 0.05$). These findings indicate possible interactions of the PDE4, Epac1, and Cx43 proteins, which commonly play roles in rectal cancer occurrence.

This study also demonstrated a correlation between PDE4 and cyclin E1. Cyclin E1 is an important protein in the G1/S stage of the cell cycle. The association of PDE4 with cyclin E1 suggests that the two proteins may exert synergistic effects on the G1/S transition during cell proliferation. However, there was no correlation between PDE4 and cyclin D1.

The Epac protein of rabbit myocardial cells regulates Cx43 phosphorylation at ser368, which affects Cx43 protein function [10]. Studies confirmed that Cx43 plays a role of tumor inhibition in multiple organisms [19–22]. In this study, Epac1 level was associated with Cx43 expression, further illustrating a close relationship for inducing rectal cancer.

In T cell leukemia patients, PDE4 and AKAP95 levels are associated in T cells [23]. However, as shown above, no correlation between PDE4 and AKAP95 was found in rectal cancer tissues. The discrepancy caused by the histological differences remains unclear. In rat myocardial cells, mAKAP, which is a member of the AKAP family, can bind with Epac1 to regulate signaling and modulate rat myocardial hypertrophy [24]. Our experimental study revealed no correlation between Epac1 and AKAP95 protein levels. This phenomenon may be associated with tumorigenesis, related to different members of the AKAP family or histological differences. The specific mechanism requires further assessment.

In summary, there are some close correlations in PDE4, Epac1, cyclin E1, and Cx43 in rectal cancer. This may be an important network of proteins for regulating cell cycle in rectal cancer. And it may become a new therapeutic target in the future. However, this needs further study.

Data Availability

(1) The data of AKAP95, Cx43, cyclin E1, and cyclin D1 expression in rectal carcinoma tissues used to support the findings of this study have been deposited in the PubMed repository [PMID: 25973052 or PMCID: PMC4396224]. The prior studies are cited at relevant places within the text as references [11]. (2) The data of associations of PDE4 and Epac1 with AKAP95, Cx43, cyclin E1, and cyclin D1 used to support the findings of this study are included within the article.

Conflicts of Interest

The authors declare that they have no conflicts of interest.

Authors' Contributions

Xiangyu Kong and Ganghao Ai contributed equally to this work.

Acknowledgments

This work is supported by the Department of Education of Liaoning Province (L2015022), the Dalian Municipal Commission of Health and Family Planning (2016), Natural Science Foundation of Fujian Province of China (nos. 2016J01407 and 2015J01345), Xiamen University Training Programs of Innovation and Entrepreneurship for Undergraduates (nos. 2016X0433 and 2015X0453), and the Fundamental Research Funds for the Central Universities (no. 20720160060).

References

[1] A. Martinez and C. Gil, "cAMP-specific phosphodiesterase inhibitors: promising drugs for inflammatory and neurological diseases," *Expert Opinion on Therapeutic Patents*, vol. 24, no. 12, pp. 1311–1321, 2014.

[2] T. Eide, V. Coghlan, S. Ørstavik et al., "Molecular cloning, chromosomal localization, and cell cycle-dependent subcellular distribution of the A-kinase anchoring protein, AKAP95," *Experimental Cell Research*, vol. 238, no. 2, pp. 305–316, 1998.

[3] E. A. Wall, J. R. Zavzavadjian, M. S. Chang et al., "Suppression of LPS-induced TNF-α production in macrophages by cAMP

is mediated by PKA-AKAP95-p105," *Science Signaling*, vol. 2, no. 75, p. ra28, 2009.

[4] T. Arsenijevic, C. Degraef, J. E. Dumont, P. P. Roger, and I. Pirson, "G1/S cyclins interact with regulatory subunit of PKA via A-kinase anchoring protein, AKAP95," *Cell Cycle*, vol. 5, no. 11, pp. 1217–1222, 2006.

[5] M. Gloerich and J. L. Bos, "Epac: defining a new mechanism for cAMP action," *Annual Review of Pharmacology and Toxicology*, vol. 50, no. 1, pp. 355–375, 2010.

[6] H. Kawasaki, G. M. Springett, N. Mochizuki et al., "A family of cAMP-binding proteins that directly activate Rap1," *Science*, vol. 282, no. 5397, pp. 2275–2279, 1998.

[7] J. de Rooij, F. J. T. Zwartkruis, M. H. G. Verheijen et al., "Epac is a Rap1 guanine-nucleotide-exchange factor directly activated by cyclic AMP," *Nature*, vol. 396, no. 6710, pp. 474–477, 1998.

[8] C. Ulucan, X. Wang, E. Baljinnyam et al., "Developmental changes in gene expression of Epac and its upregulation in myocardial hypertrophy," *American Journal of Physiology. Heart and Circulatory Physiology*, vol. 293, no. 3, pp. H1662–H1672, 2007.

[9] X. Chen, X. Kong, W. Zhuang et al., "Dynamic changes in protein interaction between AKAP95 and Cx43 during cell cycle progression of A549 cells," *Scientific Reports*, vol. 6, no. 1, article 21224, 2016.

[10] N. Duquesnes, M. Derangeon, M. Métrich et al., "Epac stimulation induces rapid increases in connexin43 phosphorylation and function without preconditioning effect," *Pflügers Archiv*, vol. 460, no. 4, pp. 731–741, 2010.

[11] F. Qi, Y. Yuan, X. Zhi et al., "Synergistic effects of AKAP95, cyclin D1, cyclin E1, and Cx43 in the development of rectal cancer," *International Journal of Clinical and Experimental Pathology*, vol. 8, no. 2, pp. 1666–1673, 2015.

[12] M. Grandoch, S. S. Roscioni, and M. Schmidt, "The role of Epac proteins, novel cAMP mediators, in the regulation of immune, lung and neuronal function," *British Journal of Pharmacology*, vol. 159, no. 2, pp. 265–284, 2010.

[13] M. Schmidt, F. J. Dekker, and H. Maarsingh, "Exchange protein directly activated by cAMP (epac): a multidomain cAMP mediator in the regulation of diverse biological functions," *Pharmacological Reviews*, vol. 65, no. 2, pp. 670–709, 2013.

[14] W. Sun, W. Jiao, Y. Huang et al., "Exchange proteins directly activated by cAMP induce the proliferation of rat anterior pituitary GH3 cells via the activation of extracellular signal-regulated kinase," *Biochemical and Biophysical Research Communications*, vol. 485, no. 2, pp. 355–359, 2017.

[15] X. Wang, C. Luo, X. Cheng, and M. Lu, "Lithium and an EPAC-specific inhibitor ESI-09 synergistically suppress pancreatic cancer cell proliferation and survival," *Acta Biochimica et Biophysica Sinica*, vol. 49, no. 7, pp. 573–580, 2017.

[16] D. P. Sun, C. L. Fang, H. K. Chen et al., "EPAC1 overexpression is a prognostic marker and its inhibition shows promising therapeutic potential for gastric cancer," *Oncology Reports*, vol. 37, no. 4, pp. 1953–1960, 2017.

[17] C. Zhang, Y. Cheng, H. Wang et al., "RNA interference-mediated knockdown of long-form phosphodiesterase-4D (PDE4D) enzyme reverses amyloid-β42-induced memory deficits in mice," *Journal of Alzheimer's Disease*, vol. 38, no. 2, pp. 269–280, 2013.

[18] F. Ahmad, T. Murata, K. Shimizu, E. Degerman, D. Maurice, and V. Manganiello, "Cyclic nucleotide phosphodiesterases: important signaling modulators and therapeutic targets," *Oral Diseases*, vol. 21, no. 1, pp. e25–e50, 2015.

[19] M. K. Elzarrad, A. Haroon, K. Willecke, R. Dobrowolski, M. N. Gillespie, and A. B. Al-Mehdi, "Connexin-43 upregulation in micrometastases and tumor vasculature and its role in tumor cell attachment to pulmonary endothelium," *BMC Medicine*, vol. 6, no. 1, p. 20, 2008.

[20] Y. D. Chen, X. X. Chen, L. N. Shen et al., "Expression of A-kinase anchor protein 95, cyclin E2, and connexin 43 in lung cancer tissue, clinical significance of their expression, and their expression correlation," *Zhonghua Lao Dong Wei Sheng Zhi Ye Bing Za Zhi*, vol. 30, no. 10, pp. 725–729, 2012.

[21] A. W. Tate, T. Lung, A. Radhakrishnan, S. D. Lim, X. Lin, and M. Edlund, "Changes in gap junctional connexin isoforms during prostate cancer progression," *Prostate*, vol. 66, no. 1, pp. 19–31, 2006.

[22] D. I. Dovzhanskiy, W. Hartwig, N. G. Lázár et al., "Growth inhibition of pancreatic cancer by experimental treatment with 4-phenylbutyrate is associated with increased expression of connexin 43," *Oncology Research*, vol. 20, no. 2, pp. 103–111, 2012.

[23] A. L. Asirvatham, S. G. Galligan, R. V. Schillace et al., "A-kinase anchoring proteins interact with phosphodiesterases in T lymphocyte cell lines," *Journal of Immunology*, vol. 173, no. 8, pp. 4806–4814, 2004.

[24] G. McConnachie, L. K. Langeberg, and J. D. Scott, "AKAP signaling complexes: getting to the heart of the matter," *Trends in Molecular Medicine*, vol. 12, no. 7, pp. 317–323, 2006.

Hindawi
Analytical Cellular Pathology
Volume 2018, Article ID 9432375, 12 pages
https://doi.org/10.1155/2018/9432375

Research Article

Comparison of Syndecan-1 Immunohistochemical Expression in Lobular and Ductal Breast Carcinoma with Nodal Metastases

Ivana Miše[1] **and Majda Vučić**[2]

[1]*Department for Clinical Cytology, University Hospital "Sestre Milosrdnice", Zagreb, Croatia*
[2]*Department of Pathology, University Hospital "Sestre Milosrdnice", Zagreb, Croatia*

Correspondence should be addressed to Ivana Miše; ivana.mise@gmail.com

Received 8 March 2018; Accepted 3 June 2018; Published 29 July 2018

Academic Editor: Jennifer E. Koblinski

Syndecan-1 (Sdc1) is a transmembrane heparan sulfate proteoglycan, an extracellular matrix receptor involved in intercellular communication, proliferation, angiogenesis, and metastasis. This study determined and compared Sdc1 expression in the tumor cells and stroma of 30 invasive lobular and 30 invasive ductal breast carcinomas (ILCs/IDCs), also in the axillary node metastases of ductal type, and correlated it with clinical and tumor parameters. Sdc1 was expressed in the epithelium of 90% carcinoma of both histological types. Also, it was most frequently expressed in their tumor stroma, but in ILC, stromal expression was negative in 40%. Sdc1 was expressed in 86.7% of the metastatic epithelium of IDC nodal metastases (in even 50% as high expression), while the nodal stroma was negative in 46.7%. Primary IDC showed a negative correlation between epithelial Sdc1 and progesterone receptors (PRs), whereas ILC showed a positive correlation between stromal Sdc1 and histological gradus. In the metastatic epithelium, Sdc1 was negatively correlated with a patient's age, estrogen receptors (ERs), and PRs in the primary tumors, while the stroma of metastases demonstrated a positive correlation with the focus number in primary tumors and a negative correlation with PRs in primary tumors. This research revealed identical overall epithelial Sdc1 expression in both breast carcinomas with no statistically significant difference in its stromal expression and confirmed the role of Sdc1 in the progression of both tumor types and in the development of ductal carcinoma's metastatic potential.

1. Introduction

Breast cancer is the most common and biologically very complex malignant tumor in women. Its incidence has been increasing lately, particularly in very young women, with often more aggressive clinical course and poor prognosis. There are numerous and intensive studies and discoveries of new molecular and genetic markers that could affect its development, growth, and potential treatment. One of them is the syndecan-1 (Sdc1), a transmembrane heparan sulfate proteoglycan (HSPG), the receptor for the extracellular matrix (ECM) and the organizer of the cell matrix adhesion which participates in tissue repair, metabolism, carcinogenesis, and development of the immune response; also, it integrates a variety of cellular signals and growth factor signals and modulates cell proliferation, migration, and angiogenesis [1–3]. As a coreceptor, Sdc1 binds, with heparan sulfate chains, to various growth factors and angiogenesis promoters by stimulating cell proliferation, and as an adhesion molecule, it enters into an interaction with ligands of ECM and cell surface. Sdc1 is the modulator of proteolytic activation and *in vivo* function of chemokines, which orchestrate leukocyte recruitment and tissue remodeling in inflammation and reparation [4]. It is predominantly expressed on/in epithelial cells, but it is also found in mesenchymal cells during their development and in the different stages of activation and differentiation of normal lymphoid cells—in centrocytes (but not in centroblasts), the mature plasma cells and the atypical plasma cells in the multiple myeloma, where it has been often investigated [5]. There are also indications that Sdc1 mediates the adhesion of the mesenchymal cells; after the mesenchymal cells disaggregate *in vitro*, it is intensely expressed in the reaggregated cells [6]. As a transmembrane protein involved in a number of the vital cellular processes,

it is an essential participant in the growth and development of the healthy and neoplastic tissues, contributing to the invasive potential of the malignant cells and metastatic spread [1–8]. By interacting with heparin-binding growth factors, it accumulates in the tumor stroma supporting the proliferation and migration of malignant cells, neoangiogenesis, and multiplication of the stroma of invasive tumors [9–13].

The significance of the expression of Sdc1 and its distribution and localization and association with established prognostic factors and prognostic value have been tested so far in pancreatic cancer [14, 15], stomach cancer [16–18], colon cancer [19, 20], liver cancer [21], prostate cancer [22–24], lung cancer [25–28], endometrial cancer [29, 30], ovarian cancer [31], squamous head and neck cancer [32–36], melanoma [37], laryngeal cancer [38], cervical cancer [39], urothelial carcinoma of the bladder [40], multiple myeloma [5, 41–43], and breast cancer [44–46] where its overexpression generally means a poor prognosis, although various studies have shown conflicting results.

The topics that associate the Sdc1 expression in the primary breast tumors and metastases with established prognostic and predictive factors are extremely rare, as well as the significance of the possible associations for the oncology practice. The aim of our study was to determine and compare the immunohistochemical (IHC) expression of Sdc1 in the malignant epithelial cells and tumor stroma of the two, by far, most common histological types of breast cancer, invasive lobular carcinoma (ILC) and invasive ductal carcinoma (IDC), and in the axillary lymph node metastases of ductal type. The goal was also to establish the correlation of the Sdc1 expression with clinical and tumor parameters and the expression of the estrogen/progesterone receptors (ERs/PRs) and HER2/neu oncoprotein in both types of primary tumors and to determine the possibility of defining and isolating the group of tumors with more aggressive biological behavior prone to metastasis.

2. Materials and Methods

2.1. Materials. We retrospectively analyzed 30 IDC with the axillary lymph node metastasis and 30 ILC archived in the paraffin blocks in the Department of Pathology "Ljudevit Jurak" at the University Hospital Centre "Sestre Milosrdnice" in Zagreb, Croatia, in the period from January 1, 2005, to December 31, 2010. The Sdc1 expression in the lobular cancer metastasis was not taken into consideration because of their lower frequency and lower metastatic potential and therefore an insufficient number of metastatic ILC in the observed period, which we consider to be the limitation of the study. The main clinical and epidemiological data of patients were obtained from the "Thanatos" computer database of the aforementioned Department of Pathology. In order to protect personal information, each tissue sample included in the study was assigned a unique number. The material for analysis was obtained by surgery based on preoperative cytological diagnosis or, rarely, by biopsy of breast tissue. Histopathological diagnosis was made on tumor tissue sections stained by the routine hemalaun-eosin (HE) method. Specimen processing began with prompt standard fixation of tumor tissue in 10 percent buffered formalin, continued by embedding it into paraffin blocks and cutting it in 3–5 μm thick sections, and ended with the HE staining method. All preparations, both histological and IHC, were analyzed by a light microscope Olympus BX41 (Tokyo, Japan). Diagnostic criteria for ductal and lobular carcinomas were based on the mode of growth and the typical architecture of both tumors and on the malignant cell morphology [47]. Considerably simplified tumor-node-metastasis (TNM) classification was used for determining the tumor (T) status and axillary lymph node (N) status [48]. No women at the time of diagnosis had proved distant metastases, and Mx was valid for all.

2.2. Immunohistochemical Detection of ERs, PRs, and HER/2neu. All samples were IHC stained to determine the presence of the nuclear ERs and PRs and HER2/neu transmembrane oncoprotein and Sdc1 by using the indirect IHC avidin-biotin complex (ABC) method or the labeled streptavidin-biotin (LSAB) method. The 1D5 monoclonal antibody against the estrogen receptors M7047 (diluted at 1 : 100, Dako, Glostrup, Denmark) and the NCL monoclonal antibody against the progesterone receptors M3569 (diluted at 1 : 100, Novocastra, Newcastle, England) were used in the IHC determination of the ERs and PRs. The results of the immunological reactions were read semiquantitatively in the area showing the strongest staining intensity, the so-called "hot spot." According to the strength of the IHC reactions or the intensity of nucleus staining, the results were graded as negative (0) (up to 5% of positive tumor cells), weakly positive (1+) (5–10% of positive tumor cells), moderately positive (2+) (10–50% of positive tumor cells), and strongly positive (3+) (over 50% of positive tumor cells).

In IHC determination of HER2/neu, the polyclonal antibody DA485 was used against HER2/neu oncoprotein K5206 (Dako, Glostrup, Denmark). The indirect streptavidin-biotin method was used to visualize the reaction (ChemMate Detection Kit and Peroxidase/DAB in the TechMate device, Dako, Glostrup, Denmark). The staining results were evaluated only in the invasive tumor component, and only the membrane staining was considered positive. The distribution of membrane positivity and the percentage of immunoreactive cells were assessed in the most positive part of the tumor. As in the most laboratories, we used the following evaluation system [49]: 0—no membrane staining or it is present in less than 10% of tumor cells, 1—weak/barely visible membrane staining in more than 10% of tumor cells (partial membrane staining), 2—low/moderate, complete membrane staining in more than 10% of tumor cells, and 3—strong, complete membrane staining in more than 10% of tumor cells.

2.3. Immunohistochemical Expression of Sdc1 and "Scoring" System. Sdc1, one of the cluster of differentiation (CD) antigens, categorized as CD138, is mainly expressed on the surface of adherent cells; for example, in adult mice, it is located on the basal and lateral surfaces of the simple epithelia and over the entire surface of the stratified epithelia [50]. During differentiation, stratification, and keratinocyte maturation, when the intercellular adhesion is normally enhanced,

the amount of the Sdc1 on the cell surface increases compared to that on the unstratified cells [51, 52], suggesting its direct involvement in the process of the cell adhesion of the contact surfaces. Sdc1 in breast tissue shows the characteristic localization with the IHC intense staining of the basal and lateral surfaces of the normal epithelial cells of most ducts, rarely lobule, while the healthy stromal tissue is not stained [46, 52]. The myoepithelial cells are intensely stained with Sdc1, whereas the luminal cells show heterogeneous reactivity [45]. In the breast cancers, Sdc1 is expressed on the malignant epithelial cells, in the stromal tumor component, and at both locations [46], as also confirmed by our study. The immunoreactivity of tumor cells to the Sdc1 in the invasive carcinomas is different and heterogeneous—it differs from strong diffuse positivity of the tumor epithelium to the focal reactivity of some groups of cells or single cells or to a complete lack of staining (negative reaction). The tumor cells often show the membrane positivity, but sometimes the cytoplasmic one is indicated too. The tumor stroma also shows the heterogeneous Sdc1 expression, so it can be strong, moderate, weak, or absent, and the stromal cells and the collagen fibers can show it too [45, 46]. The dense desmoplastic stroma usually shows strong immunoreactivity, while weaker stromal reaction with stronger lymphoplasmocytic infiltration shows weaker Sdc1 staining [46].

A monoclonal antibody FLEX MO A HU CD138 (diluted at 1 : 50, Dako, Glostrup, Denmark) was used in the study. The indirect ABC technique (LSAB plus kit/HRP, Dako, Glostrup, Denmark) was used for detecting expression. The whole sections of the tumor tissue were examined by two independent examiners (Ivana Miše and Majda Vučić) at the magnification of ×40 and ×100, and then most of the preparation or at least 2000 cells at the magnification of ×400. The proportion of the stained cells and their staining intensity were assessed. Tumors with more than 5% of cells expressing Sdc1 were considered to demonstrate overexpression of Sdc1. The results were expressed by semiquantitative evaluation of the reaction intensity from 0–3 in the area of the greatest intensity of IHC reaction, the strongest staining intensity of the tumor cells ("hot spot"), at an average of five consecutive visual fields at the magnification of ×400 with cca 200 tumor cells [16, 22, 23, 46]. They were graded according to the following: 0 or Sdc1 negative—staining in less than 5% of tumor cells, 1 or weak Sdc1 expression—staining in 5–25% of tumor cells, 2 or moderate Sdc1 expression—staining in 25–50% of tumor cells, and 3 or strong Sdc1 expression—staining in >50% of tumor cells (Figures 1–3). The Sdc1 expression in the stroma of both types of primary tumors, as well as in the tumor epithelium and stroma of the ductal carcinoma metastases in the axillary lymph nodes, was evaluated in the same way (Figures 4–8).

The absence of staining of the normal ductal epithelium or removal of the primary antibody constituted an internal negative control in the preparations of both primary tumors, while the staining of the normal ductal epithelium and/or sometimes the presence of the stratified squamous epithelium of the skin or nipple represented an internal positive control. The normal lymphatic tissue of a lymph node is not stained with Sdc1. The lymphatic tissue of the tonsil

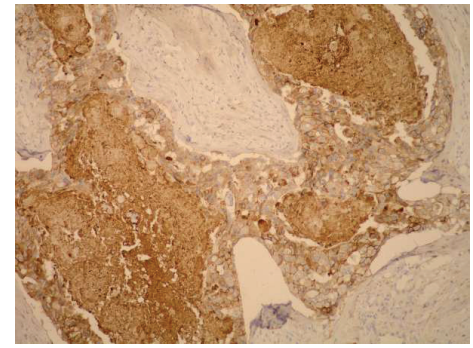

Figure 1: Strong epithelial (both membranous and cytoplasmic) Sdc1 expression and the absence of the stromal Sdc1 expression, with the accumulation of Sdc1 in the intraluminal necrotic tumor mass, IDC (IHC, ×100).

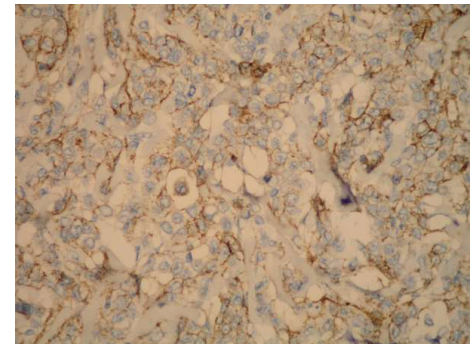

Figure 2: Moderate epithelial Sdc1 expression in the ILC (IHC, ×200).

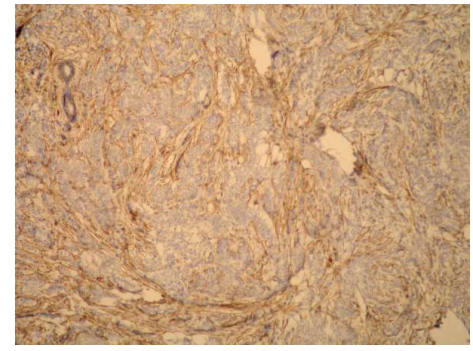

Figure 3: Weak epithelial and strong stromal Sdc1 expression in the ILC (IHC, ×100).

constituted the external negative control of the IHC reaction in the axillary lymph nodes, while the positive control was represented by the multilayer squamous epithelium that lines the surface of the tonsil, as well as the plasma cells, located mainly in the medullary cords of the lymph nodes.

2.4. Statistical Methods. The results obtained in the study are presented in tables and figures. The chi-square test was used to analyze the differences between categorical variables in relation to the cancer types. The Spearman correlation coefficients between Sdc1 expression in the epithelium and the stroma in both primary and metastatic ductal carcinomas

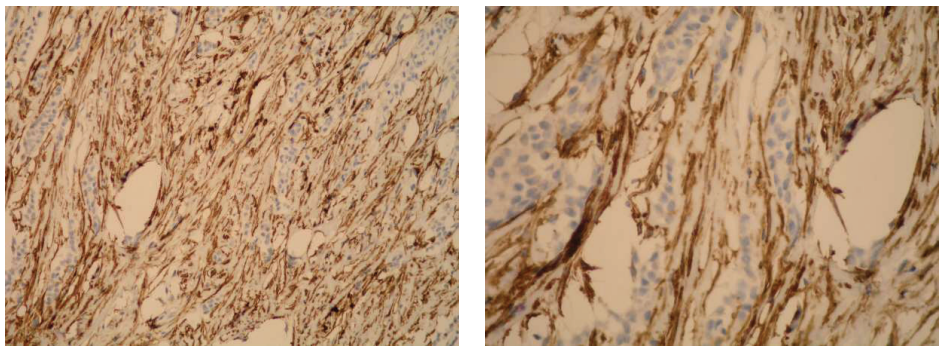

(a) (b)

Figure 4: Strong stromal Sdc1 expression in the ILC (the same slide, IHC; ×200 for (a) and ×400 for (b)).

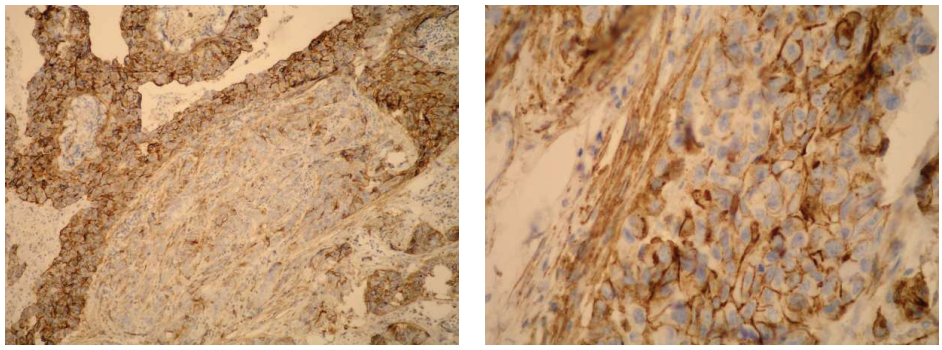

(a) (b)

Figure 5: (a) Strong Sdc1 expression in the metastatic epithelium of the ductal carcinoma in the axillary lymph node (IHC, ×100). (b) Strong epithelial (membranous) and stromal Sdc1 expression in the metastasis of the ductal carcinoma in the axillary lymph node (IHC, ×400).

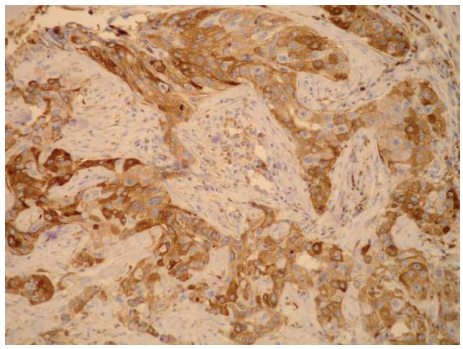

Figure 6: Strong epithelial (both membranous and cytoplasmic) Sdc1 expression in the IDC metastasis in the axillary lymph node (IHC, ×200).

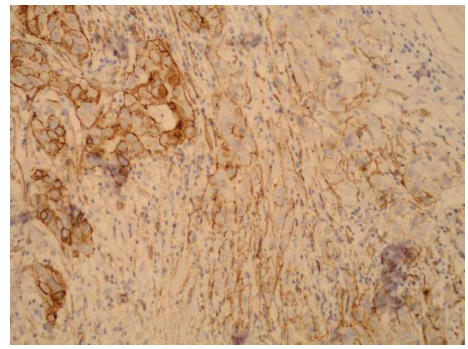

Figure 7: Change of the Sdc1 expression—from the strong epithelial Sdc1 expression to the moderate stromal Sdc1 expression, on the edge of the ductal carcinoma metastasis in the axillary node (subcapsular) (IHC, ×200).

with different clinical and histological parameters were calculated. All P values below 0.05 were considered significant. The computer software IBM SPSS Statistics 19.0.0.1 was used to perform the analysis (http://www.ibm.com/analytics/spss-statistics-software, Chicago, IL).

3. Results

The clinical and tumor parameters of the primary IDC and ILC included in our research are shown in Table 1.

The statistically significant differences were found between some of the examined parameters of IDC and ILC. They were found in the tumor size (the ductal carcinomas were significantly higher ($P = 0.002$)), in the total number of the isolated lymph nodes (the lobular carcinomas had a significantly greater number of the removed lymph nodes ($P = 0.006$)), in the number of the positive lymph nodes (the ductal carcinomas had a significantly greater number of the positive lymph nodes ($P = 0.035$)), and in

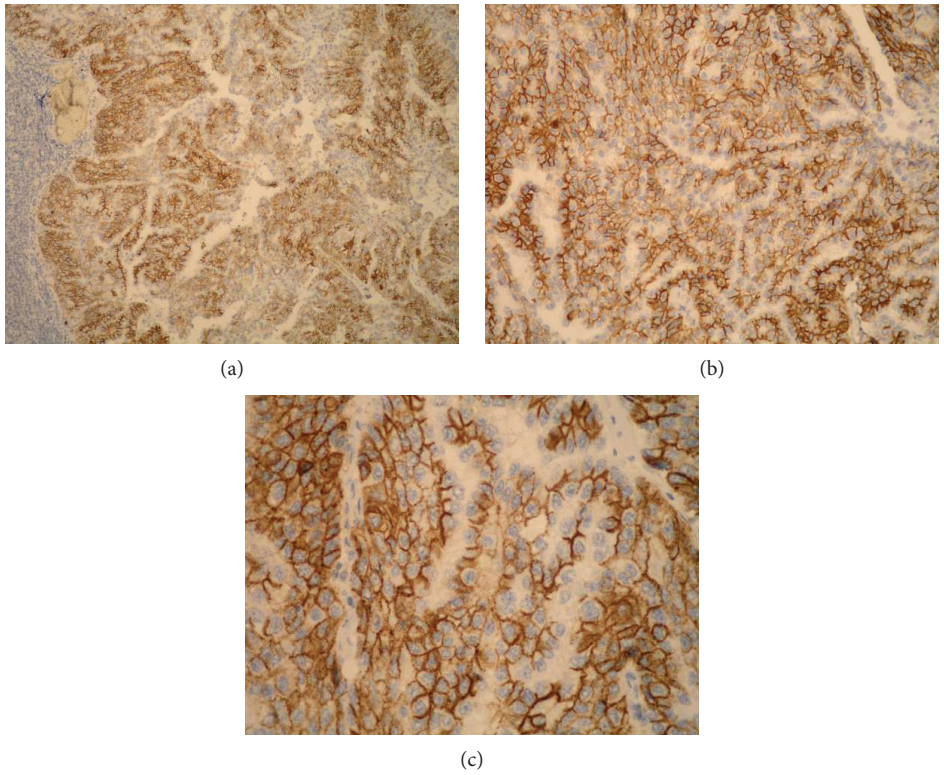

(a) (b) (c)

Figure 8: Strong Sdc1 expression in the tumor epithelium of the ductal carcinoma metastasis in the axillary lymph node (the micropapillar histological subtype) (the same slide, IHC; ×100 for (a), ×200 for (b), and ×400 for (c)).

Table 1: Differences in the investigated quantitative values between the invasive ductal and lobular breast carcinomas: the statistical analysis was done with the Mann–Whitney *U* test.

	Histological types	*N*	Arithmetic mean	Standard deviation	Min	Max	Percentiles			*P* value
							25	Median	75	
Age (years)	Ductal carcinoma	30	65.13	14.98	37	87	55.00	**67.00**	77.75	0.096
	Lobular carcinoma	30	59.63	11.99	36	77	50.75	**63.50**	69.50	
Tumor size (cm)	Ductal carcinoma	30	3.89	1.59	1.20	8.50	2.50	**3.65**	5.05	**0.002**
	Lobular carcinoma	30	2.77	1.90	0.70	8.00	1.50	**2.00**	3.28	
Total number of lymph nodes	Ductal carcinoma	30	10.80	4.48	4	21	6.75	**11.00**	14.00	**0.006**
	Lobular carcinoma	29*	14.45	4.59	8	26	10.50	**13.00**	17.00	
Number of positive lymph nodes	Ductal carcinoma	30	5.27	3.48	1	13	2.00	**4.00**	8.00	**0.035**
	Lobular carcinoma	29*	4.90	7.26	0	25	0.00	**2.00**	6.00	
Percentage of positive lymph nodes (%)	Ductal carcinoma	30	50.92	28.66	5.26	100.00	26.70	**46.43**	77.00	**0.007**
	Lobular carcinoma	29*	30.58	36.72	0.00	100.00	0.00	**11.76**	53.57	

*For one invasive lobular carcinoma, the number of the total isolated and positive lymph nodes was not known (Nx).

the proportion of the positive lymph nodes in relation to the total number of the removed lymph nodes (the ductal carcinomas had a significantly greater number of the positive lymph nodes ($P = 0.007$)) (Table 1).

According to our results, the strong (3+) Sdc1 expression was significantly higher in the tumor epithelium of the primary IDC than in that of the ILC ($P = 0.027$), while there were no significant differences in the stromal expression of Sdc1 between the two types of cancer ($P = 0.305$) (Table 2).

A significant difference in the absence of the Sdc1 expression (null expression) between the tumor epithelium and the stroma of the ductal carcinoma metastases was found (13.3% versus 46.7%, $P = 0.005$) (Table 3). The Yates correction for a small sample also showed a significant difference between them ($P = 0.011$), which means that the stroma of the ductal carcinoma metastases in the axillary lymph nodes more frequently demonstrates the absence of the Sdc1 expression compared to the tumor epithelium of metastases.

Table 2: The distribution of the intensity of the Sdc1 expression by the levels in the tumor epithelium and the stroma of primary IDC and ILC.

		Histological types				Chi-square value	P
		Ductal carcinoma		Lobular carcinoma			
		N	%	N	%		
Syndecan-1 expression in the tumor epithelium	0	3	10.0	3	10.0	9.17	**0.027**
	1	4	13.3	2	6.7		
	2	6	20.0	17	56.7		
	3	17	56.7	8	26.7		
Syndecan-1 expression in the tumor stroma	0	8	26.7	12	40.0	3.62	0.305
	1	8	26.7	5	16.7		
	2	7	23.3	3	10.0		
	3	7	23.3	10	33.3		

Table 3: The distribution of the intensity of the Sdc1 expression by levels in the tumor epithelium and the stroma of the metastases of the ductal breast cancer in the axillary nodes.

Metastases of ductal carcinoma		Intensity of syndecan-1 expression				Total
		0	1	2	3	
Tumor epithelium of metastases	N	4	2	9	15	30
	%	13.3	6.7	30.0	50.0	100.0
Stroma of metastases	N	14	5	5	6	30
	%	46.7	16.7	16.7	20.0	100.0

The negative correlation between the Sdc1 expression in the tumor epithelium and the PR expression was significant in the ductal carcinomas ($P = 0.014$), as the positive correlation between the Sdc1 expression in the tumor stroma and the histological grade was in the lobular carcinomas ($P = 0.014$) (Table 4). In the total sample of both primary cancers, the positive correlation between the Sdc1 expression in the tumor epithelium with grade ($P = 0.080$) and the expression of the ERs ($P = 0.068$), as well as the positive correlation between the Sdc1 expression in the tumor stroma and the tumor size $P = 0.063$, was marginally significant (Table 4).

The negative correlations between the Sdc1 expression in the malignant epithelium of the metastases with the age of the patients and the ER/PR expression were significant in the ductal carcinoma metastases ($P = 0.043$, $P = 0.038$, and $P = 0.010$) (Table 5). The positive correlation between the Sdc1 expression in the stroma of the metastases and the number of the primary tumor foci ($P = 0.022$) was significant, as well as the negative correlation with the PR expression ($P = 0.032$) in the primary tumors (Table 5).

4. Discussion

This study showed that the Sdc1 was expressed in the tumor epithelium in the vast majority or 90% of the primary IDC, and most frequently, it was a strong expression (56.7%). The tumor epithelium of the primary ILC showed the identical overall Sdc1 expression, in 90% of them, but the intensity distribution was slightly different, and it most frequently showed a moderate expression in 56.7% and a strong expression in 26.7% (Table 2). The Chi-square distribution test showed a significantly stronger Sdc1 expression in the primary ductal carcinomas than in the lobular ones (Pearson χ^2 test = 9.17, df = 3, $P = 0.027$). The equal overall epithelial Sdc1 expression in the primary IDC and ILC can be explained by the same origin of both histological types—the epithelium of the terminal ductal lobular unit (TDLU), from which most breast cancers originate [47, 53]. The reason why the molecular profile of the two different histological types of cancer, in spite of the same origin, shows an identical epithelial Sdc1 expression, but, for example, completely opposite E-cadherin expression [47], remains unclear and requires further studies. High levels of Sdc1 are associated with the maintenance of the epithelial cell morphology and the inhibition of invasiveness due to the increased cell adhesion to the matrix components via Sdc1 [54]. The control of the cell adhesion is partly mediated by the Sdc1, and understanding the underlying molecular mechanism, besides the physiological phenomena of growth and development, is necessary in the pathological processes such as tumor cell invasion, angiogenesis, and metastasis [55–57]. By interacting with heparin-binding growth factors, the Sdc1 accumulates in the malignant breast stroma, where its amount can be more than 10 times greater than that in the adjacent normal tissue, with a marked redistribution from the epithelium to the stroma [58], thus contributing to the angiogenesis and proliferation of the stroma of the invasive tumors [59]. In this research, the stroma of the primary IDC demonstrated the overall Sdc1 expression in most tumors (73.3%), with almost equal distribution in all levels (Table 2). The stroma of the ILC included the Sdc1 less frequently, in 60% of tumors. A possible reason for this may be a gentler stromal reaction in the lobular tumors, more pronounced in the elastosis, unlike desmoplasia in the IDC. It is partially weaker due to the typical single-file or "Indian file" arrangement of the tumor cells (in the most common classical histological subtype of the ILC) [47], which makes the contact

Table 4: The correlation between the Sdc1 expression in the tumor epithelium and the stroma of the total sample of both types of the primary tumors and separately of the invasive ductal and the lobular carcinomas, with various clinical and histological parameters analyzed using Spearman's correlation coefficient.

Spearman correlation		Syndecan-1 expression in the tumor epithelium			Syndecan-1 expression in the tumor stroma		
		Total sample ($N = 60$)	Ductal carcinoma ($N = 30$)	Lobular carcinoma ($N = 30$)	Total sample ($N = 60$	Ductal carcinoma ($N = 30$)	Lobular carcinoma ($N = 30$)
Age (years)	Coefficient rho	−0.159	−0.179	−0.288	−0.1	0.096	−0.346
	P	0.225	0.345	0.123	0.447	0.612	0.061
Tumor size (cm)	Coefficient rho	0.141	0.129	−0.021	0.242	0.114	0.28
	P	0.283	0.498	0.912	0.063	0.548	0.134
Focus numbers (1–3)	Coefficient rho	0.103	−0.007	0.295	−0.099	−0.139	−0.06
	P	0.435	0.97	0.113	0.451	0.463	0.752
Histological grade	Coefficient rho	0.228	0.185	0.078	0.187	0.000	0.442
	P	0.08	0.329	0.683	0.153	0.999	**0.014**
T status	Coefficient rho	0.023	−0.253	0.025	0.203	0.145	0.254
	P	0.863	0.177	0.895	0.119	0.443	0.175
N status	Coefficient rho	0.176	0.136	0.115	0.122	0.062	0.169
	P	0.182	0.475	0.553	0.357	0.744	0.38
Percentage of positive lymph nodes	Coefficient rho	0.213	0.254	0.071	0.002	−0.153	0.11
	P	0.105	0.175	0.713	0.989	0.421	0.57
ER	Coefficient rho	−0.237	−0.205	−0.268	−0.034	−0.099	0.021
	P	0.068	0.277	0.152	0.799	0.604	0.911
PR	Coefficient rho	−0.156	−0.442	0.187	0.022	−0.007	0.034
	P	0.235	**0.014**	0.323	0.868	0.971	0.86
HER2/neu	Coefficient rho	−0.054	−0.09	−0.052	−0.028	−0.101	0.072
	P	0.683	0.637	0.787	0.831	0.597	0.705

surface with the surrounding stroma larger. Loussouarn et al. describe a strong immunoreactivity to the Sdc1 of the dense desmoplastic stroma than that of the soft connective stroma [46]. In addition, the change in the Sdc1 expression from the malignant epithelial to the reactive stromal cells [60, 61], with the loss of the E-cadherin, is a critical molecular event in the amazing process of the epithelial-mesenchymal transition (EMT), in which malignant cells lose their epithelial properties and obtain the mesenchymal-like properties in the invasion process [62, 63]. Furthermore, the E-cadherin gene, responsible for the cohesion of the epithelial cells and the suppression of the malignant cell invasion, is absent in 80–100% of the ILC, and its inactivation is an early event in the oncogenesis of the lobular lesions [47]. All the above suggests a stronger connection between the Sdc1 and the E-cadherin in the lobular carcinomas than in the ductal ones. We can assume that the somewhat weaker stromal Sdc1 expression in the lobular tumors is probably associated with a greater E-cadherin loss; that is, the tumor cells of the lobular cancers lose more Sdc1 during the EMT than the ductal carcinoma cells undergoing the EMT. It is supported by the fact that the epithelium of both primary carcinomas expresses the Sdc1 in exactly the same way, in 90% of cases (Table 2). However, either it unevenly loses the Sdc1 during the EMT (which is probably associated with a loss of the E-cadherin as described above) or for some reason, the induction of the Sdc1 is weaker in the stroma of the lobular cancers. Namely, the Sdc1, besides being a transmembrane protein and the native cell membrane HSPG, released from the membrane into the adjacent

Table 5: The correlation between the Sdc1 expression in the tumor epithelium and the stroma of the metastases of the ductal breast carcinoma and some clinical and histological features of the primary tumors, analyzed using Spearman's correlation coefficient.

Spearman correlation		Syndecan-1 expression in the epithelium of metastases ($N = 30$)	Syndecan-1 expression in the stroma of metastases ($N = 30$)
Age (years)	Coefficient rho	−0.373	0.014
	P	**0.043**	0.940
Tumor size (cm)	Coefficient rho	−0.223	0.061
	P	0.237	0.750
Focus numbers (1–3)	Coefficient rho	0.07	0.417
	P	0.714	**0.022**
Histological grade	Coefficient rho	0.138	0.164
	P	0.466	0.385
T status	Coefficient rho	−0.299	0.229
	P	0.109	0.223
N status	Coefficient rho	0.11	0.179
	P	0.562	0.343
Percentage of positive lymph nodes	Coefficient rho	0.08	0.267
	P	0.676	0.153
ER	Coefficient rho	−0.381	−0.302
	P	**0.038**	0.105
PR	Coefficient rho	−0.461	−0.393
	P	**0.01**	**0.032**
HER2/neu	Coefficient rho	0.138	0.287
	P	0.468	0.124

matrix when excessively expressed [64–66], is partly synthesized in the stroma itself, that is, in the stromal fibroblasts [67–70]. This raises the hypothesis of its possible lower synthesis in the stromal fibroblasts of the ILC, which would be very valuable to investigate. Such a concept is supported by our result of distribution of the Sdc1 expression in the primary ILC (by level), according to which the stroma of the ILC often, in as many as 40%, did not show even a weak expression of the Sdc1 (Table 2). Stanley et al. described a significantly lower epithelial Sdc1 expression in the IDC than in the healthy breast tissue and the epithelial-stromal tumors, with the emphasizing difference in the expression between the stromas of malignant and nonmalignant tissue; the Sdc1 was highly expressed in the stroma and the epithelial-stromal border of the IDC and absent in the stroma of normal tissue and the epithelial-stromal tumors [59]. Such redistribution of the Sdc1 in the direction of the epithelium to the stroma in the malignant epithelial tumors [58] is related to the loss of the Sdc1 expression on/in the malignant epithelial cells [59–61], and it precisely means the EMT—when cancer cells lose their Sdc1 by transition from the epithelial to the weaker differentiated mesenchymal phenotype [62, 63]. The changed or altered Sdc1 expression from the malignant epithelial to the reactive stromal cells is crucial for the transformation of a ductal breast carcinoma to the metastatic disease, but it is also found during progression of other malignant tumors.

In our study, the tumor epithelium of the metastatic IDC in the axillary lymph nodes showed the Sdc1 expression in even 86.7% of metastases, almost the same as the malignant epithelia of the primary IDC; the Sdc1 expression was mostly strong (50%) or moderate (30%), while 13.3% of the metastatic tumor epithelium did not show even a weak expression (Table 3). Thanakit et al. also found a high expression of the Sdc1 in the affected axillary nodes at the primary IDC, with a significant expression increase during the tumor progression from the lymph node to the extracapsular adipose tissue [71], while the E-cadherin expression showed no significant difference between the metastatic nodes and the extracapsular tumor invasion. According to our results, a high Sdc1 expression in the tumor epithelium of the metastasis, almost equal to that of a primary tumor, suggests direct involvement of the Sdc1 in progression, not only of primary ductal carcinomas but also of metastatic carcinomas. It is very important to emphasize that this strong Sdc1 expression in the tumor epithelium of lymph nodes might be a possible prerequisite for the further progression and metastasis of a ductal carcinoma, in the loco-regional and remote areas. However, Wang et al. found a significantly reduced Sdc1 expression in the metastatic breast cancer cell lines compared to the nonmetastatic breast cancer cell lines under *in vitro* conditions [72]. Our study determined that the stroma of the metastatic IDC showed an overall Sdc1 expression in 53.4% of the lymph nodes (i.e., it was absent in almost half of them or 46.7% (Table 3)), which is lower (but not

statistically significant) than the expression in the stroma of the primary ductal carcinomas (73.3%). The probable reason for this is the smaller amount of stromas in a lymph node and therefore its lower reactivity to the metastatic epithelium compared to the primary tumors (a lymph node shows a discrete stroma in the physiological state too), and also a different microenvironment for the metastatic epithelium in the new "host"—the lymph node, which determines different epithelial-stromal interactions.

The HER2/neu is overexpressed in 25–30% of the invasive breast cancers and even in 50% of the breast ductal carcinoma in situ (DCIS) [49]. Götte et al. demonstrated a strong Sdc1 expression in 72% of the DCIS, with a correlation between the levels of Sdc1 and HER2/neu expression [73]. Kim et al. showed a significant association between the epithelial Sdc1 and EGFR expression in the colorectal carcinomas [74]. It seems that some syndecans (Sdc1 and Sdc4) play a key role in the activation of the $\alpha 6\beta 4$ integrin by receptor tyrosine kinases (HER1 and HER2) [75]. Besides, the action of a trastuzumab, an antibody in the therapy of the breast cancer cases positive for human EGFR2 (HER2/neu), depends on the availability of the heparan sulfate on the surface of the breast cancer cell lines [76]. All these indicate an association between the Sdc1 and HER2/neu, that is, their signaling pathways. Nevertheless, our total sample of the primary tumors did not demonstrate it, most likely because the half of them were the lobular carcinomas in which the HER2/neu is rarely expressed [47, 77–79], nor the IDC, probably because of the weaker HER2/neu expression in the invasive carcinomas than in in situ carcinomas [49]. Since HER2/neu is particularly expressed in the carcinomas in situ, it is probably more involved in the initiation of carcinogenesis than in the growth of the already established tumors, hence showing no correlation with the Sdc1 in our research.

In this study, the lobular carcinomas demonstrated a positive correlation between the stromal Sdc1 expression and histological grade ($P = 0.014$) (Table 4). Loussouarn et al. associated a strong epithelial Sdc1 expression with a low-grade and well-differentiated breast carcinomas and a reduction of expression with poorly differentiated ones [46]. Leivonen et al. discovered an epithelial Sdc1 expression in 61% of the IDC [44], which is lower than our result, and a stromal expression in 67%, which is very similar to our result. Barbareschi et al. identified the increased Sdc1 expression in 42% of cancers, mostly in large tumors, with a high grade and a high mitotic index, a negative ER/PR status, and an HER2/neu overexpression [45]. According to our results, the primary IDC showed a significant negative correlation between the epithelial Sdc1 expression and the PR expression ($P = 0.014$) (Table 4). The axillary node metastases from the IDC demonstrated a negative relationship between the Sdc1 expressed in the tumor epithelium and the patient age ($P = 0.043$), as well as the ER ($P = 0.038$) and PR expression ($P = 0.010$) in the primary tumors (Table 5). Thus, a higher expression of the Sdc1 in the tumor epithelium of the metastatic IDC is associated with younger patients and a lower expression of both hormone receptors in the primary tumors, which is very significant and can be a basis for further studies. The Sdc1 expression in the stroma of metastases positively correlated with the number of tumor foci ($P = 0.022$) in the primary tumor and negatively correlated with the PR expression ($P = 0.032$) in the primary tumor. Baba et al. related the Sdc1 overexpression (but in the primary tumor) and the negative ERs to the aggressive, highly proliferative type of a breast cancer [80]. Leivonen et al. associated the epithelial Sdc1 expression with the negative ERs and the stromal Sdc1 expression with the positive ERs [44]. As noted, Barbareschi et al. also have linked the Sdc1 expression (in a primary tumor) with the negative ER/PR [45]. All the above indicates the existence of certain relations between the Sdc1 expression and ER/PR status in the primary ductal carcinomas, while the results trying to define this relationship in the metastases were not found in the reviewed literature.

5. Conclusion

The aim of our study was to determine and compare the Sdc1 expression in the malignant epithelial cells and stroma of 30 ILCs and 30 IDCs, as well as in the axillary lymph node metastases of ductal type, and to correlate it with the clinical and tumor parameters. This research has shown the identical overall epithelial Sdc1 expression with no statistically significant difference in its stromal expression between by far the two most common primary breast cancers—ductal and lobular cancers. However, it has shown some differences in the correlation between the Sdc1 expression and the important hormonal ER/PR status as the unavoidable prognostic/predictive factors in the routine diagnostic-therapeutic procedure of each breast carcinoma. The involvement of Sdc1 in the progression of both primary cancers was proved, as well as the involvement of Sdc1 in the development of the metastatic potential of ductal tumors when invading the axillary lymph nodes. Moreover, the frequent and strong Sdc1 expression in the nodal metastasis (found in almost 90% of cases) assumes a very high probability of further disintegration of the malignant cells, and it presents a significant source of the new metastases. A further research on a larger number of patients with different types of breast cancer is needed in order to define the role and behavior of the Sdc1 in different histologic tumor types and to include the results of selected types of the Sdc1 expression (both are positive/negative or one of them is positive) into the comprehensive molecular and gene profile at the level of an individual tumor. Such research will continue the path towards understanding the numerous mutually dependent or autonomous molecular processes in the complex biopathology and carcinogenesis of breast cancer.

Data Availability

The data that support the findings of this study are available from the corresponding author upon reasonable request.

Disclosure

This article is based on own doctoral dissertation (by Ivana Miše), under the same name, which is not yet published

and is written as the final part of the postgraduate research study programme at the Division of Biology, Faculty of Science, University of Zagreb, Croatia, defended on 22 July 2011.

Conflicts of Interest

The authors declared no potential conflict of interests with respect to the research, authorship, and/or publication of this paper.

References

[1] J. R. Couchman and A. Woods, "Syndecans, signaling, and cell adhesion," *Journal of Cellular Biochemistry*, vol. 61, no. 4, pp. 578–584, 1996.

[2] M. Bernfield, M. Götte, P. W. Park et al., "Functions of cell surface heparan sulfate proteoglycans," *Annual Review of Biochemistry*, vol. 68, no. 1, pp. 729–777, 1999.

[3] P. Inki and M. Jalkanen, "The role of syndecan-1 in malignancies," *Annals of Medicine*, vol. 28, no. 1, pp. 63–67, 1996.

[4] M. Götte, "Syndecans in inflammation," *The FASEB Journal*, vol. 17, no. 6, pp. 575–591, 2003.

[5] Y. B. Khotskaya, Y. Dai, J. P. Ritchie et al., "Syndecan-1 is required for robust growth, vascularization, and metastasis of myeloma tumors in vivo," *Journal of Biological Chemistry*, vol. 284, no. 38, pp. 26085–26095, 2009.

[6] S. Vainio, M. Jalkanen, M. Bernfield, and L. Saxén, "Transient expression of syndecan in mesenchymal cell aggregates of the embryonic kidney," *Developmental Biology*, vol. 152, no. 2, pp. 221–232, 1992.

[7] S. Tumova, A. Woods, and J. R. Couchman, "Heparan sulfate proteoglycans on the cell surface: versatile coordinators of cellular functions," *The International Journal of Biochemistry & Cell Biology*, vol. 32, no. 3, pp. 269–288, 2000.

[8] M. Palaiologou, I. Delladetsima, and D. Tiniakos, "CD138 (syndecan-1) expression in health and disease," *Histology and Histopathology*, vol. 29, no. 2, pp. 177–189, 2014.

[9] V. Nikolova, C. Y. Koo, S. A. Ibrahim et al., "Differential roles for membrane-bound and soluble syndecan-1 (CD138) in breast cancer progression," *Carcinogenesis*, vol. 30, no. 3, pp. 397–407, 2009.

[10] N. Yang, R. Mosher, S. Seo, D. Beebe, and A. Friedl, "Syndecan-1 in breast cancer stroma fibroblasts regulates extracellular matrix fiber organization and carcinoma cell motility," *The American Journal of Pathology*, vol. 178, no. 1, pp. 325–335, 2011.

[11] M. R. Akl, P. Nagpal, N. M. Ayoub et al., "Molecular and clinical profiles of syndecan-1 in solid and hematological cancer for prognosis and precision medicine," *Oncotarget*, vol. 6, no. 30, pp. 28693–28715, 2015.

[12] R. Gharbaran, "Advances in the molecular functions of syndecan-1 (SDC1/CD138) in the pathogenesis of malignancies," *Critical Reviews in Oncology/Hematology*, vol. 94, no. 1, pp. 1–17, 2015.

[13] T. Szatmári, R. Ötvös, A. Hjerpe, and K. Dobra, "Syndecan-1 in cancer: implications for cell signaling, differentiation, and prognostication," *Disease Markers*, vol. 2015, Article ID 796052, 13 pages, 2015.

[14] L. Kylänpää, J. Hagström, A. Lepistö et al., "Syndecan-1 and tenascin expression in cystic tumors of the pancreas," *Journal of the Pancreas*, vol. 10, no. 4, pp. 378–382, 2009.

[15] A. Juuti, S. Nordling, J. Lundin, J. Louhimo, and C. Haglund, "Syndecan-1 expression – a novel prognostic marker in pancreatic cancer," *Oncology*, vol. 68, no. 2-3, pp. 97–106, 2005.

[16] J. P. Wiksten, J. Lundin, S. Nordling, A. Kokkola, and C. Haglund, "Comparison of the prognostic value of a panel of tissue tumor markers and established clinicopathological factors in patients with gastric cancer," *Anticancer Research*, vol. 28, no. 4C, pp. 2279–2287, 2008.

[17] X. F. Hu, J. Yao, S. G. Gao, Y. T. Yang, X. Q. Peng, and X. S. Feng, "Midkine and syndecan-1 levels correlate with the progression of malignant gastric cardiac adenocarcinoma," *Molecular Medicine Reports*, vol. 10, no. 3, pp. 1409–1415, 2014.

[18] B. Geramizadeh, O. A. Adeli, M. Rahsaz, M. Mokhtari, and S. Sefidbakht, "Comparison of the expression of cell adhesion molecule markers (E-cadherin and syndecan-1) between young and older age patients with gastric carcinoma," *Journal of Gastrointestinal Cancer*, vol. 41, no. 3, pp. 193–196, 2010.

[19] M. Jary, T. Lecomte, O. Bouché et al., "Prognostic value of baseline seric syndecan-1 in initially unresectable metastatic colorectal cancer patients: a simple biological score," *International Journal of Cancer*, vol. 139, no. 10, pp. 2325–2335, 2016.

[20] H. T. Wei, E. N. Guo, B. G. Dong, and L. S. Chen, "Prognostic and clinical significance of syndecan-1 in colorectal cancer: a meta-analysis," *BMC Gastroenterology*, vol. 15, no. 1, p. 152, 2015.

[21] S. Yu, H. Lv, H. Zhang et al., "Heparanase-1-induced shedding of heparan sulfate from syndecan-1 in hepatocarcinoma cell facilitates lymphatic endothelial cell proliferation via VEGF-C/ERK pathway," *Biochemical and Biophysical Research Communications*, vol. 485, no. 2, pp. 432–439, 2017.

[22] B. Sharpe, D. A. Alghezi, C. Cattermole et al., "A subset of high Gleason grade prostate carcinomas contain a large burden of prostate cancer syndecan-1 positive stromal cells," *The Prostate*, vol. 77, no. 13, pp. 1312–1324, 2017.

[23] T. Szarvas, H. Reis, F. vom Dorp et al., "Soluble syndecan-1 (SDC1) serum level as an independent pre-operative predictor of cancer-specific survival in prostate cancer," *The Prostate*, vol. 76, no. 11, pp. 977–985, 2016.

[24] K. Shimada, M. Nakamura, M. A. De Velasco, M. Tanaka, Y. Ouji, and N. Konishi, "Syndecan-1, a new target molecule involved in progression of androgen-independent prostate cancer," *Cancer Science*, vol. 100, no. 7, pp. 1248–1254, 2009.

[25] A. Anttonen, S. Leppä, T. Ruotsalainen, H. Alfthan, K. Mattson, and H. Joensuu, "Pretreatment serum syndecan-1 levels and outcome in small cell lung cancer patients treated with platinum-based chemotherapy," *Lung Cancer*, vol. 41, no. 2, pp. 171–177, 2003.

[26] A. Anttonen, P. Heikkilä, M. Kajanti, M. Jalkanen, and H. Joensuu, "High syndecan-1 expression is associated with favourable outcome in squamous cell lung carcinoma treated with radical surgery," *Lung Cancer*, vol. 32, no. 3, pp. 297–305, 2001.

[27] T. Pasqualon, J. Pruessmeyer, V. Jankowski et al., "A cytoplasmic C-terminal fragment of syndecan-1 is generated by sequential proteolysis and antagonizes syndecan-1 dependent lung tumor cell migration," *Oncotarget*, vol. 6, no. 31, pp. 31295–31312, 2015.

[28] T. Pasqualon, J. Pruessmeyer, S. Weidenfeld et al., "A transmembrane C-terminal fragment of syndecan-1 is generated by the metalloproteinase ADAM17 and promotes lung epithelial tumor cell migration and lung metastasis formation," *Cellular and Molecular Life Sciences*, vol. 72, no. 19, pp. 3783–3801, 2015.

[29] D. S. Choi, J. H. Kim, H. S. Ryu et al., "Syndecan-1, a key regulator of cell viability in endometrial cancer," *International Journal of Cancer*, vol. 121, no. 4, pp. 741–750, 2007.

[30] H. Kim, D. S. Choi, S. J. Chang et al., "The expression of syndecan-1 is related to the risk of endometrial hyperplasia progressing to endometrial carcinoma," *Journal of Gynecologic Oncology*, vol. 21, no. 1, pp. 50–55, 2010.

[31] Q. Guo, X. Yang, Y. Ma, and L. Ma, "Syndecan-1 serves as a marker for the progression of epithelial ovarian carcinoma," *European Journal of Gynaecological Oncology*, vol. 36, no. 5, pp. 506–513, 2015.

[32] P. Mukunyadzi, K. Liu, E. Y. Hanna, J. Y. Suen, and C. Y. Fan, "Induced expression of syndecan-1 in the stroma of head and neck squamous cell carcinoma," *Modern Pathology*, vol. 16, no. 8, pp. 796–801, 2003.

[33] A. Martínez, M. L. Spencer, U. Brethauer, P. Grez, F. J. Marchesani, and I. G. Rojas, "Reduction of syndecan-1 expression during lip carcinogenesis," *Journal of Oral Pathology & Medicine*, vol. 38, no. 7, pp. 580–583, 2009.

[34] M. S. Shegefti, M. Malekzadeh, Z. Malek-Hosseini, B. Khademi, A. Ghaderi, and M. Doroudchi, "Reduced serum levels of syndecan-1 in patients with tongue squamous cell carcinoma," *The Laryngoscope*, vol. 126, no. 5, pp. E191–E195, 2016.

[35] P. Inki, H. Joensuu, R. Grénman, P. Klemi, and M. Jalkanen, "Association between syndecan-1 expression and clinical outcome in squamous cell carcinoma of the head and neck," *British Journal of Cancer*, vol. 70, no. 2, pp. 319–323, 1994.

[36] S. H. Lee, E. J. Choi, M. S. Kim et al., "Prognostic significance of syndecan-1 expression in squamous cell carcinoma of the tonsil," *International Journal of Clinical Oncology*, vol. 19, no. 2, pp. 247–253, 2014.

[37] C. Wang, T. Tseng, Y. Jhang et al., "Loss of cell invasiveness through PKC-mediated syndecan-1 downregulation in melanoma cells under anchorage independency," *Experimental Dermatology*, vol. 23, no. 11, pp. 843–849, 2014.

[38] A. Anttonen, S. Leppä, P. Heikkilä, R. Grenman, and H. Joensuu, "Effect of treatment of larynx and hypopharynx carcinomas on serum syndecan-1 concentrations," *Journal of Cancer Research and Clinical Oncology*, vol. 132, no. 7, pp. 451–457, 2006.

[39] Y. I. Kim, A. Lee, B. H. Lee, and S. Y. Kim, "Prognostic significance of syndecan-1 expression in cervical cancers," *Journal of Gynecologic Oncology*, vol. 22, no. 3, pp. 161–167, 2011.

[40] K. Shimada, M. Nakamura, M. A. De Velasco et al., "Role of syndecan-1 (CD138) in cell survival of human urothelial carcinoma," *Cancer Science*, vol. 101, no. 1, pp. 155–160, 2010.

[41] M. N. Sanaee, M. Malekzadeh, A. Khezri, A. Ghaderi, and M. Doroudchi, "Soluble CD138/syndecan-1 increases in the sera of patients with moderately differentiated bladder cancer," *Urologia Internationalis*, vol. 94, no. 4, pp. 472–478, 2015.

[42] K. Matsue, Y. Matsue, K. Kumata et al., "Quantification of bone marrow plasma cell infiltration in multiple myeloma: usefulness of bone marrow aspirate clot with CD138 immunohistochemistry," *Hematological Oncology*, vol. 35, no. 3, pp. 323–328, 2017.

[43] N. F. Andersen, I. B. Kristensen, B. S. Preiss, J. H. Christensen, and N. Abildgaard, "Upregulation of syndecan-1 in the bone marrow microenvironment in multiple myeloma is associated with angiogenesis," *European Journal of Haematology*, vol. 95, no. 3, pp. 211–217, 2015.

[44] M. Leivonen, J. Lundin, S. Nordling, K. von Boguslawski, and C. Haglund, "Prognostic value of syndecan-1 expression in breast cancer," *Oncology*, vol. 67, no. 1, pp. 11–18, 2004.

[45] M. Barbareschi, P. Maisonneuve, D. Aldovini et al., "High syndecan-1 expression in breast carcinoma is related to an aggressive phenotype and to poorer prognosis," *Cancer*, vol. 98, no. 3, pp. 474–483, 2003.

[46] D. Loussouarn, L. Campion, C. Sagan et al., "Prognostic impact of syndecan-1 expression in invasive ductal breast carcinomas," *British Journal of Cancer*, vol. 98, no. 12, pp. 1993–1998, 2008.

[47] I. O. Ellis, S. J. Schnitt, X. Sastre-Garau et al., "Invasive breast carcinoma," in *World Health Organization Classification of Tumours: Tumours of the Breast and Female Genital Organs*, F. A. Tavassoli and P. Devilee, Eds., pp. 13–59, IARC Press, Lyon, France, 2003.

[48] S. E. Singletary and J. L. Connolly, "Breast cancer staging: working with the sixth edition of the *AJCC Cancer Staging Manual*," *CA: A Cancer Journal for Clinicians*, vol. 56, no. 1, pp. 37–47, 2006.

[49] J. Jakić-Razumović, J. Unušić, and D. Vrbanec, "Assessment of oncogene HER-2/neu in breast cancer – why, when, how?," in *Breast Diseases: Proceedings of the 12th Scientific Meeting "Breast Diseases" in Organization of Croatian Academy of Sciences and Arts, Department of Medical Sciences, Committee on Tumors*, pp. 51–59, Zagreb, Croatia, October 2002.

[50] K. Hayashi, M. Hayashi, M. Jalkanen, J. H. Firestone, R. L. Trelstad, and M. Bernfield, "Immunocytochemistry of cell surface heparan sulfate proteoglycan in mouse tissues. A light and electron microscopic study," *Journal of Histochemistry & Cytochemistry*, vol. 35, no. 10, pp. 1079–1088, 1987.

[51] R. D. Sanderson, M. T. Hinkes, and M. Bernfield, "Syndecan-1, a cell-surface proteoglycan, changes in size and abundance when keratinocytes stratify," *Journal of Investigative Dermatology*, vol. 99, no. 4, pp. 390–396, 1992.

[52] P. Inki, H. Larjava, K. Haapasalmi, H. M. Miettinen, R. Grenman, and M. Jalkanen, "Expression of syndecan-1 is induced by differentiation and suppressed by malignant transformation of human keratinocytes," *European Journal of Cell Biology*, vol. 63, no. 1, pp. 43–51, 1994.

[53] J. Jakić-Razumović, "Significance of stem cells in occurrence and spreading of breast cancer," in *Breast Diseases: Proceedings of the 17th Scientific Meeting "Breast Diseases" in Organization of Croatian Academy of Sciences and Arts, Department of Medical Sciences, Committee on Tumors*, pp. 17–26, Zagreb, Croatia, September 2007.

[54] T. Y. Eshchenko, V. I. Rykova, A. E. Chernakov, S. V. Sidorov, and E. V. Grigorieva, "Expression of different proteoglycans in human breast tumors," *Biochemistry*, vol. 72, no. 9, pp. 1016–1020, 2007.

[55] D. M. Beauvais and A. C. Rapraeger, "Syndecans in tumor cell adhesion and signaling," *Reproductive Biology and Endocrinology*, vol. 2, no. 1, p. 3, 2004.

[56] D. M. Beauvais, B. J. Ell, A. R. McWhorter, and A. C. Rapraeger, "Syndecan-1 regulates $\alpha_v\beta_3$ and $\alpha_v\beta_5$ integrin activation during angiogenesis and is blocked by synstatin, a novel

peptide inhibitor," *Journal of Experimental Medicine*, vol. 206, no. 3, pp. 691–705, 2009.

[57] C. C. Lopes, C. P. Dietrich, and H. B. Nader, "Specific structural features of syndecans and heparan sulfate chains are needed for cell signaling," *Brazilian Journal of Medical and Biological Research*, vol. 39, no. 2, pp. 157–167, 2006.

[58] L. Lofgren, L. Sahlin, S. Jiang et al., "Expression of syndecan-1 in paired samples of normal and malignant breast tissue from postmenopausal women," *Anticancer Research*, vol. 27, no. 5A, pp. 3045–3050, 2007.

[59] M. J. Stanley, M. W. Stanley, R. D. Sanderson, and R. Zera, "Syndecan-1 expression is induced in the stroma of infiltrating breast carcinoma," *American Journal of Clinical Pathology*, vol. 112, no. 3, pp. 377–383, 1999.

[60] M. Guarino, B. Rubino, and G. Ballabio, "The role of epithelial-mesenchymal transition in cancer pathology," *Pathology*, vol. 39, no. 3, pp. 305–318, 2007.

[61] L. Larue and A. Bellacosa, "Epithelial-mesenchymal transition in development and cancer: role of phosphatidylinositol 3′ kinase/AKT pathways," *Oncogene*, vol. 24, no. 50, pp. 7443–7454, 2005.

[62] M. Kato, S. Saunders, H. Nguyen, and M. Bernfield, "Loss of cell surface syndecan-1 causes epithelia to transform into anchorage-independent mesenchyme-like cells," *Molecular Biology of the Cell*, vol. 6, no. 5, pp. 559–576, 1995.

[63] S. Leppä, K. Vleminckx, F. Van Roy, and M. Jalkanen, "Syndecan-1 expression in mammary epithelial tumor cells is E-cadherin-dependent," *Journal of Cell Science*, vol. 109, Part 6, pp. 1393–1403, 1996.

[64] D. Mennerich, A. Vogel, I. Klaman et al., "Shift of syndecan-1 expression from epithelial to stromal cells during progression of solid tumours," *European Journal of Cancer*, vol. 40, no. 9, pp. 1373–1382, 2004.

[65] B. J. Burbach, A. Friedl, C. Mundhenke, and A. C. Rapraeger, "Syndecan-1 accumulates in lysosomes of poorly differentiated breast carcinoma cells," *Matrix Biology*, vol. 22, no. 2, pp. 163–177, 2003.

[66] Y. Yang, V. MacLeod, H. Q. Miao et al., "Heparanase enhances syndecan-1 shedding: a novel mechanism for stimulation of tumor growth and metastasis," *Journal of Biological Chemistry*, vol. 282, no. 18, pp. 13326–13333, 2007.

[67] T. Maeda, J. Desouky, and A. Friedl, "Syndecan-1 expression by stromal fibroblasts promotes breast carcinoma growth in vivo and stimulates tumor angiogenesis," *Oncogene*, vol. 25, no. 9, pp. 1408–1412, 2006.

[68] T. Maeda, C. M. Alexander, and A. Friedl, "Induction of syndecan-1 expression in stromal fibroblasts promotes proliferation of human breast cancer cells," *Cancer Research*, vol. 64, no. 2, pp. 612–621, 2004.

[69] G. Su, S. A. Blaine, D. Qiao, and A. Friedl, "Shedding of syndecan-1 by stromal fibroblasts stimulates human breast cancer cell proliferation via FGF2 activation," *Journal of Biological Chemistry*, vol. 282, no. 20, pp. 14906–14915, 2007.

[70] G. Su, S. A. Blaine, D. Qiao, and A. Friedl, "Membrane type 1 matrix metalloproteinase–mediated stromal syndecan-1 shedding stimulates breast carcinoma cell proliferation," *Cancer Research*, vol. 68, no. 22, pp. 9558–9565, 2008.

[71] V. Thanakit, P. Ruangvejvorachai, and P. Sampatanukul, "Expression of E-cadherin and syndecan-1 in axillary lymph node metastases of breast cancer with and without extracapsular extension," *Journal of the Medical Association of Thailand*, vol. 91, no. 7, pp. 1087–1092, 2008.

[72] Y. Wang, X. Ao, H. Vuong et al., "Membrane glycoproteins associated with breast tumor cell progression identified by a lectin affinity approach," *Journal of Proteome Research*, vol. 7, no. 10, pp. 4313–4325, 2008.

[73] M. Götte, C. Kersting, I. Radke, L. Kiesel, and P. Wülfing, "An expression signature of syndecan-1 (CD138), E-cadherin and c-met is associated with factors of angiogenesis and lymphangiogenesis in ductal breast carcinoma in situ," *Breast Cancer Research*, vol. 9, no. 1, article R8, 2007.

[74] S. Y. Kim, E. J. Choi, J. A. Yun et al., "Syndecan-1 expression is associated with tumor size and EGFR expression in colorectal carcinoma: a clinicopathological study of 230 cases," *International Journal of Medical Sciences*, vol. 12, no. 2, pp. 92–99, 2015.

[75] H. Wang, H. Jin, D. M. Beauvais, and A. C. Rapraeger, "Cytoplasmic domain interactions of syndecan-1 and syndecan-4 with $\alpha 6\beta 4$ integrin mediate human epidermal growth factor receptor (HER1 and HER2)-dependent motility and survival," *Journal of Biological Chemistry*, vol. 289, no. 44, pp. 30318–30332, 2014.

[76] E. R. Suarez, E. J. Paredes-Gamero, A. Del Giglio, I. L. dos Santos Tersariol, H. B. Nader, and M. A. S. Pinhal, "Heparan sulfate mediates trastuzumab effect in breast cancer cells," *BMC Cancer*, vol. 13, no. 1, p. 444, 2013.

[77] A. L. Bane, S. Tjan, R. K. Parkes, I. Andrulis, and F. P. O'Malley, "Invasive lobular carcinoma: to grade or not to grade," *Modern Pathology*, vol. 18, no. 5, pp. 621–628, 2005.

[78] A. García-Fernández, J. M. Lain, C. Chabrera et al., "Comparative long-term study of a large series of patients with invasive ductal carcinoma and invasive lobular carcinoma. Loco-regional recurrence, metastasis, and survival," *The Breast Journal*, vol. 21, no. 5, pp. 533–537, 2015.

[79] I. Miše, M. Vučić, I. Maričević, M. Šokčević, and S. Ćuric-Jurić, "Histologic subtypes of invasive lobular carcinoma in correlation with tumor status and hormone receptors," *Acta Clinica Croatica*, vol. 49, no. 3, pp. 275–281, 2010.

[80] F. Baba, K. Swartz, R. van Buren et al., "Syndecan-1 and syndecan-4 are overexpressed in an estrogen receptor-negative, highly proliferative breast carcinoma subtype," *Breast Cancer Research and Treatment*, vol. 98, no. 1, pp. 91–98, 2006.

Hindawi
Analytical Cellular Pathology
Volume 2018, Article ID 9275685, 11 pages
https://doi.org/10.1155/2018/9275685

Research Article

LncRNA LOXL1-AS1 Promotes the Proliferation and Metastasis of Medulloblastoma by Activating the PI3K/AKT Pathway

Ran Gao,[1] Rui Zhang,[2] Cuicui Zhang,[3] Yingwu Liang,[1] and Weining Tang[1]

[1]*Department of Pediatrics, Jining No. 1 People's Hospital, Shandong, China*
[2]*Department of Pediatrics, Sishui People's Hospital, Shandong, China*
[3]*Intensive Care Unit, Affiliated Hospital of Jining Medical University, Shandong, China*

Correspondence should be addressed to Weining Tang; weiningtang_s@sina.com

Received 30 November 2017; Revised 11 March 2018; Accepted 22 May 2018; Published 27 June 2018

Academic Editor: Mamoun Ahram

Medulloblastoma is the most common malignant brain tumor of childhood, with great potential to metastasize. However, the mechanisms of how medulloblastoma develops and progresses remain to be elucidated. The present study assessed the role of long noncoding RNA LOXL1-AS1 (lncRNA LOXL1-AS1) in the cell proliferation and metastasis in human medulloblastoma. It was initially found that LOXL1-AS1 was significantly overexpressed in clinical medulloblastoma tissues compared with the adjacent noncancerous tissues. LOXL1-AS1 was also highly expressed in medulloblastoma at advanced stages and differentially expressed in a series of medulloblastoma cell lines. Knockdown of LOXL1-AS1 using shRNAs significantly inhibited cell viability and colony formation capacities in D283 and D341 cells. Moreover, the cell proportion in the S phase was significantly increased, while the cell proportion in the G2/M phase was decreased after knockdown of LOXL1-AS1 in D283 cells and D341 cells. Cell cycle arrest led to eventual cell apoptosis by LOXL1-AS1 knockdown. Moreover, in a xenograft model of human medulloblastoma, knockdown of LOXL1-AS1 significantly inhibited tumor growth and promoted tumor cell apoptosis. In addition, knockdown of LOXL1-AS1 inhibited cell migration and reversed epithelial-to-mesenchymal transition (EMT). Western blot analysis further revealed that knockdown of LOXL1-AS1 decreased the phosphorylated levels of PI3K and AKT without affecting their total protein levels. These results suggest that LncRNA LOXL1-AS1 promoted the proliferation and metastasis of medulloblastoma by activating the PI3K-AKT pathway, providing evidence that knockdown of LncRNA LOXL1-AS1 might be a potential therapeutic strategy against medulloblastoma.

1. Introduction

Medulloblastoma is the most common malignant brain tumor of childhood characterized with frequent extraneural metastasis [1]. Current therapies for medulloblastoma were introduced primarily in the 1980s and consist of predominantly cytotoxic, nontargeted approaches. However, mortality from medulloblastoma remains significant [2]. Moreover, many survivors suffer from severe treatment-related effects of radiation and cytotoxic chemotherapy such as endocrinological dysfunction and intellectual damage [3, 4]. Therefore, novel therapeutic strategies targeting critical regulatory pathways in the development and progression of medulloblastoma are warranted.

Currently, the origin of cancer is considered as a step-by-step accumulation of alterations in cell function and molecular expression, which are widely reported to relate with mechanisms involving transcriptional regulation [5], posttranscriptional regulation [6], and epigenetic modification [7]. Among the posttranscriptional regulatory machineries, long noncoding RNAs (lncRNAs) have recently been identified as key regulators of various biological processes, including cell proliferation, differentiation, apoptosis, migration, and invasion [8–10]. lncRNAs are a class of RNA over 200 nucleotides in length. The role of lncRNAs in solid tumors has received increasing attention from worldwide studies. Moreover, lncRNAs, such as SNHG1, have been associated with cancer malignancy in pan-cancer including

medulloblastoma [11]. However, our knowledge of lncRNAs remains limited, and it has become a major research challenge in discovering novel disease-related lncRNAs in cancers such as medulloblastoma [11].

Emerging data has shown the critical role of lncRNAs in the development and progression of medulloblastoma. Tumor growth and metastasis of medulloblastoma have been reported to be strictly controlled by lncRNAs such as CCAT1 [10], linc-NeD125 [12], and CRNDE [9]. However, other critical lncRNAs significantly associated with medulloblastoma remain to be elucidated.

lncRNA LOXL1-antisense RNA (LOXL1-AS1) is encoded on the opposite strand of LOXL1. It is a novel lncRNA that has recently been identified using sequencing and genetic analysis [13]. LOXL1-AS1 expression is significantly altered in response to oxidative stress in human lens epithelial cells and in response to cyclic mechanical stress in human Schlemm's canal endothelial cells [13], supporting a functional role for the lncRNA LOXL1-AS1 in cellular stress response.

The role of LOXL1-AS1 in human tumorigenesis remains unknown, so the present study aimed to investigate the expression profile and functional role of LOXL1-AS1 in medulloblastoma. To this end, the LOXL1-AS1 level was initially evaluated in clinical medulloblastoma tissues and in a series of medulloblastoma cell lines. Specific shRNAs targeting LOXL1-AS1 were then synthesized to modulate the expression of LOXL1-AS1. Cell viability, colony formation, and cell migration capacities were examined *in vivo* and *in vitro*. Our results showed that LOXL1-AS1 was highly expressed in medulloblastoma tissues. Knockdown of LOXL1-AS1 significantly inhibited cell proliferation and metastasis in medulloblastoma. In addition, the PI3K/AKT pathway was regulated by LOXL1-AS1, which might suggest a regulatory mechanism contributing to LOXL1-AS1-mediated medulloblastoma progression.

2. Materials and Methods

2.1. Human Tissues and Ethical Statements. A total of 50 cases that were clinically diagnosed with medulloblastoma at Jining No. 1 People's Hospital and Sishui People's Hospital were included in the present study. For each case, its cancerous tissues and the matched adjacent noncancerous tissues were obtained. All patients showed their full consent to participate in our study, and a written consent form was obtained from each patient. Protocols for using human tissues were approved by the ethical committee board at Jining No. 1 People's Hospital and Sishui People's Hospital University.

2.2. Cells and Reagents. Human medulloblastoma cell lines Daoy, D283, D425, D341, and D458 were purchased from the Cell Bank of the Chinese Academy of Sciences (Shanghai, China). All cell lines were maintained in Dulbecco's Modified Eagle Medium (DMEM) (Gibco, Los Angeles, CA, USA) supplied with 10% fetal bovine serum (FBS) (Gibco). Culture medium was refreshed every two days unless otherwise stated. Primary antibodies were commercially purchased from Santa Cruz Biotechnology (Santa Cruz, CA, USA) except for the phosphorylation detection antibodies which were obtained from Cell Signaling Technology (Boston, MA, USA). For knockdown of lncRNA LOXL1-AS1, two specific shRNAs were chemically synthesized by GenePharma (Shanghai, China). A scramble shRNA was also synthesized serving as control shRNA.

2.2.1. Quantitative Real-Time PCR. Total RNAs of human tissues and cultured cells were isolated using TRIzol Reagent (Thermo Fisher Scientific, Waltham, MA, USA) according to the manufacturer's instruction. The quality and concentration of extracted RNAs were determined by collecting the absorbance at 260 nm with Nanodrop 2000. The RNAs were immediately transcribed into cDNAs using the PrimeScript RT Master Mix Perfect Real Time (TaKaRa, Shiga, Japan). All real-time PCRs were performed with the SYBR Premix Ex Taq Kit (TaKaRa, Japan) in an ABI PRISM 7500 Real-Time System. *Glyceraldehyde-3-phosphate dehydrogenase (GAPDH)* was included as the internal control. Each experiment was repeated three times with each one performed in triplicate.

2.3. Western Blot Analysis. Total proteins were extracted using a RIPA lysis buffer (pH = 7.5, Beyotime Biotechnology, Nantong, China) to generate the whole protein lysate. An equal amount of 40 μg protein was loaded to each lane in a 12% SDS-PAGE gel. Proteins were then transferred to a polyvinylidene fluoride (PVDF) membrane after electrophoresis. After blockade of nonspecific antigens with 5% skim milk, membranes were incubated with primary antibodies overnight at 4°C. A secondary antibody which recognizes the primary antibody was then added, and the immunoreactivity was determined with enhanced chemoluminescent autoradiography (Thermo Scientific, PA, USA). GAPDH was synchronously developed for loading control.

2.4. Immunofluorescent Assay. D283 and D341 cells with indicated treatments were seeded on sterile coverslips in a 24-well plate in DMEM with 10% FBS. After 24 h, cells were rinsed with PBS and fixed for 30 min in 4% paraformaldehyde. Subsequently, cells were penetrated with 2% Triton X-100 for 20 min and then blocked in 5% FBS for 1 h. After that, cells were incubated with primary antibodies at 4°C overnight. After washing by PBS, cells were incubated with corresponding secondary antibody in the dark for 1 h and counterstained for 30 min with 4′, 6-diamidino-2-phenylindole (DAPI). Samples were finally mounted and observed/photographed by an Olympus IX71 inverted microscope (Olympus Optical Co., Tokyo, Japan).

2.5. Cell Viability Detection. D283 and D341 cell viability were assessed using a cell counting kit-8 (CCK-8) assay (Beyotime, Nantong, China) according to the manufacturer's protocol. Briefly, cells were seeded into 6 cm dishes and transfected with specific shRNAs against LOXL1-AS1 (shRNA1 or shRNA2 group) or with a scramble shRNA (control group). Twenty-four hours later, each group of cells were trypsinized and resuspended. Cells were then seeded into a 96-well plate at an initial concentration of 8000 cells per well. Cell proliferative rates were monitored for the

following 5 days. On each monitored time point, an aliquot of 10 μl of CCK-8 solution was added to each well. After further incubation of cells with CCK-8 solution for 4 h, the absorbance of each well was measured by an ELISA reader at a wave length of 450 nm. For data analysis, the cell viability on day 1 was set as 1.

2.6. Colony Formation Assay. Human medulloblastoma cell lines D283 and D341 were pretransfected with specific shRNA against LOXL1-AS1 and spread into 12-well plates. Then, all plates were incubated for 2 weeks to allow colony formation. After that, colonies were stained with crystal violet (0.1%) for 30 min. A colony is defined as cell accumulation with over 50 cells. The total number of colonies was manually counted and averaged for each group.

2.7. Wound-Healing Assay and Transwell Migration Assay. For the wound-healing assay, cells were plated on 6-well plates to form a confluent monolayer. Wounds were made with sterile pipette tips. Wound recovery was observed every 6 hours. The wound recovery rate was then calculated after each monitored time point. A migration assay was carried out using Boyden chambers (tissue culture-treated, 6.5 mm diameter, 8 μm pores, Transwell, Costar, Cambridge, MA, USA) containing polycarbonate membrane. Briefly, 100 μl of 1×10^6 cells in serum-free medium was added to the upper chamber, and 600 μl of DMEM with 10% FBS was added to the lower chamber. Cells were incubated for 12 h. Migrated cells on the undersurface of the membrane were fixed and stained with crystal violet for 10 minutes at room temperature. Photographs of five random regions were taken, and the number of cells was counted to calculate the average number of migrated cells per plate.

2.8. Cell Cycle Analysis. Flow cytometry analysis was performed to analyze cell cycle progression. Briefly, control or LOXL1-AS1-depleted D283 cells and D341 cells were washed with PBS twice and fixed with 70% ethanol for 30 min on ice. To degrade RNAs, 20 mg/ml of RNase (Sigma-Aldrich, NY, USA) was added for 1 h at 37°C. After RNA degradation, samples were then stained with 20 mg/ml propidium iodide (PI, Sigma-Aldrich), and cell proportion at each phase was assessed by FACSCalibur flow cytometry (BD Biosciences, San Jose, CA, USA) equipped with the ModiFit LT v2.0 software.

2.9. Cell Apoptosis Analysis. Cell apoptosis was analyzed using the Annexin V/PI apoptosis kit (Invitrogen, Shanghai, China) according to the manufacturer's instruction. Briefly, D283 and D341 cells were seeded in a 6-well plate (2×10^6 cells/well) and transfected with a scramble shRNA (control group) or with the specific shRNA against LOXL1-AS1 (shRNA group). Both cell lines were then cultured with complete medium for 48 h. After that, cells were washed with iced PBS and resuspended with 100 μl binding buffer. Then, 5 μl of annexin V-FITC and 5 μl of PI working solution (100 μg/ml) were added to the 100 μl aliquots of cell suspension. Cell suspensions were further incubated at room temperature for 15 min in the dark. Subsequently, another 400 μl of binding buffer was added to the cell suspension. Samples were then analyzed by flow cytometry. Each sample was tested in triplicate three times.

2.10. Xenograft Model of Medulloblastoma In Vivo. Male athymic BALB/c nude mice that were 5 weeks old were maintained in a special pathogen-free (SPF) condition. A total of 10 mice were fed and randomly divided into the control or shRNA group ($n = 5$ per group). D283 cells were pretransfected with the scramble shRNA (control) or specific shRNA1 against LOXL1-AS1 (shRNA1 group) prior to inoculation into mice. A total of 5×10^6 D283 cells with indicated treatments were then injected subcutaneously into the right flank in each mouse. Tumor dimensions (length, L, and width, W) were then measured once a week for a total of 4 weeks. Tumor volumes (TV) were calculated as $\mathrm{TV} = L \times W^2/2$. After 4 weeks feeding, the mice were sacrificed and tumor tissues were dissected for subsequent analyses. All efforts were made to minimize suffering.

2.11. Histology and Immunohistochemistry (IHC) Analysis. Tumor tissues from the mouse model were paraffin embedded and cut into 4 μm slides. The slides were then subject to hematoxylin and eosin (H&E) staining for pathology confirmation. After H&E staining, the slides were subjected to antigen retrieval in a microwave in 0.1 M citric acid solution (pH 6.0) for 10 min. After incubation with primary antibodies at 4°C overnight, the slides were incubated with corresponding secondary antibody at room temperature for 1 h. The reactivity was developed using 0.05% diaminobenzidine (DAB) containing 0.01% H_2O_2. Representative images were photographed for each slide.

2.12. Statistical Analysis. Data were expressed as means ± standard deviation (SD). Comparisons between groups were analyzed using Student's t-test. Differences with a two-sided p value < 0.05 were considered to be statistically significant.

3. Results

3.1. lncRNA LOXL1-AS1 Was Overexpressed in Medulloblastoma. Initially, the expression of LOXL1-AS1 was examined in clinical medulloblastoma tissues. In the 50 cases, the mean level of LOXL1-AS1 in medulloblastoma tissues was approximately 1.5-fold that in the adjacent noncancerous tissues (Figure 1(a)). After analysis of the paired tissues, it was found that 36 of the 50 cases showed a higher level of LOXL1-AS1 in medulloblastoma tissues as compared with the paired adjacent tissues (Figure 1(b)). Moreover, the relative LOXL1-AS1 level was significantly higher in tumors with the size categorized as T3 and T4 (Figure 1(c)). In a series of medulloblastoma cell lines, LOXL1-AS1 was differentially expressed and showed the highest levels in D283 and D341 cells (Figure 1(d)). Taken together, these data suggest that LOXL1-AS1 was overexpressed in medulloblastoma tissues.

3.2. Knockdown of LOXL1-AS1 Inhibited Cell Viability and Colony Formation Capacity in D283 and D341 Cells. In view of the highest expression of LOXL1-AS1 in D283 and D341 cells, these two cell lines were selected as optimal to

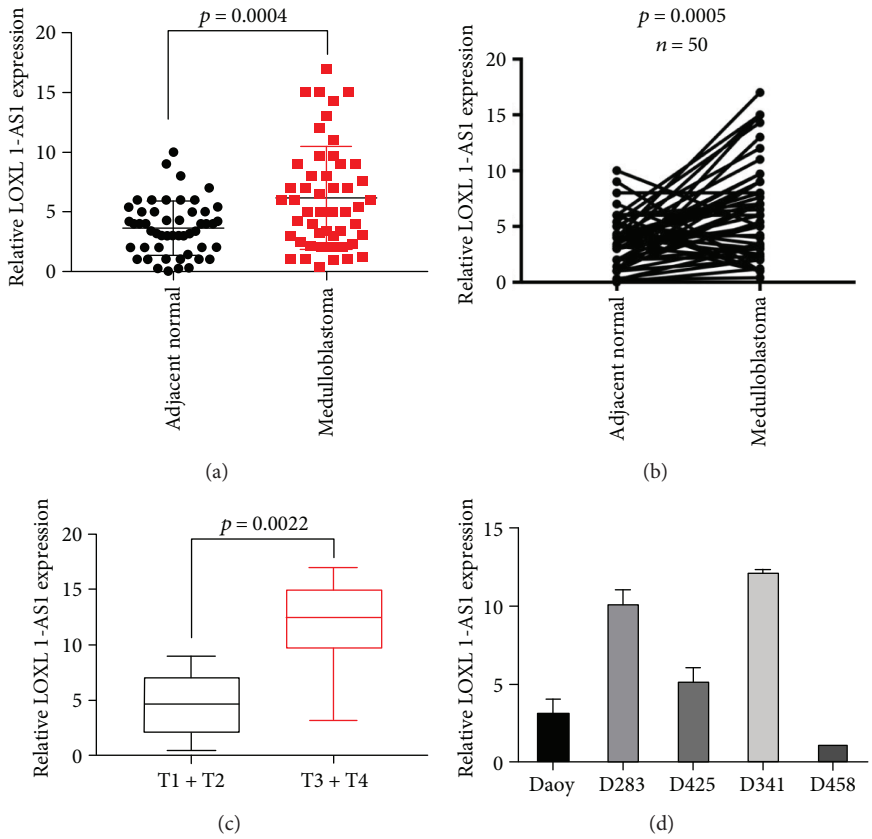

Figure 1: lncRNA LOXL1-AS1 was highly expressed in medulloblastoma. (a) qRT-PCR analysis of LncRNA LOXL1-AS1 in 50 cases of clinical medulloblastoma as well as their adjacent normal tissues. (b) The paired expression of LOXL1-AS1 was shown in the 50 cases. (c) All the 50 cases were subgrouped as T1, T2, T3, and T4 based on the tumor size. Relative level of LOXL1-AS1 in T3 and T4 cancerous tissues was significantly higher than that in T1 and T2 tissues. (d) qRT-PCR analysis of the relative level of LOXL1-AS1 in 5 medulloblastoma cell lines. The level of LOXL1-AS1 in the D458 cells was set as 1. LOXL1-AS1 levels in other cell lines were normalized to those in D458 cells. The p value for each comparison was indicated in each panel.

investigate the functional roles of LOXL1-AS1 in medulloblastoma. Specific shRNAs against LOXL1-AS1 were synthesized. It was shown that specific shRNAs depleted the expression of LOXL1-AS1 in D283 cells (Figure 2(a)) and D341 cells (Figure 2(b)). Next, cell viability was determined in both cell lines with or without LOXL1-AS1 depletion. In D283 cells, it was observed that depletion of LOXL1-AS1 impaired cell proliferative abilities from day 3. On day 5, the proliferative rate in LOXL1-AS1-depleted cells was only half of that in control cells (Figure 2(c)). Depletion of LOXL1-AS1 using either shRNA also inhibited cell proliferation by up to 70% in D341 cells (Figure 2(d)). Likewise, in the colony formation assay, it was visually observed that depletion of LOXL1-AS1 in either cell line decreased the colonies that were stained with crystal violet (Figure 2(e)). Quantification of the colonies showed that only approximately 40–50 colonies were formed in LOXL1-AS1-depleted D283 cells, which was in contrast to the mean 120 colonies in control D283 cells (Figure 2(f)). Decreases in the formed colonies were also found in LOXL1-AS1-depleted D341 cells (Figure 2(g)). All these data suggested that knockdown of LOXL1-AS1 inhibited cell viability and clonogenic potential in medulloblastoma cells.

3.3. Knockdown of LOXL1-AS1 Arrested Cell Cycle at the S Phase and Led to Eventual Cell Apoptosis in Medulloblastoma. The effects of LOXL1-AS1 knockdown were then assessed on cell survival (Figure 3(a)). In the cell cycle analysis, it was found that knockdown of LOXL1-AS1 arrested the cell cycle progression (Figure 3(a)). Particularly, the cell proportion in the S phase was significantly increased from approximately 30% in control D283 cells to nearly 45% in LOXL1-AS1-depleted D283 cells. Accordingly, the cell proportion in the G2/M phase was decreased by approximately 50% after knockdown of LOXL1-AS1 in D283 cells (Figure 3(b)). Comparable cell cycle arrest at the S phase was also observed in D341 cells (Figure 3(c)).

Subsequently, cell apoptosis was analyzed (Figure 4(a)). While there was only approximately 4% control D283 cells that were apoptotic, the cell apoptosis rate was up to 14% in shRNA1-transfected D283 cells and 15.2% in shRNA2-transfected D283 cells (Figure 4(b)). Knockdown of LOXL1-AS1 in D341 also promoted cell apoptosis rates, a 200% increase by shRNA1 and 250% increase by shRNA2 (Figure 4(c)). These data suggest that knockdown of LOXL1-AS1 arrested the cell cycle, leading to eventual cell apoptosis in medulloblastoma.

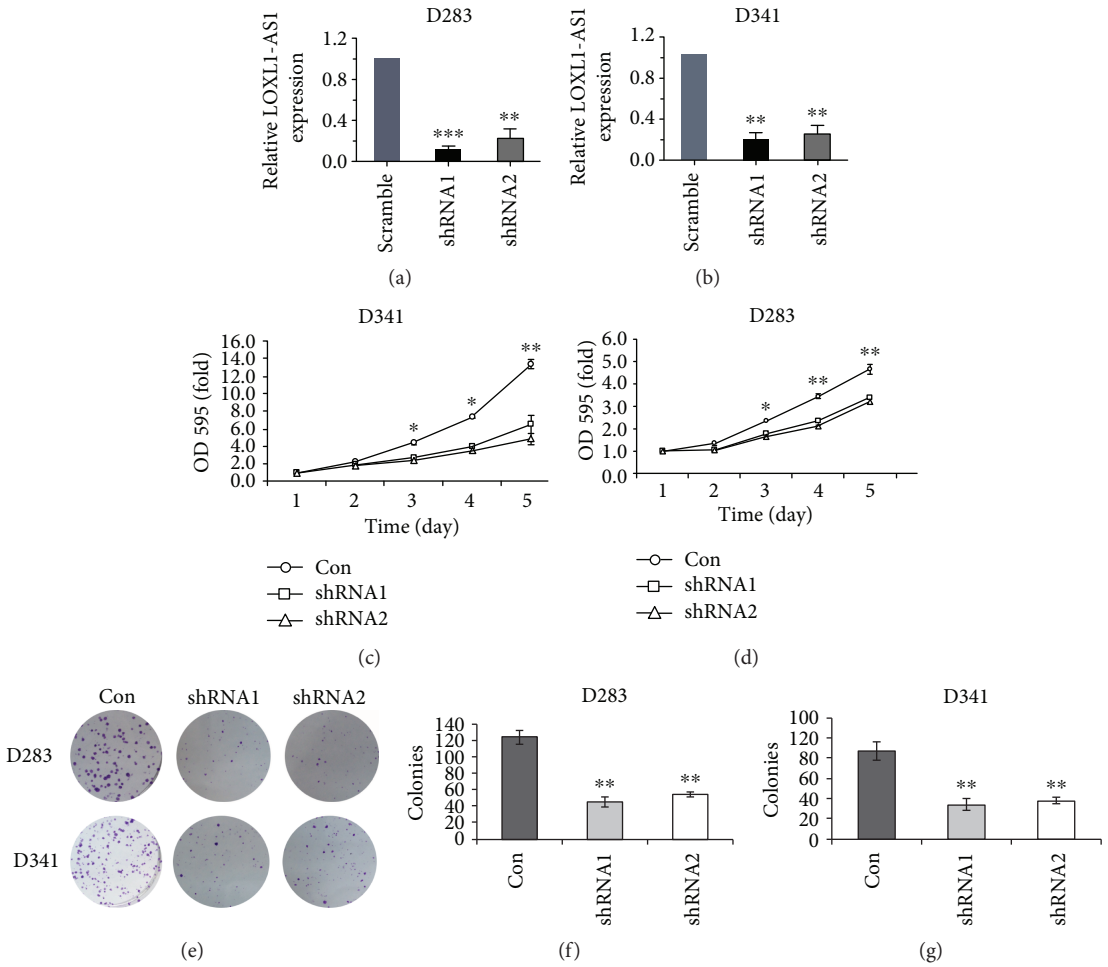

Figure 2: Knockdown of LOXL1-AS1 inhibited cell viability and colony formation capacity in D283 and D341 cells. (a, b) Knockdown efficiency of two synthesized shRNAs against LOXL1-AS1 (termed as shRNA1 and shRNA2) was assessed in D283 cells and D341 cells, respectively. (c, d) After knockdown of LOXL1-AS1 in D283 and D341 cells, cell proliferative rates were monitored in a consecutive of 5 days. The absorbance on day 1 was set as 1 for each group of cells. (e, f, g) Control and LOXL1-AS1-depleted cells were subject to colony formation assay in D283 cells and D341 cells. Formed colonies were stained with crystal violet, and all colonies in each group were manually counted and averaged from three independent assays. $^{*}p < 0.05$; $^{**}p < 0.01$.

3.4. Depletion of LOXL1-AS1 Inhibited Tumor Growth in Medulloblastoma In Vivo. A xenograft model of human medulloblastoma was established by inoculating D283 cells into nude mice. D283 cells were pretreated with a scrambled shRNA or the shRNA1 prior to inoculation. QRT-PCR analysis was performed to confirm the efficiency of the shRNA1 to knockdown LOXL1-AS1 (Figure 5(a)). The use of shRNA1 was due to the observation that shRNA1 exhibited relatively higher efficacy to deplete LOXL1-AS1 than shRNA2 as shown in Figures 2(a) and 2(b). Four weeks after inoculation, tumors in each group of mice were resected, and the shRNA1-treated mice exhibited visibly smaller sized tumors as compared with the control mice. The weight of tumors from the shRNA1 group was also significantly less than that from the control group (Figure 5(b)). Indeed, during the monitored 4 weeks, shRNA1-treated mice began to exhibit smaller tumor sizes from the second week, and LOXL1-AS1-depleted mice showed slower tumor growth rate during the following weeks (Figure 5(c)). Immunohistochemical analysis revealed that the neoplasia from the shRNA1-treated mice showed relatively less positivity of Ki-67, a marker of tumor cell proliferation (Figures 5(d) and 5(e)). Instead, neoplasia from the LOXL1-AS1-depleted mice showed more TUNEL-positive cells (Figures 5(d) and 5(f)), which indicated the increased cell apoptosis within the tissues, supporting the *in vitro* observations and suggesting that LOXL1-AS1 depletion inhibited tumor growth in medulloblastoma.

3.5. Knockdown of LOXL1-AS1 Inhibited Cell Migration in Medulloblastoma. Cell migration capacity was then assessed using a wound-healing assay. It was observed that both D283 and 341 cells recovered the artificial wound, regardless of what treatments they received. However, the shRNA-treated cells showed slower recovery ability at 18 h in comparison with control cells (Figure 6(a)). In fact, the wound recovery rates were decreased by nearly 46.7% in D283 cells and 55.6% in D341 cells (Figure 6(b)). The Transwell migration assay also confirmed that LOXL1-AS1-depleted cells were less capable of transmigrating to the lower surface of

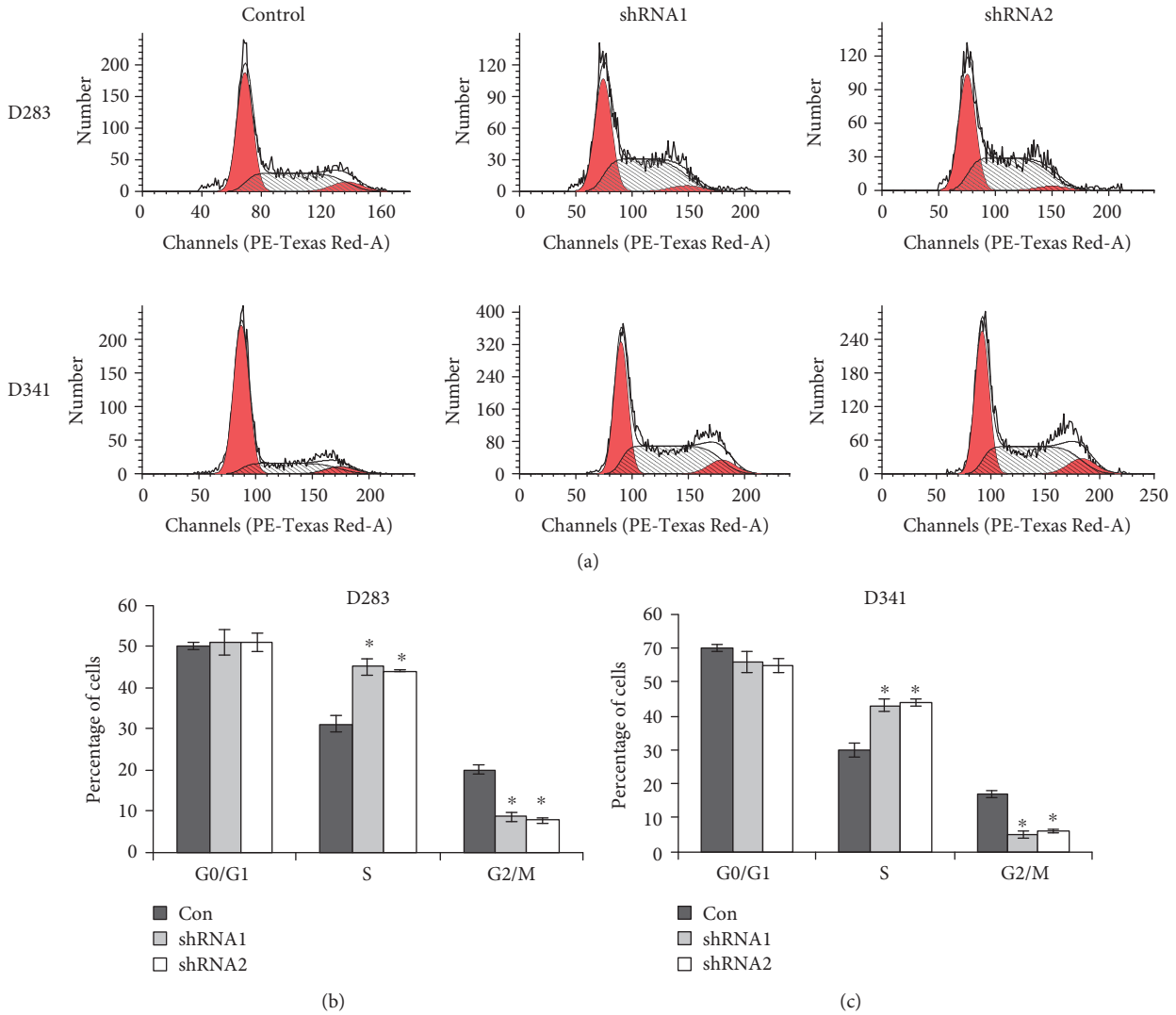

Figure 3: Knockdown of LOXL1-AS1 arrested cell cycle at the S phase in medulloblastoma. (a) Cell cycle progression was analyzed in both D283 cells and D341 cells that were pretreated with or without specific shRNAs against LOXL1-AS1. (b, c) Cell proportions in the G0/G1, S, and G2/M phases were calculated in D283 cells and D341 cells, respectively. It was found that cells were proportionally accumulated in the S phase while cells in the G2/M phase were significantly decreased in both cell lines. $^*p < 0.05$.

the chamber (Figure 6(c)). The migrated cells in shRNA-treated groups were less than half of that in control groups (Figure 6(d)).

In addition, the epithelial marker, E-cadherin, and mesenchymal marker, vimentin, were detected, with an increase in E-cadherin immunofluorescence and a decrease in vimentin immunofluorescence observed after knockdown of LOXL1-AS1 (Figure 6(e)). Consistently, Western blot analysis also showed that the protein level of vimentin decreased, whereas that of E-cadherin increased in response to LOXL1-AS1 depletion in both D283 cells and D341 cells (Figure 6(f)), suggesting that knockdown of LOXL1-AS1 inhibited cell migration and reversed EMT processes.

3.6. LOXL1-AS1 Positively Regulated the PI3K/AKT Pathway in Medulloblastoma Cell Lines. The molecular mechanisms that contributed to the LOXL1-AS1-mediated phenotype were explored. It was detected that the phosphorylated levels of PI3K (p-PI3K) and AKT (p-AKT) were remarkably decreased in LOXL1-AS1-depleted cells, whereas the total protein levels of PI3K and AKT remained unaffected by LOXL1-AS1 knockdown, indicating that LOXL1-AS1 activated the PI3K/AKT pathway in medulloblastoma (Figure 7).

4. Discussion

Medulloblastoma remains a major health problem threating children's lives worldwide. Forty percent of patients suffering from medulloblastoma were found to have distant metastasis at diagnosis [14], making it a real challenge to treat this malignancy. Moreover, traditional therapies for medulloblastoma are associated with significant side effects [3]. Therefore, investigation of novel molecular changes during medulloblastoma initiation and progression is necessary to identify novel therapeutic targets and individualize treatments for medulloblastoma patients.

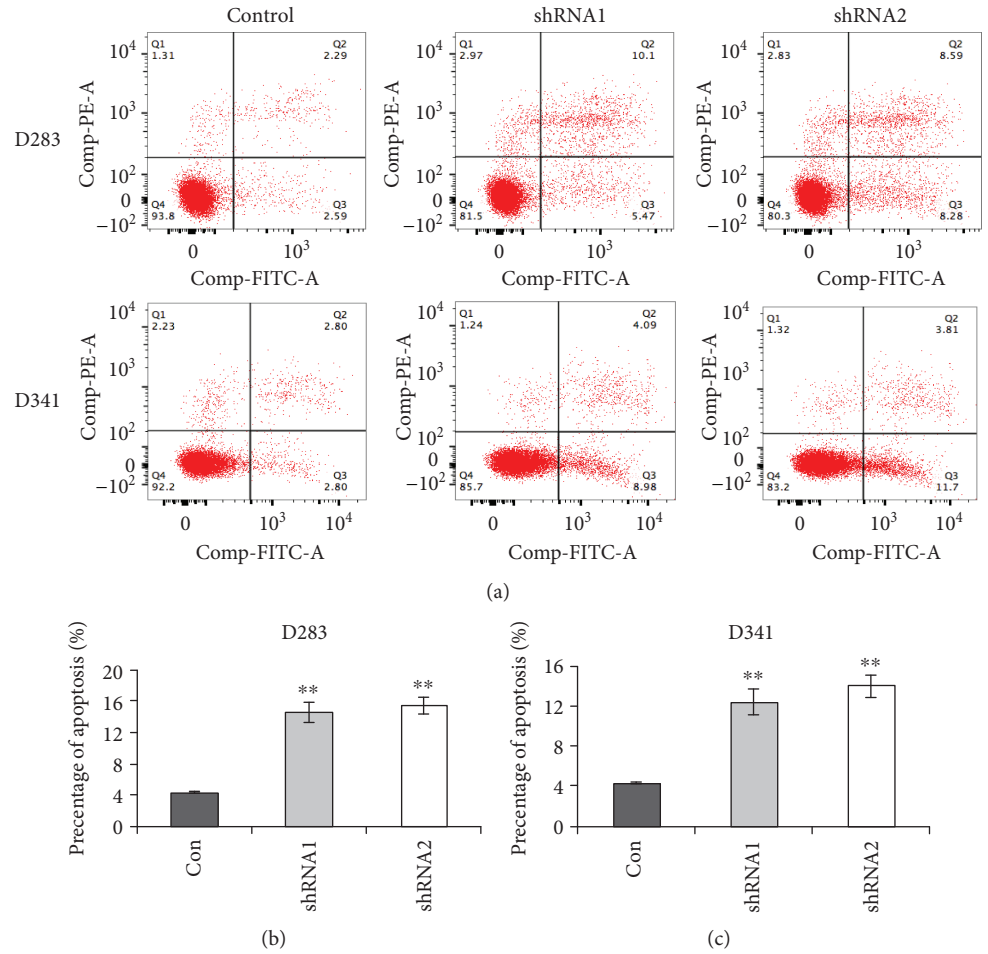

Figure 4: Knockdown of LOXL1-AS1 promoted cell apoptosis in D283 and D341 cells. (a) Cell survival was determined in both cell lines with or without LOXL1-AS1 depletion. (b, c) The percentage of cell apoptosis was shown for D283 cells and D341 cells. It was found that the cell apoptosis was significantly promoted by either shRNA in both cell lines. $^{**}p < 0.01$.

The present study provided *in vitro* and *in vivo* evidence that LOXL1-AS1 displayed potent prooncogenic functions in medulloblastoma and commends itself as a possible therapeutic target to current medulloblastoma treatment. LOXL1-AS1 is a recently identified lncRNA that is critically associated with cellular stress response [13], but there is a lack of expression data for LOXL1-AS1, especially in tumor tissues. This is the first report that LOXL1-AS1 is significantly overexpressed in clinical medulloblastoma tissues. Its expression was even higher in medulloblastoma with advanced tumor sizes, indicating a critical involvement in tumor growth regulation. In fact, cell viability and clonogenic potential was significantly inhibited after knockdown of LOXL1-AS1 in medulloblastoma cell lines. Tumor growth was also inhibited in an *in vivo* xenografted model of human medulloblastoma with LOXL1-AS1 depletion. Furthermore, the *in vitro* and *in vivo* tumor growth-inhibition effect by LOXL1-AS1 depletion was associated with tumor cell cycle arrest at the S phase. Deregulation of cell cycle progression is a hallmark of tumor growth [15] and closely linked with cell apoptosis [16, 17]. Cell cycle arrest by LOXL1-AS1 depletion supports the tumor growth promotion effect by LOXL1-AS1, as well as the eventual cell apoptosis in D283 and D341 cells, and in the xenografted model of medulloblastoma. Taken together, these observations indicate that LOXL1-AS1 promotes cell growth in medulloblastoma.

In addition, it was also found that knockdown of LOXL1-AS1 impaired cell migration capacities as evidenced by the wound-healing and Transwell migration assays. Cell migration was inhibited by approximately 50% in LOXL1-AS1-depleted D283 cells and D341 cells. EMT is a common manifestation of tumor metastasis and reflects epithelial cell plasticity, in which multiple regulatory molecules are involved, including the Zeb and Snail families [18]. The EMT process is induced by various cellular procedures, including increased expression of mesenchymal markers (N-cadherin and vimentin), decreased protein levels of epithelial markers (E-cadherin), and overexpressed ECM compounds (fibronectin) [19]. EMT is associated with a wide range of human tumorigenesis; activation of EMT in ovarian cancer has been shown to be associated with chemoresistance, which can cause cancer recurrence and metastasis after traditional treatment for ovarian cancer [2, 20, 21]. The

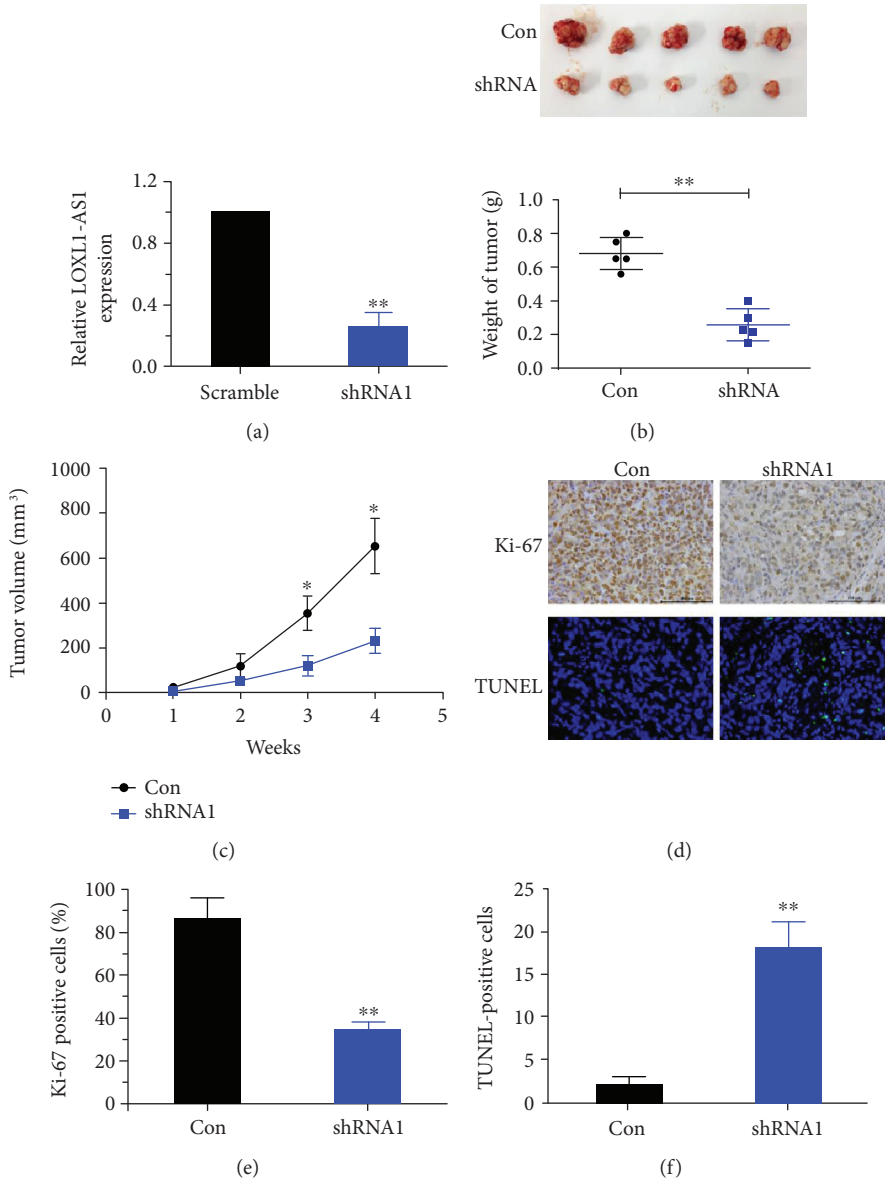

Figure 5: Depletion of LOXL1-AS1 inhibited tumor growth in medulloblastoma *in vivo*. (a) qRT-PCR analysis of relative LOXL1-AS1 levels in D283 cells to confirm the knockdown efficacy of shRNA1 (the first synthesized shRNA against LOXL1-AS1). (b) D283 cells were pretreated with the scramble (control group) or shRNA1 prior to inoculation into mice. Four weeks after inoculation, neoplasia were resected and weighed. (c) During the 4-week monitoring, tumor dimensions were measured and tumor volume was calculated for each group of mice. (d) The neoplasia from control mice or shRNA1-treated mice were subject to immunohistochemistry analysis of Ki-67 (an indicator of cell proliferation) or TUNEL staining (indicating cell apoptosis). (e) The Ki-67-positive cells were calculated for control and shRNA1-treated mice. (f) TUNEL-positive cells were also quantified to show tumor cell apoptosis. $^{*}p < 0.05$; $^{**}p < 0.01$.

present study observed that after depletion of LOXL1-AS1, expression of the mesenchymal marker, vimentin, was downregulated, while the epithelial marker, E-cadherin, was upregulated, suggesting that the EMT process was reversed by LOXL1-AS1 knockdown. Hence, LOXL1-AS1-depleted medulloblastoma cells are more epithelial and less migratory. The EMT assessment supported the wound-healing and Transwell migration assays. Taken together with the tumor growth observations, it can be concluded that LOXL1-AS1 regulates tumor growth and migration in medulloblastoma.

Phosphorylation of PI3K and AKT is pivotal for their activation. Upon phosphorylation, PI3K activates and phosphorylates the downstream AKT to cause a cascade reaction [22]. Interestingly, it was found that the phosphorylated levels of PI3K (p-PI3K) and AKT (p-AKT) were decreased after LOXL1-AS1 depletion, while their total protein levels remained unchanged, suggesting that LOXL1-AS1 positively regulates the PI3K/AKT pathway. PI3K/AKT signaling has been identified as a key driver of cellular proliferation, migration, and angiogenesis in human tumorigenesis, including medulloblastoma, in which activation of PI3K/

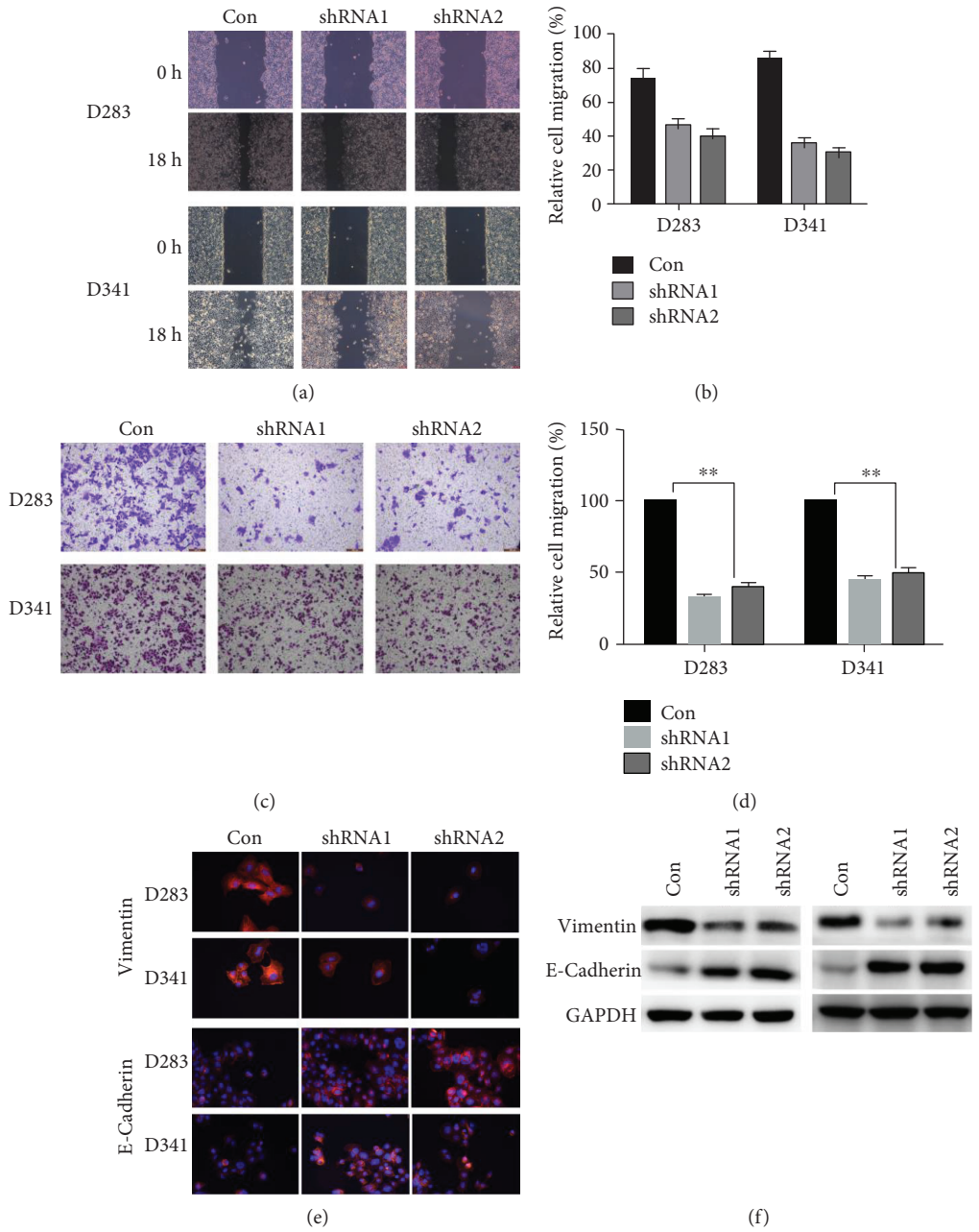

Figure 6: Knockdown of LOXL1-AS1 inhibited cell metastasis and reversed EMT processes in medulloblastoma. (a, b) Control or shRNA-treated D283 and D341 cells were subject to wound-healing assay. Representative images showing the wound recovery were shown at 0 h and 18 h for both cell lines. The wound-recovered area which represented the cell migration capacity was calculated for each group of cells. (c, d) Both D283 and D341 cells were subject to Transwell migration assay. Cells that migrated to the lower surface were stained with crystal violet. Transmigrated cells were counted and averaged from 5 randomly selected fields. (e) Immunofluorescent analysis of vimentin (mesenchymal marker) and E-cadherin (epithelial marker). (f) Western blot analysis of vimentin and E-cadherin in D283 and D341 cells. Expression of vimentin was less detected, whilst that of E-cadherin was largely detected after knockdown of LOXL1-AS1. $^{*}p < 0.05$; $^{**}p < 0.01$.

AKT signaling enhances tumor growth, metastasis, and chemoresistance [23–25]. PI3K/AKT signaling also serves as an integration node in a network of tumor-promoting signal pathways. Inhibition of PI3K activity using the GDC-0941 inhibitor displayed promising *in vitro* and *in vivo* efficacy for targeted medulloblastoma therapy [26]. Targeting the PI3K p110alpha isoform inhibited medulloblastoma proliferation, chemoresistance, and migration [25]. As LOXL1-AS1 promotes cell proliferation and migration in medulloblastoma *via* regulating the PI3K/AKT pathway, any compound or reagent targeting LOXL1-AS1 and consequently inhibiting the PI3K/AKT pathway might serve as a promising therapeutic strategy for the treatment of medulloblastoma.

In summary, the present study identified a novel lncRNA, LOXL1-AS1, as a critical mediator of cell proliferation and

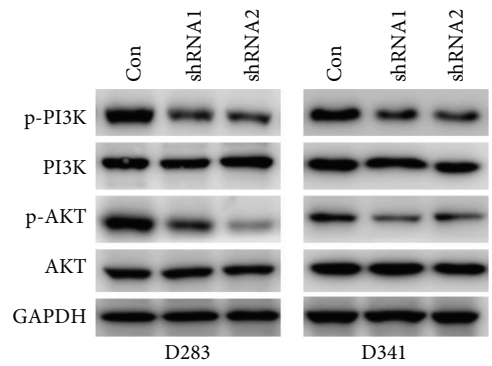

Figure 7: LOXL1-AS1 positively regulated the PI3K/AKT pathway in medulloblastoma cell lines. D283 cells and D341 cells were pretreated with scramble shRNA or specific shRNA1 or shRNA2 before collection of cell lysates. PI3K and AKT were detected at both the dephosphorylated and phosphorylated forms using Western blot analysis.

migration in medulloblastoma. LOXL1-AS1 is significantly overexpressed in clinical medulloblastoma tissues, while knockdown of LOXL1-AS1 expression impairs tumor cell growth and migration, as well as inactivation of PI3K/AKT. This is the first report of the expression profile and functional role of LOXL1-AS1 in human tumorigenesis, providing strong evidence that a synthetic compound or reagent targeting LOXL1-AS1 or the PI3K/AKT pathway might serve as promising clinical therapeutics against medulloblastoma.

Conflicts of Interest

The authors declare that they have no conflicts of interest.

Authors' Contributions

Ran Gao and Rui Zhang contributed equally to this study.

References

[1] A. Mazloom, A. H. Zangeneh, B. S. Teh, and A. C. Paulino, "Extraneural metastasis of medulloblastoma," *Journal of Clinical Oncology*, vol. 27, no. 15S, p. 2065, 2009.

[2] V. Ramaswamy and M. D. Taylor, "Medulloblastoma: from myth to molecular," *Journal of Clinical Oncology*, vol. 35, no. 21, pp. 2355–2363, 2017.

[3] A. Gajjar, M. Chintagumpala, D. Ashley et al., "Risk-adapted craniospinal radiotherapy followed by high-dose chemotherapy and stem-cell rescue in children with newly diagnosed medulloblastoma (St Jude Medulloblastoma-96): long-term results from a prospective, multicentre trial," *The Lancet Oncology*, vol. 7, no. 10, pp. 813–820, 2006.

[4] R. J. Packer, "Risk-adapted craniospinal radiotherapy followed by high-dose chemotherapy and stem-cell rescue in children with newly diagnosed medulloblastoma," *Current Neurology and Neuroscience Reports*, vol. 7, no. 2, pp. 130–132, 2007.

[5] L. L. Li, A. M. Xue, B. X. Li et al., "JMJD2A contributes to breast cancer progression through transcriptional repression of the tumor suppressor ARHI," *Breast Cancer Research*, vol. 16, no. 3, p. R56, 2014.

[6] E. Pennisi, "Genomics. ENCODE project writes eulogy for junk DNA," *Science*, vol. 337, no. 6099, pp. 1159–1161, 2012.

[7] V. Hovestadt, D. T. W. Jones, S. Picelli et al., "Decoding the regulatory landscape of medulloblastoma using DNA methylation sequencing," *Nature*, vol. 510, no. 7506, pp. 537–541, 2014.

[8] L. Chen, W. Wang, L. Cao, Z. Li, and X. Wang, "Long noncoding RNA CCAT1 acts as a competing endogenous RNA to regulate cell growth and differentiation in acute myeloid leukemia," *Molecules and Cells*, vol. 39, no. 4, pp. 330–336, 2016.

[9] H. Song, L. M. Han, Q. Gao, and Y. Sun, "Long non-coding RNA CRNDE promotes tumor growth in medulloblastoma," *European Review for Medical and Pharmacological Sciences*, vol. 20, no. 12, pp. 2588–2597, 2016.

[10] R. Gao, R. Zhang, C. Zhang, L. Zhao, and Y. Zhang, "Long noncoding RNA CCAT1 promotes cell proliferation and metastasis in human medulloblastoma via MAPK pathway," *Tumori*, vol. 104, no. 1, pp. 43–50, 2018.

[11] C. Xu, R. Qi, Y. Ping et al., "Systemically identifying and prioritizing risk lncRNAs through integration of pan-cancer phenotype associations," *Oncotarget*, vol. 8, no. 7, pp. 12041–12051, 2017.

[12] P. Laneve, A. Po, A. Favia et al., "The long noncoding RNA linc-NeD125 controls the expression of medulloblastoma driver genes by microRNA sponge activity," *Oncotarget*, vol. 8, no. 19, pp. 31003–31015, 2017.

[13] M. A. Hauser, I. F. Aboobakar, Y. Liu et al., "Genetic variants and cellular stressors associated with exfoliation syndrome modulate promoter activity of a lncRNA within the LOXL1 locus," *Human Molecular Genetics*, vol. 24, no. 22, pp. 6552–6563, 2015.

[14] X. Wu, P. A. Northcott, A. Dubuc et al., "Clonal selection drives genetic divergence of metastatic medulloblastoma," *Nature*, vol. 482, no. 7386, pp. 529–533, 2012.

[15] C. J. Sherr, "Cancer cell cycles," *Science*, vol. 274, no. 5293, pp. 1672–1677, 1996.

[16] X. Y. Xu, P. Xia, M. Yu et al., "The roles of REIC gene and its encoding product in gastric carcinoma," *Cell Cycle*, vol. 11, no. 7, pp. 1414–1431, 2014.

[17] X. Li, K. F. Cheung, X. Ma et al., "Epigenetic inactivation of paired box gene 5, a novel tumor suppressor gene, through direct upregulation of p53 is associated with prognosis in gastric cancer patients," *Oncogene*, vol. 31, no. 29, pp. 3419–3430, 2012.

[18] M. A. Nieto, "Epithelial-mesenchymal transitions in development and disease: old views and new perspectives," *International Journal of Developmental Biology*, vol. 53, no. 8-9-10, pp. 1541–1547, 2009.

[19] R. Strauss, Z. Y. Li, Y. Liu et al., "Analysis of epithelial and mesenchymal markers in ovarian cancer reveals phenotypic heterogeneity and plasticity," *PLoS One*, vol. 6, no. 1, article e16186, 2011.

[20] M. Iwatsuki, K. Mimori, T. Yokobori et al., "Epithelial-mesenchymal transition in cancer development and its clinical significance," *Cancer Science*, vol. 101, no. 2, pp. 293–299, 2010.

[21] K. Sakurai, K. Tomihara, K. Furukawa, W. Heshiki, Z. Moniru, and M. Noguchi, "Mechanism of autophagy in chemoresistance in oral cancer stem cells," *Cancer Science*, vol. 109, pp. 1050–1050, 2018.

[22] V. Dimitrova and A. Arcaro, "Targeting the PI3K/AKT/mTOR signaling pathway in medulloblastoma," *Current Molecular Medicine*, vol. 15, no. 1, pp. 82–93, 2015.

[23] W. Hartmann, B. Digon-Söntgerath, A. Koch et al., "Phosphatidylinositol 3'-kinase/AKT signaling is activated in medulloblastoma cell proliferation and is associated with reduced expression of PTEN," *Clinical Cancer Research*, vol. 12, no. 10, pp. 3019–3027, 2006.

[24] N. Baryawno, B. Sveinbjornsson, S. Eksborg, C. S. Chen, P. Kogner, and J. I. Johnsen, "Small-molecule inhibitors of phosphatidylinositol 3-kinase/Akt signaling inhibit Wnt/beta-catenin pathway cross-talk and suppress medulloblastoma growth," *Cancer Research*, vol. 70, no. 1, pp. 266–276, 2010.

[25] A. S. Guerreiro, S. Fattet, B. Fischer et al., "Targeting the PI3K p110alpha isoform inhibits medulloblastoma proliferation, chemoresistance, and migration," *Clinical Cancer Research*, vol. 14, no. 21, pp. 6761–6769, 2008.

[26] M. Ehrhardt, R. B. Craveiro, M. I. Holst, T. Pietsch, and D. Dilloo, "The PI3K inhibitor GDC-0941 displays promising in vitro and in vivo efficacy for targeted medulloblastoma therapy," *Oncotarget*, vol. 6, no. 2, pp. 802–813, 2015.

Hindawi
Analytical Cellular Pathology
Volume 2018, Article ID 5917470, 9 pages
https://doi.org/10.1155/2018/5917470

Research Article

Metformin Treatment Inhibits Motility and Invasion of Glioblastoma Cancer Cells

Marwa Al Hassan,[1] **Isabelle Fakhoury**,[1] **Zeinab El Masri**,[1] **Noura Ghazale**,[1] **Rayane Dennaoui**,[1] **Oula El Atat**,[1] **Amjad Kanaan**,[2] **and Mirvat El-Sibai**[1]

[1]*Department of Natural Sciences, School of Arts and Sciences, Lebanese American University, Beirut, Lebanon*
[2]*Department of Biomedical Sciences, Faculty of Medicine and Medical Sciences, University of Balamand, El-Kurah, Lebanon*

Correspondence should be addressed to Mirvat El-Sibai; mirvat.elsibai@lau.edu.lb

Received 2 February 2018; Revised 7 April 2018; Accepted 18 April 2018; Published 26 June 2018

Academic Editor: Lubna H. Tahtamouni

Glioblastoma multiforme (GBM) is one of the most common and deadliest cancers of the central nervous system (CNS). GBMs high ability to infiltrate healthy brain tissues makes it difficult to remove surgically and account for its fatal outcomes. To improve the chances of survival, it is critical to screen for GBM-targeted anticancer agents with anti-invasive and antimigratory potential. Metformin, a commonly used drug for the treatment of diabetes, has recently emerged as a promising anticancer molecule. This prompted us, to investigate the anticancer potential of metformin against GBMs, specifically its effects on cell motility and invasion. The results show a significant decrease in the survival of SF268 cancer cells in response to treatment with metformin. Furthermore, metformin's efficiency in inhibiting 2D cell motility and cell invasion in addition to increasing cellular adhesion was also demonstrated in SF268 and U87 cells. Finally, AKT inactivation by downregulation of the phosphorylation level upon metformin treatment was also evidenced. In conclusion, this study provides insights into the anti-invasive antimetastatic potential of metformin as well as its underlying mechanism of action.

1. Introduction

Gliomas are brain tumors that originate within the central nervous system (CNS). Glioblastomas (GBMs), which account for about 80% of malignant gliomas, contain self-renewing cancer stem cells (CSCs) that contribute to tumor initiation and resistance to treatment [1, 2]. Death due to malignant gliomas is the third most common cause of cancer death [3, 4]. The management of malignant gliomas, especially GBMs, remains challenging despite medical and scientific advancements in cancer therapeutics. This is largely attributed to their increased resistance to chemotherapy as well as their highly invasive behavior which makes them difficult to surgically remove [5, 6]. Such shortcomings have called forth for the screening for new GBM-targeted anticancer agents with antimigratory and anti-invasive potential.

Metformin, (N, N-dimethylbiguanide) is an antihyperglycemic agent that belongs to the biguanide class. It is commonly used to treat type 2 diabetes mellitus [7, 8]. Metformin decreases hyperglycemia by suppressing glucose production in the liver, increasing insulin sensitivity and glucose uptake by the peripheral tissues, and inhibiting glucose absorption by the gastrointestinal tract as well as inhibiting the mitochondrial respiration [7, 9–11]. The drug's mechanism of action has been shown to be both adenosine monophosphate protein kinase- (AMPK) dependent and AMPK-independent [7, 10, 12]. Cancer cells resort to an increased glucose metabolism to meet their energy requirements needed for rapid expansion and proliferation [13, 14]. Consequently, metformin has emerged as a promising anticancer agent in various cancers including GBMs [15–23]. Specifically, metformin has been shown to inhibit GBMs growth *in vitro* and *in vivo* alone or in combination with other chemotherapeutics as well as radiation therapy [24–31]. Furthermore, metformin's anticancer potential has also been demonstrated against glioma

cancer stem cells and brain tumor-initiating cells [26, 27, 30, 32–35]. However, the effects of metformin on glioma cell motility and invasion as well as its mechanism of action remain poorly understood.

Glioma invasion is a multistep process regulated by extracellular and intracellular interactions [36–38]. It starts with the detachment of cancer cells from primary tumor sites, their binding to the extracellular matrix (ECM) and subsequent degradation of the ECM to finalize the invasion process. Cell motility is essential for the migration and invasion of cancer cells. Cell motility requires the formation and liberation of cell protrusions from adhesion structures [36, 37, 39, 40].

In this study, we sought to assess the anticancer potential of metformin on SF268 brain cancer cells and investigate the drug's antimigratory and anti-invasive potential as well as its mechanism of action. To this aim, we first evaluated metformin's cytotoxic effects against SF268 cancer cells using WST-1 proliferation assay. We then performed 2D motility, adhesion, and invasion assays to determine the drug's antimigratory and anti-invasive potential. Finally, we examined the mechanism of action of metformin, by assessing its effects on the PI3K pathway, one of the most deregulated signaling pathways in glioblastoma. Specifically, we studied the involvement of the antiapoptotic protein AKT of the PI3K pathway in metformin's anticancer, anti-invasive, and antimigratory potential.

2. Materials and Methods

2.1. Cell Culture. Human astrocytoma cell lines SF268 and U87 were purchased from the American Type Culture Collection (Manassas, VA, USA). The cells were cultured in DMEM (Dulbecco's Modified Eagle's Medium) supplemented with 10% FBS and 100 U penicillin/streptomycin and were maintained under standard cell culture conditions at 37°C and 5% CO_2 in a humid environment.

2.2. Antibodies and Reagents. Rabbit monoclonal antibody against pan-Akt and rabbit monoclonal antibody against Akt1 phosphorylated at S473 were purchased from Abcam (Cambridge, UK). Anti-rabbit HRP-conjugated secondary antibody was obtained from Promega (Promega, CO., WI, USA). Collagen was purchased from Invitrogen (Rockville, MD, USA), metformin (1, 1-dimethylbiguanide hydrochloride) (purity > 99%) from Sigma-Aldrich (St. Louis, MO, USA), WST-1 from Roche (Germany), the ECL chemiluminescent reagent from GE Healthcare (Little Chalfont, UK), X-ray films from Agfa HealthCare (Mortsel, Belgium), and the collagen-based invasion assay from Millipore (Burlington, MA, USA).

2.3. Proliferation Assay. Cells were seeded in flat-bottom 96-well plates (growth area: 0.6 cm^2) at a density of 10^5cells/ml before treatment with or without metformin dissolved in DMSO. Following treatment period, 10 μl of Cell Proliferation Reagent (WST-1) was added to each well. The plates were then incubated for 2 h at 37°C and 5% CO_2, and absorbance was read at 450 nm using Multiskan FC microplate ELISA reader from Thermo Fisher Scientific (Rockford, IL, USA). Results were normalized to the corresponding controls, and the percent of cell proliferation was reported. For the next set of experiments, we followed the methods of Khoury et al. [41].

2.4. Western Blot. Control and treated cells were scraped and lysed in buffer consisting of 4% SDS, 10% β-mercaptoethanol, 20% glycerol, 0.004% bromophenol blue, and 0.125 M Tris-HCl at a pH of 6.8. Cell lysates were boiled for 5 min before separating protein samples by SDS-PAGE on 8% or 15% denaturing polyacrylamide gels. Proteins were then transferred to PVDF membranes overnight at 30 V before blocking with 5% nonfat dry milk in PBS containing 0.1% Tween-20 for 1 h at room temperature. Following, the membranes were incubated with primary antibody at a concentration of 1 : 500 for 2 h at room temperature before washing and incubation with the appropriate secondary antibody at a concentration of 1 : 1000 for 2 h. Finally, the membranes were washed, and the bands were visualized by treatment with Western blotting ECL chemiluminescent reagent from GE Healthcare (Little Chalfont, UK). The results were obtained on X-ray films from Agfa HealthCare (Mortsel, Belgium). Protein expression levels were quantified by densitometry analysis using ImageJ.

2.5. Wound Healing Assay. Cells were grown to confluency on culture plates, and a wound was made in the monolayer with a sterile pipette tip. The cells were then washed twice with PBS to remove debris and supplemented with new medium. Phase-contrast images of the wounded area were taken at 0 and 24 h after wounding. ImageJ was used to quantify wound widths at 12 different points for each wound, and the average rate of wound closure was calculated in μm/h.

2.6. Random Motility Assay. For motility analysis, cells were treated with wortmannin or metformin or left untreated. Images of cells moving randomly in serum were collected every 60 seconds or every 3 minutes for 2 h using a 20x objective. During imaging, the temperature was controlled using a heating stage which was set at 37°C. The medium was buffered using HEPES and overlaid with mineral oil. Cell movement was quantified using the ROI tracker plugin in the ImageJ software, written by Dr. David Entenberg. This was used to calculate the total distance travelled by individual cells. The net distance travelled by the cell was calculated by measuring the distance travelled between the first and the last frames.

2.7. Invasion Assay. Invasion assay was performed 48 h after treatment with metformin using the collagen-based invasion assay kit from Millipore (Burlington, MA, USA) according to the manufacturer's protocol. Briefly, SF268 cells were starved in serum-free medium for 24 h before harvesting and resuspension in quenching medium (serum-free). Culture plate inserts were rehydrated using 300 μl of serum-free medium for 30 min at room temperature before plating the cells at a density of 0.6×10^6 cells/ml. Specifically, 250 μl of the serum-free medium was removed from inserts and replaced by 250 μl of cell suspension. Inserts were then placed in a

24-well plate containing 500 μl of complete medium in each well before incubation for 24 h at 37°C in a CO_2 incubator. Following incubation, nonmigrating cells inside the upper cup were removed using a cotton swab and cells migrating through the membrane to the bottom surface of the cup were stained for 20 min at room temperature with 400 μl of cell stain provided with the kit. The stain was then extracted with extraction buffer and 100 μl of extracted stain was transferred to a 96-well plate suitable for colorimetric measurement using the Multiskan FC microplate ELISA reader, and optical density was measured at 560 nm.

2.8. Adhesion Assay. To perform the adhesion assay, 96-well plates were covered with collagen using Collagen Solution Type I from rat tail and incubated overnight at 37°C. After washing with washing buffer (0.1% BSA in DMEM), the plates were blocked with 0.5% BSA in DMEM at 37°C in a CO_2 incubator for 1 h. Next, the plates were washed and chilled on ice. In parallel, SF268 cells were trypsinized and diluted to the density of 4×10^5cell/ml before adding 50 μl of the cell suspension to each well and incubating at 37°C in a 5% CO_2 incubator for 30 min. Plates were then shaken and washed 3 times. Next, the cells were fixed with 4% paraformaldehyde at room temperature for 10 min, washed, and stained with crystal violet (5 mg/ml in 2% ethanol) for 10 min. Following staining, the plates were washed with water and left to dry. Finally, crystal violet was solubilized by incubating the cells with 2% SDS for 30 min. The absorption of the plates was read at 550 nm using the Multiskan FC microplate ELISA reader.

2.9. Statistical Analysis. All the results reported represent the average values of three independent experiments. All error estimates are given as mean ± standard error of the mean (SEM). Statistical analysis was performed using the t-test or the one-way analysis of variance (ANOVA). Results showed statistical significance with a p value ≤ 0.05.

3. Results

3.1. Metformin Treatment Decreases Cell Viability in SF268 and U87 Cells. First, we investigated the anticancer potential of metformin against human glioblastoma SF268 and U87 cancer cells. To this aim, cells were treated with increasing concentrations of metformin (1, 1.5, 2, 2.5, 5, 10, 15, 20, or 50 mM) for 24 h before assessing cell proliferation and viability. The results presented in Figure 1(a) for SF268 and 1B for U87 show that metformin significantly reduces cell viability of both cell lines in a dose-dependent manner as compared to the untreated control. In SF268, metformin exerted a maximum cytotoxic effect at a concentration of 2.5 mM, whereby the proliferation of glioblastoma cells decreases about twofold in response to treatment with metformin as compared to the untreated control. The effect on cytotoxicity in SF268 plateaued beyond the 2.5 mM concentration. This concentration was thus chosen for further investigation in the study.

3.2. Metformin Treatment Inhibits Cell Motility in SF268 and U87 Cells. After determining the cytotoxic potential of metformin against SF268 glioblastoma cancer cell line, we tested the drug's ability to modulate cell motility. Therefore, SF268 cancer cells were exposed to metformin and the motility of treated versus untreated cancer cells was evaluated in 2D using wound healing and time-lapse assays. Figures 2(a)–2(c) (as well as supplemental movies S1 and S2) show that exposure of SF268 glioblastoma cells to 2.5 mM metformin for 24 h significantly inhibits cell motility. Quantitatively, the rates of wound closure reached 1 μm/h and 0.22 μm/h for control and metformin-treated cells, respectively. Also, the total migrated distance decreased by approximately 50% upon treatment with metformin. The time-lapse analysis traces individual cell migration, thus eliminating the potential interference from the effect on proliferation. We also wanted to see the effect of metformin on cellular migration of U87 cells. The time-lapse assay showed a 40% decrease in the total migrated distance of U87 cells after treatment with metformin (2.5 mM) for 24 h (Figure 2(d) and supplemental movies S3 and S4).

3.3. Metformin Treatment Decreases Cellular Invasion in SF268 and U87 Cells. Having established that metformin inhibits cell motility in 2D, we further studied the effect of metformin on invasion, one of the main cancer hallmarks. Using a transwell migration assay and FBS as a chemoattractant in the lower wells, SF268 and U87 cells were treated with 2.5 mM metformin for 24 h before assessing their ability to invade *in vitro* in a collagen-based invasion assay. Figures 3(a) and 3(b) show less invading cells upon treatment with metformin as compared to the control.. Quantitatively, metformin inhibits cell invasion by around 30% in SF268 as compared to the untreated control and by 50% in U87 cells (Figures 3(b) and 3(d), resp.).

3.4. Metformin Treatment Increases SF268 Adhesion to Collagen. To further investigate the inhibition of 2D cell motility and invasion in response to treatment with metformin, we assessed metformin's effects on the adhesion of SF268 cells to collagen, a major component of the ECM. Results in Figure 4(a) show an increase in the stabilization and adhesion of SF268 metformin-treated cells (2.5 mM for 24 h) to collagen as compared to the control. As shown in Figure 4(b), about 35% increase in adhesion was noted following treatment with metformin as compared to the untreated control.

3.5. Effect of Metformin on SF268 Cell Motility Is Mimicked by Inhibiting PI3K. Since previous work showed that metformin inhibits cellular migration and invasion by inhibiting Akt, we wanted to see if this model applies to SF268 glioblastoma cells. We examined the effect of metformin on the PI3K/Akt signaling pathway. Figure 5(a) shows that treatment of SF268 cells with 2.5 mM of metformin for 24 h has no effect on the expression levels of the Akt protein. However, as seen in both Figures 5(a) and 5(b), treatment with metformin significantly inhibits the phosphorylation of Akt which reflects the activation of the PI3K pathway. Specifically,

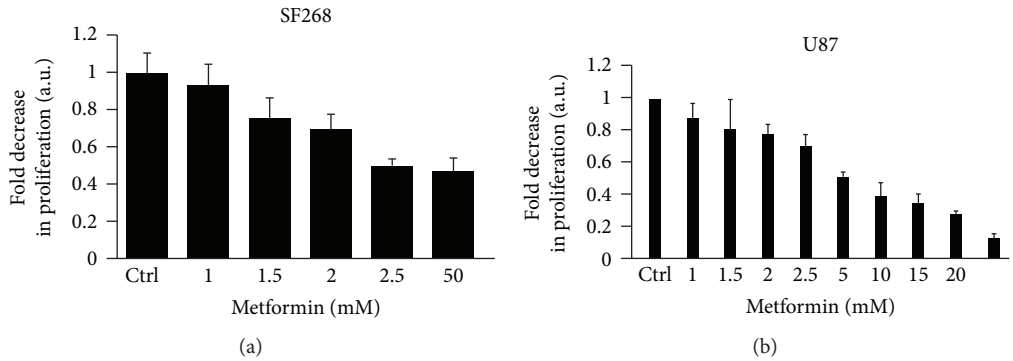

Figure 1: Metformin treatment decreases cell viability in SF268 and U87 cells. Cells were treated with increasing concentrations of metformin (1, 1.5, 2, 2.5, 5, 10, 15, 20, or 50 mM) for 24 h or left untreated. Cell proliferation was assessed using the WST-1 reagent. The data represents the mean ± SEM from 3 independent experiments.

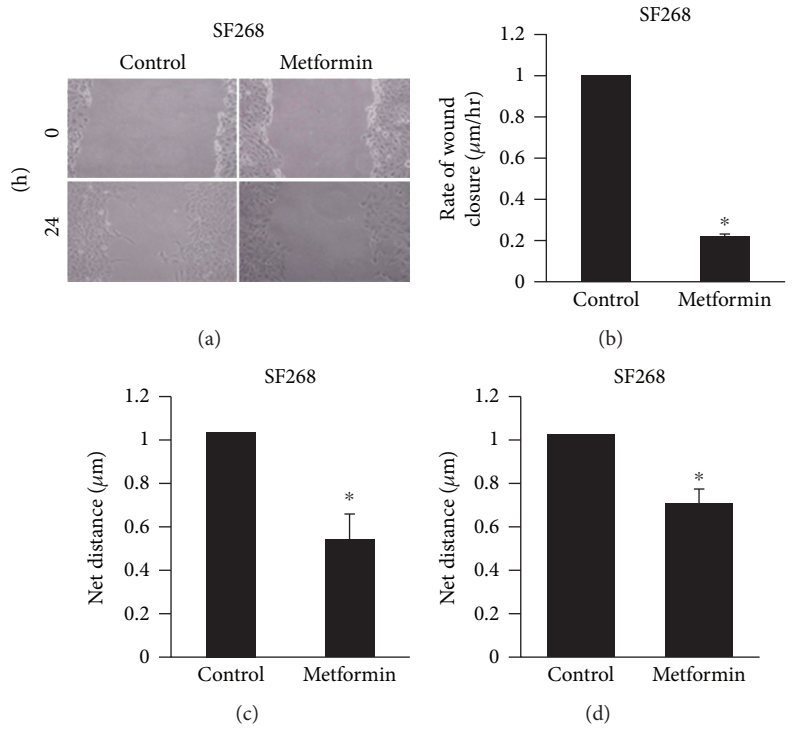

Figure 2: Metformin treatment inhibits cell motility in SF268 and U87 cells. (a) Control and metformin-treated SF268 cells were allowed to form monolayers before wounding with a micropipette. The same frame was imaged directly (upper micrographs) or 24 h (lower micrographs) after wound. (b) Mobility in (a) was quantified by measuring the width of single wound at 12 distinct points. The average rate of wound closure was calculated in μm/hr. Data are the mean ± SEM from 3 different wound healing experiments. * indicates that the values are significant with $p < 0.05$. (c) SF268 cells were treated with metformin (2.5 mM) (Supplemental movie S2) for 24 h or left untreated (Supplemental movie S1). Quantitation of their net path is expressed in μm. * indicates that the values are significant with $p < 0.001$. U87 cells were treated with metformin (2.5 mM) (Supplemental movie S4) for 24 h or left untreated (Supplemental movie S3). Quantitation of their net path is expressed in μm. * indicates that the values are significant with $p < 0.001$.

Akt phosphorylation was reduced by 30% upon treatment with metformin indicating a partial inactivation of this protein.

To assess the role of the PI3K/Akt pathway in glioblastoma migration, we inhibited PI3K using wortmannin. The inhibition leads to a significant decrease in cellular motility in a 2D random motility assay as seen in Figure 5(c) and Supplemental movies S5 and S6. Our results indicate that PI3K/Akt pathway plays an important role in GBM invasiveness.

4. Discussion

This work provides an understanding of metformin treatment effects on SF268 and U87 glioblastoma cancer cell viability, motility and invasion. It also establishes the Akt

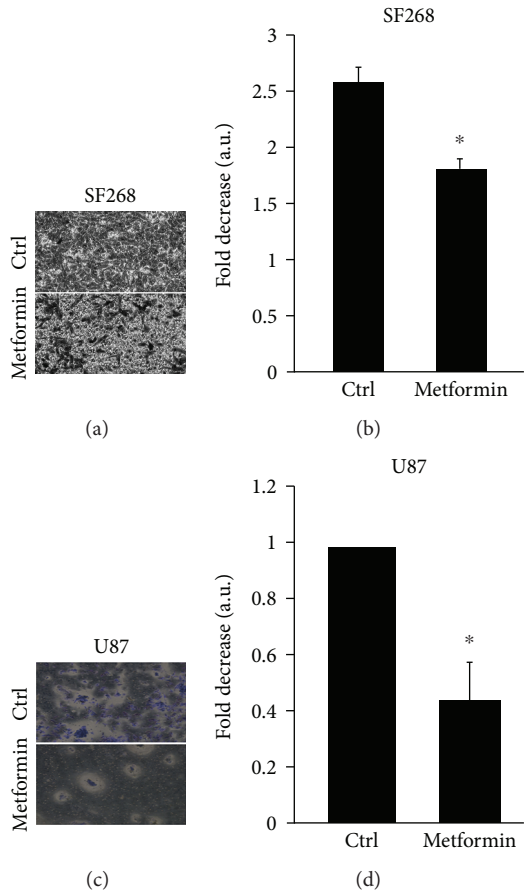

Figure 3: Metformin treatment decreases cellular invasion in SF268 and U87 cells. Representative images showing invasive cells at the bottom side of the membrane for SF268 cells in (a) and U87 cells in (c). The cells were stained with crystal violet as per the manufacturer's recommendations (b) and (d) show quantitation of stained SF268 and U87 cells, respectively, by colorimetric measurement using ELISA (560 nm). Data is measured in arbitrary units and normalized to the control. Data are the mean ± SEM from 3 independent experiments. * indicates that the values are significant with $p < 0.001$.

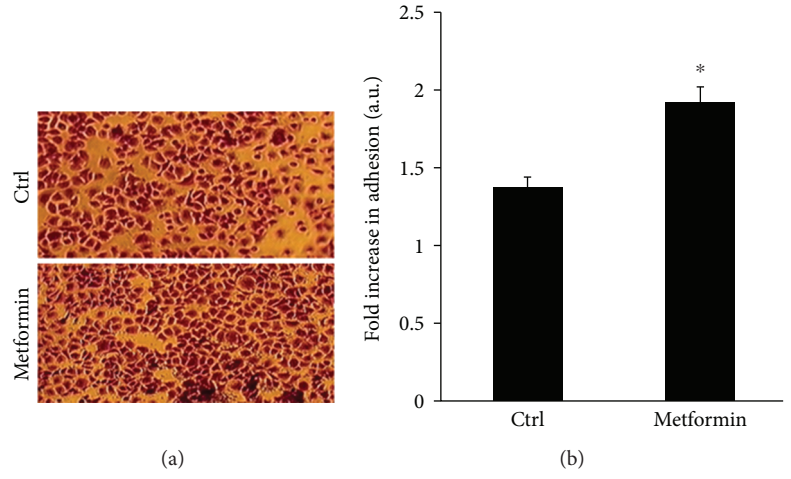

Figure 4: Metformin treatment increases SF268 adhesion to collagen. (a) Representative images of cells that were fixed and stained with crystal violet to detect adhesion. (b) Quantitation of stained cells by colorimetric measurement using ELISA (560 nm). Data is measured in arbitrary units and normalized to the control. Data are the mean ± SEM from 3 independent experiments. The results were significant with $p = 0.02$.

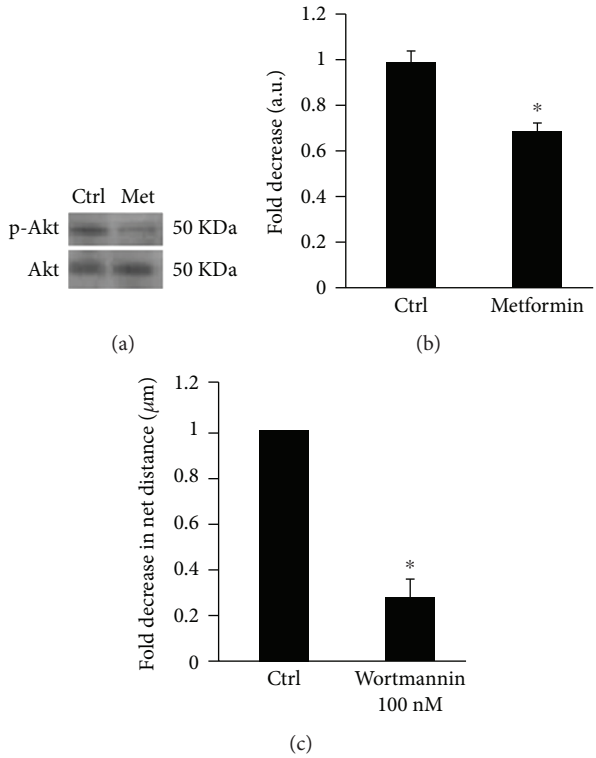

Figure 5: Effect of metformin on SF268 cell motility is mimicked by inhibiting PI3K. (a) Cells were treated with metformin for 24 h before blotting for Akt and p-Akt. (b) Densitometry analysis was performed using the ImageJ software, and the values were normalized to the control. Data are the mean ± SEM from 3 independent experiments. The results were significant with $p = 0.03$. (c) SF268 cells were treated with wortmannin (100 nM) (Supplemental movie S6) or with DMSO alone (Supplemental movie S5). Quantitation of their net path is expressed in μm. Data are the mean ± SEM. * indicates that the values are significant with $p < 0.001$.

antiapoptotic protein of the PI3K signaling pathway as a key mediator of metformin's mechanism of action. To our knowledge, this is one of the few studies investigating the anticancer potential of metformin against the aggressive SF268 and U87 and assessing the anti-invasive and antimigratory effects of this drug in this GBM cancer model.

First, we examined the anticancer potential of the drug *in vitro* and established that metformin is cytotoxic to SF268 and U87 cancer cells as evidenced by the reduced cell viability following treatment with metformin. This was consistent with a similar study which shows that treatment of T98G glioblastoma multiform cells with metformin decreases cell viability and triggers apoptotic morphological alterations in the cells [28]. The decrease in SF268 and U87 cell viability following treatment with 2.5 mM was also similar to the results obtained by another group which have reported a decrease in U87MG, T98G, and U251 cancer cell viability by 46%, 92% and 99%, respectively, upon treatment with 2.5 mM metformin as compared to the control [42].

Our findings further revealed that metformin decreases 2D cell motility by 80%, hence almost abrogating it. This property has been previously reported in other cancer models including pancreatic, breast, renal cell, colon, lung, ovarian, glioma, and prostate [43–47]. For instance, metformin was shown to inhibit wound healing in cholangiocarcinoma cells and metformin in combination with cisplatin was shown to inhibit the migration of nasopharyngeal carcinoma cells [46, 47]. This is thus the first evidence of metformin's antimigratory effects in GBMs in 2D, *in vitro*.

In addition, we observed an increase in the adhesion of SF268 cancer cells to collagen upon treatment with metformin. Focal adhesion dissolution is required for cell movement; hence, the increase in adhesion is in line with the reduced cell motility findings discussed earlier. However, one other group found that cell adhesion and invasion of U251 GBM cancer cells were suppressed following treatment with metformin [48]. The increase in adhesion we report herein is consistent with previous work performed in our lab which shows that the RhoGAP STARD13 maintains RhoA active and prevents focal adhesion dissolution [49, 50]. Indeed, the metformin-treated cells exhibited a more elongated phenotype (Supplemental movie S2) which is reminiscent of the StarD13 KnDn phenotype in SF268 cells previously observed in our laboratory, which can be explained by the increase in adhesion and lack of detachment at the tail while the cells migrate. We are thus currently testing the effect of metformin on STARD13 and RhoA and the interplay with cell adhesion and cell motility.

In parallel, we investigated the effects of metformin on the 3D motility or the invasion of SF268 and U87 cancer cells and demonstrated the efficient reduction cell invasion in response to treatment with metformin. This was consistent with the literature and was reported in melanoma, ovarian cancer, U251 brain cancer, and others [48, 51, 52].

Finally, we showed that metformin inactivates AKT, a major signaling molecule of the PI3K pathway suggesting a potential role for PI3K inhibition in the mediation of the anticancer potential and anti-invasive as well as antimigratory effects exerted by metformin. The importance of the PI3K/Akt pathway in glioblastoma was validated when we treated cells with wortmannin, a PI3K inhibitor. Wortmannin treatment decreased cellular motility and inhibited EGF stimulated protrusions correlating with our metformin results. Similar studies have supported this conclusion whereby the effects of metformin correlated with a significant inhibition of Akt-dependent cell survival pathway [34].

5. Conclusions

This study elucidates the anticancer potential of metformin treatment in a new GBMs *in vitro* model which have not been previously studied. It also demonstrates the drug's anti-invasive and antimigratory potentials. Invasion is a major obstacle for GBM therapy; hence, these findings enhance metformin's chances as a therapeutic candidate for GBM treatment. Further studies are thus needed to investigate metformin's efficiency in treating GBMs *in vivo*.

Data Availability

The data that support the findings of this study are available from the corresponding author upon reasonable request.

Conflicts of Interest

The authors declare that they have no conflicts of interest.

Acknowledgments

This work was supported by the annual departmental grant from the Department of Natural Sciences at the Lebanese American University, Beirut, Lebanon. The ROI_Tracker software was supplied by David Entenberg and John Condeelis as supported by CA100324 and GM064346. This work was supported by the Natural Science Department at the Lebanese American University and by the School of Arts and Science Research and Development Council (SRDC) at LAU.

Supplementary Materials

Supplementary 1. Supplemental movie S1. Control SF268 cells undergoing 2D motility.

Supplementary 2. Supplemental movie S2. SF268 cells treated with Metformin undergoing 2D motility.

Supplementary 3. Supplemental movie S3. U87 cells undergoing 2D motility.

Supplementary 4. Supplemental movie S4. U87 cells treated with Metformin undergoing 2D motility.

Supplementary 5. Supplemental movie S5. SF268 cells treated with DMSO undergoing 2D motility.

Supplementary 6. Supplemental movie S6. SF268 cells treated with wortmannin undergoing 2D motility.

References

[1] T. J. Abou-Antoun, J. S. Hale, J. D. Lathia, and S. M. Dombrowski, "Brain cancer stem cells in adults and children: cell biology and therapeutic implications," *Neurotherapeutics*, vol. 14, no. 2, pp. 372–384, 2017.

[2] J. D. Lathia, S. C. Mack, E. E. Mulkearns-Hubert, C. L. L. Valentim, and J. N. Rich, "Cancer stem cells in glioblastoma," *Genes & Development*, vol. 29, no. 12, pp. 1203–1217, 2015.

[3] Q. T. Ostrom, H. Gittleman, P. M. de Blank et al., "American brain tumor association adolescent and young adult primary brain and central nervous system tumors diagnosed in the United States in 2008-2012," *Neuro-Oncology*, vol. 18, Supplement 1, pp. i1–i50, 2015.

[4] Q. T. Ostrom, H. Gittleman, J. Xu et al., "CBTRUS statistical report: primary brain and other central nervous system tumors diagnosed in the United States in 2009-2013," *Neuro-Oncology*, vol. 18, Supplement_5, pp. v1–v75, 2016.

[5] E. Angelopoulou and C. Piperi, "Emerging role of plexins signaling in glioma progression and therapy," *Cancer Letters*, vol. 414, pp. 81–87, 2018.

[6] A. Omuro and L. M. DeAngelis, "Glioblastoma and other malignant gliomas: a clinical review," *JAMA*, vol. 310, no. 17, pp. 1842–1850, 2013.

[7] L. B. A. Rojas and M. B. Gomes, "Metformin: an old but still the best treatment for type 2 diabetes," *Diabetology & Metabolic Syndrome*, vol. 5, no. 1, p. 6, 2013.

[8] E. Sanchez-Rangel and S. E. Inzucchi, "Metformin: clinical use in type 2 diabetes," *Diabetologia*, vol. 60, no. 9, pp. 1586–1593, 2017.

[9] M. P. Wróbel, B. Marek, D. Kajdaniuk, D. Rokicka, A. Szymborska-Kajanek, and K. Strojek, "Metformin - a new old drug," *Endokrynologia Polska*, vol. 68, no. 4, pp. 482–496, 2017.

[10] G. Rena, D. G. Hardie, and E. R. Pearson, "The mechanisms of action of metformin," *Diabetologia*, vol. 60, no. 9, pp. 1577–1585, 2017.

[11] M.-Y. El-Mir, V. Nogueira, E. Fontaine, N. Avéret, M. Rigoulet, and X. Leverve, "Dimethylbiguanide inhibits cell respiration via an indirect effect targeted on the respiratory chain complex I," *The Journal of Biological Chemistry*, vol. 275, no. 1, pp. 223–228, 2000.

[12] M. Foretz, S. Hébrard, J. Leclerc et al., "Metformin inhibits hepatic gluconeogenesis in mice independently of the LKB1/AMPK pathway via a decrease in hepatic energy state," *The Journal of Clinical Investigation*, vol. 120, no. 7, pp. 2355–2369, 2010.

[13] S. Abbadi, J. J. Rodarte, A. Abutaleb et al., "Glucose-6-phosphatase is a key metabolic regulator of glioblastoma invasion," *Molecular Cancer Research*, vol. 12, no. 11, pp. 1547–1559, 2014.

[14] D. Hanahan and R. A. Weinberg, "Hallmarks of cancer: the next generation," *Cell*, vol. 144, no. 5, pp. 646–674, 2011.

[15] R. Ge, Z. Wang, S. Wu et al., "Metformin represses cancer cells via alternate pathways in N-cadherin expressing vs. N-cadherin deficient cells," *Oncotarget*, vol. 6, no. 30, pp. 28973–28987, 2015.

[16] S. Gou, P. Cui, X. Li, P. Shi, T. Liu, and C. Wang, "Low concentrations of metformin selectively inhibit CD133(+) cell proliferation in pancreatic cancer and have anticancer action," *PLoS One*, vol. 8, no. 5, article e63969, 2013.

[17] T. H. Kim, D. H. Suh, M. K. Kim, and Y. S. Song, "Metformin against cancer stem cells through the modulation of energy metabolism: special considerations on ovarian cancer," *BioMed Research International*, vol. 2014, Article ID 132702, 11 pages, 2014.

[18] F. Kong, F. Gao, H. Liu et al., "Metformin use improves the survival of diabetic combined small-cell lung cancer patients," *Tumour Biology*, vol. 36, no. 10, pp. 8101–8106, 2015.

[19] A. Leone, E. di Gennaro, F. Bruzzese, A. Avallone, and A. Budillon, "New perspective for an old antidiabetic drug: metformin as anticancer agent," *Cancer Treatment and Research*, vol. 159, pp. 355–376, 2014.

[20] V. C. Miranda, R. Barroso-Sousa, J. Glasberg, and R. P. Riechelmann, "Exploring the role of metformin in anticancer treatments: a systematic review," *Drugs of Today*, vol. 50, no. 9, pp. 623–640, 2014.

[21] P. Nangia-Makker, Y. Yu, A. Vasudevan et al., "Metformin: a potential therapeutic agent for recurrent colon cancer," *PLoS One*, vol. 9, no. 1, article e84369, 2014.

[22] A. M. Thompson, "Molecular pathways: preclinical models and clinical trials with metformin in breast cancer," *Clinical Cancer Research*, vol. 20, no. 10, pp. 2508–2515, 2014.

[23] G. Vlotides, A. Tanyeri, M. Spampatti et al., "Anticancer effects of metformin on neuroendocrine tumor cells in vitro," *Hormones*, vol. 13, no. 4, pp. 498–508, 2014.

[24] R. Ferla, E. Haspinger, and E. Surmacz, "Metformin inhibits leptin-induced growth and migration of glioblastoma cells," *Oncology Letters*, vol. 4, no. 5, pp. 1077–1081, 2012.

[25] J. Sesen, P. Dahan, S. J. Scotland et al., "Metformin inhibits growth of human glioblastoma cells and enhances therapeutic response," *PLoS One*, vol. 10, no. 4, article e0123721, 2015.

[26] T. H. Mouhieddine, A. Nokkari, M. M. Itani et al., "Metformin and ara-a effectively suppress brain Cancer by targeting Cancer stem/progenitor cells," *Frontiers in Neuroscience*, vol. 9, 2015.

[27] C. Seliger, A. L. Meyer, K. Renner et al., "Metformin inhibits proliferation and migration of glioblastoma cells independently of TGF-β2," *Cell Cycle*, vol. 15, no. 13, pp. 1755–1766, 2016.

[28] A. Ucbek, Z. G. Özünal, Ö. Uzun, and A. Gepdiremen, "Effect of metformin on the human T98G glioblastoma multiforme cell line," *Experimental and Therapeutic Medicine*, vol. 7, no. 5, pp. 1285–1290, 2014.

[29] S. H. Yang, S. Li, G. Lu et al., "Metformin treatment reduces temozolomide resistance of glioblastoma cells," *Oncotarget*, vol. 7, no. 48, pp. 78787–78803, 2016.

[30] Z. Yu, G. Zhao, G. Xie et al., "Metformin and temozolomide act synergistically to inhibit growth of glioma cells and glioma stem cells in vitro and in vivo," *Oncotarget*, vol. 6, no. 32, pp. 32930–32943, 2015.

[31] S. Adeberg, D. Bernhardt, S. B. Harrabi et al., "Metformin enhanced in vitro radiosensitivity associates with G2/M cell cycle arrest and elevated Adenosine-5′-monophosphate-activated protein kinase levels in glioblastoma," *Radiology and Oncology*, vol. 51, no. 4, pp. 431–437, 2017.

[32] M. Carmignani, A. R. Volpe, M. Aldea et al., "Glioblastoma stem cells: a new target for metformin and arsenic trioxide," *Journal of Biological Regulators and Homeostatic Agents*, vol. 28, no. 1, pp. 1–15, 2014.

[33] A. Sato, J. Sunayama, M. Okada et al., "Glioma-initiating cell elimination by metformin activation of FOXO3 via AMPK," *Stem Cells Translational Medicine*, vol. 1, no. 11, pp. 811–824, 2012.

[34] R. Würth, A. Pattarozzi, M. Gatti et al., "Metformin selectively affects human glioblastoma tumor-initiating cell viability: a role for metformin-induced inhibition of Akt," *Cell Cycle*, vol. 12, no. 1, pp. 145–156, 2012.

[35] Z. Yu, G. Zhao, P. Li et al., "Temozolomide in combination with metformin act synergistically to inhibit proliferation and expansion of glioma stem-like cells," *Oncology Letters*, vol. 11, no. 4, pp. 2792–2800, 2016.

[36] M. L. Kutys, A. D. Doyle, and K. M. Yamada, "Regulation of cell adhesion and migration by cell-derived matrices," *Experimental Cell Research*, vol. 319, no. 16, pp. 2434–2439, 2013.

[37] A. Armento, J. Ehlers, S. Schötterl, and U. Naumann, "Molecular Mechanisms of Glioma Cell Motility," in *Glioblastoma*, S. Vleeschouwer, Ed., Codon Publications Copyright: The Authors, Brisbane (AU), 2017.

[38] B. A. Saykali and M. El-Sibai, "Invadopodia, regulation, and assembly in cancer cell invasion," *Cell Communication & Adhesion*, vol. 21, no. 4, pp. 207–212, 2014.

[39] M. Block, C. Badowski, A. Millonfremillon et al., "Podosome-type adhesions and focal adhesions, so alike yet so different," *European Journal of Cell Biology*, vol. 87, no. 8-9, pp. 491–506, 2008.

[40] S. Hanna and M. El-Sibai, "Signaling networks of Rho GTPases in cell motility," *Cellular Signalling*, vol. 25, no. 10, pp. 1955–1961, 2013.

[41] N. Khoury, S. El-Hayek, O. Tarras, M. El-Sabban, M. El-Sibai, and S. Rizk, "Kefir exhibits antiproliferative and proapoptotic effects on colon adenocarcinoma cells with no significant effects on cell migration and invasion," *International Journal of Oncology*, vol. 45, no. 5, pp. 2117–27, 2014.

[42] C. R. Kennedy, S. B. Tilkens, H. Guan, J. A. Garner, P. M. Y. Or, and A. M. Chan, "Differential sensitivities of glioblastoma cell lines towards metabolic and signaling pathway inhibitions," *Cancer Letters*, vol. 336, no. 2, pp. 299–306, 2013.

[43] A. Isakovic, L. Harhaji, D. Stevanovic et al., "Dual antiglioma action of metformin: cell cycle arrest and mitochondria-dependent apoptosis," *Cellular and Molecular Life Sciences*, vol. 64, no. 10, pp. 1290–1302, 2007.

[44] M. Zakikhani, R. Dowling, I. G. Fantus, N. Sonenberg, and M. Pollak, "Metformin is an AMP kinase–dependent growth inhibitor for breast cancer cells," *Cancer Research*, vol. 66, no. 21, pp. 10269–10273, 2006.

[45] R. Rattan, S. Giri, L. C. Hartmann, and V. Shridhar, "Metformin attenuates ovarian cancer cell growth in an AMP-kinase dispensable manner," *Journal of Cellular and Molecular Medicine*, vol. 15, no. 1, pp. 166–178, 2011.

[46] X.-J. Sun, P. Zhang, H. H. Li, Z. W. Jiang, C. C. Jiang, and H. Liu, "Cisplatin combined with metformin inhibits migration and invasion of human nasopharyngeal carcinoma cells by regulating E-cadherin and MMP-9," *Asian Pacific Journal of Cancer Prevention*, vol. 15, no. 9, pp. 4019–4023, 2014.

[47] S. X. Trinh, H. T. Nguyen, K. Saimuang, V. Prachayasittikul, and W. Chan On, "Metformin inhibits migration and invasion

of cholangiocarcinoma cells," *Asian Pacific Journal of Cancer Prevention*, vol. 18, no. 2, pp. 473–477, 2017.

[48] L.-B. Gao, S. Tian, H. H. Gao, and Y. Y. Xu, "Metformin inhibits glioma cell U251 invasion by downregulation of fibulin-3," *Neuroreport*, vol. 24, no. 10, pp. 504–508, 2013.

[49] B. D. Khalil and M. El-Sibai, "Rho GTPases in primary brain tumor malignancy and invasion," *Journal of Neuro-Oncology*, vol. 108, no. 3, pp. 333–339, 2012.

[50] S. Hanna, B. Khalil, A. Nasrallah et al., "StarD13 is a tumor suppressor in breast cancer that regulates cell motility and invasion," *International Journal of Oncology*, vol. 44, no. 5, pp. 1499–1511, 2014.

[51] M. Cerezo, M. Tichet, P. Abbe et al., "Metformin blocks melanoma invasion and metastasis development in AMPK/p53-dependent manner," *Molecular Cancer Therapeutics*, vol. 12, no. 8, pp. 1605–1615, 2013.

[52] B. Wu, S. Li, L. Sheng et al., "Metformin inhibits the development and metastasis of ovarian cancer," *Oncology Reports*, vol. 28, no. 3, pp. 903–908, 2012.

Hindawi
Analytical Cellular Pathology
Volume 2018, Article ID 8389595, 10 pages
https://doi.org/10.1155/2018/8389595

Review Article

Heparan Sulfate Proteoglycans in Human Colorectal Cancer

Carolina Meloni Vicente,[1] **Daiana Aparecida da Silva**,[1] **Priscila Veronica Sartorio**,[2] **Tiago Donizetti Silva**,[3] **Sarhan Sydney Saad**,[4] **Helena Bonciani Nader**,[1] **Nora Manoukian Forones**,[3] **and Leny Toma**[1]

[1]*Disciplina de Biologia Molecular, Escola Paulista de Medicina, Universidade Federal de São Paulo, Rua Três de Maio, 100 4° Andar, Vila Clementino, São Paulo, SP, Brazil*
[2]*Disciplina de Farmacologia Celular, Escola Paulista de Medicina, Universidade Federal de São Paulo, Rua Três de Maio, 100 4° Andar, Vila Clementino, São Paulo, SP, Brazil*
[3]*Disciplina de Gastroenterologia Clínica, Escola Paulista de Medicina, Universidade Federal de São Paulo, Rua Loefgreen 1726, Vila Clementino, São Paulo, SP, Brazil*
[4]*Disciplina de Gastroenterologia Cirúrgica, Escola Paulista de Medicina, Universidade Federal de São Paulo, Rua Napoleão de Barros, 715 2° Andar, Vila Clementino, São Paulo, SP, Brazil*

Correspondence should be addressed to Carolina Meloni Vicente; carolmv@yahoo.com

Received 7 March 2018; Revised 14 May 2018; Accepted 20 May 2018; Published 20 June 2018

Academic Editor: Mamoun Ahram

Colorectal cancer is the third most common cancer worldwide, accounting for more than 610,000 mortalities every year. Prognosis of patients is highly dependent on the disease stage at diagnosis. Therefore, it is crucial to investigate molecules involved in colorectal cancer tumorigenesis, with possible use as tumor markers. Heparan sulfate proteoglycans are complex molecules present in the cell membrane and extracellular matrix, which play vital roles in cell adhesion, migration, proliferation, and signaling pathways. In colorectal cancer, the cell surface proteoglycan syndecan-2 is upregulated and increases cell migration. Moreover, expression of syndecan-1 and syndecan-4, generally antitumor molecules, is reduced. Levels of glypicans and perlecan are also altered in colorectal cancer; however, their role in tumor progression is not fully understood. In addition, studies have reported increased heparan sulfate remodeling enzymes, as the endosulfatases. Therefore, heparan sulfate proteoglycans are candidate molecules to clarify colorectal cancer tumorigenesis, as well as important targets to therapy and diagnosis.

1. Background

Colorectal cancers (CRC) arise from the epithelium lining the colon or rectum. In females and males, it is the third and fourth most common cancer, respectively. This type of cancer is responsible for 610,000 mortalities worldwide yearly [1]. The incidence of CRC tends to increase considering aging and population growth [2]. The survival rate of patients with CRC is hugely dependent on the disease stage and in a projected five-year survival rate; patients with stage I tumors show range from 85 to 90% while the range is less than 5% for patients with stage IV diseases [3]. The main risk factors are the following: age over 50 years; family history of colon and rectal cancer, including some hereditary conditions (family adenomatous polyposis (FAP) and hereditary nonpolyposis colorectal cancer (HNPCC)); high-fat content in diet, meat consumption, and low calcium content; physical inactivity and obesity; and inflammatory colon diseases such as chronic ulcerative colitis and Crohn's disease [4, 5].

CRC is commonly diagnosed in advanced stages in both sexes and presents a higher incidence after 55 years of age. CRC screening methods increase the early diagnosis of this pathology and allow the identification of premalignant lesions such as adenomatous polyps [6, 7]. In addition to colonoscopy, rectosigmoidoscopy and occult blood decrease CRC mortality as screening methods. Thus, when people

are screened in their fifties and the polyps are removed, the subsequent incidence of colorectal cancer is usually very low [8, 9].

Therefore, CRC is curable in nearly 90% cases if detected at an early stage. Furthermore, screening methods detecting mucosal changes reduce the incidence and mortality rates of this disease [10]. The most accurate method of diagnosis is colonoscopy, followed by histopathological biopsy. Fecal occult blood test (FOBT) is the most noninvasive screening procedure used and is able to reduce CRC-related mortality by 20%, when executed every other year [11]. In spite of improvements in sensitivity, FOBT has a low detection rate for early-stage tumors and precancerous lesions, such as polyps [1, 12]. Even though colonoscopy and rectosigmoidoscopy are more effective in detecting CRC, they are extremely costly and require extensive preparation of the bowel and involve invasion of patient privacy and sedation [13]. As a rule, surgery is the primary treatment, removing the affected portion of the intestine and lymph nodes near this region. After surgical procedure, chemotherapy or radiotherapy can be recommended in order to reduce the tumor recurrence [14].

In 1990, Fearon and Vogelstein suggested a model for colorectal cancer tumorigenesis, which describes the genetic alterations involved in transformation from normal intestinal mucosa to colorectal carcinoma [15]. Thenceforward, CRC critical genes have already been well established, 40% of the cases of CRC have a specific point mutation in KRAS, 60% have inactivating mutations or deletions of p53, and more than 60% have mutations in the APC (adenomatous polyposis coli) tumor suppressor gene. Additional studies have revealed how these genes lead to uncontrolled cell division and metastasis [16, 17].

The inactivation of the APC gene appears to be a very early step in most CRC cases, since it can be detected already in small benign polyps at the same high frequency as in malignant tumors. Loss of APC function appears to be responsible for the increase of cell proliferation [18]. Mutations involving the KRAS oncogene appear to take place later than those in APC as they are infrequent in small polyps but common in larger ones that present undifferentiated cells [19]. Finally, mutations in p53 are rare in polyps but common in carcinomas, suggesting that they may often occur late in the sequence. Loss of p53 function leads abnormal cells to avert apoptosis, divide, and promote the accumulation of additional mutations [20].

Not only genetic mutations and chromosome instability but also another frequent genomic instability in CRC is the microsatellite instability at the nucleotide level, commonly resulting in deletions or insertions of a few nucleotides [21, 22]. Furthermore, global DNA hypomethylation and depletion of overall 5-methylcytosine content in CRC tissues were observed for the first time in 1983, by Feinberg and Vogelstein [23]. This global hypomethylation has been associated with an increased genomic instability and overexpression of genes implicated in CRC pathogenesis [24]. Moreover, this hypomethylation is believed to be associated with the hypermethylation at the promoter regions of specific genes that are involved in cell cycle regulation, DNA repair, apoptosis, angiogenesis, adhesion, and invasion [1, 25].

It has been known for decades that proteoglycans (PG) are involved in the progression of cancer at various stages. Heparan sulfate proteoglycans (HSPGs) play vital roles in tumorigenesis, allowing cancer cells to proliferate, evade immune response, invade adjacent tissues, and metastasize to distal sites away from the primary tumor [26]. In CRC, syndecan-1 and syndecan-4 are downregulated while syndecan-2 is upregulated [27–29] (Figure 1). In addition, studies have reported increased 6-OST, heparanase [30, 31], and SULFs [32, 33]. Notably, several of CRC critical genes show relationship with HSPGs. For instance, p53 has been described to regulate the expression of SULF2 or heparanase. Many growth factors, including TGF-beta and VEGF, bind to heparan sulfate chains; the WNT/beta-catenin pathway is regulated by glypicans and SULFs [34, 35].

2. Heparan Sulfate Proteoglycans

HSPGs are complex molecules presenting one or more heparan sulfate (HS) chains covalently bound to the protein backbone [36], being present on the cell surface and extracellular matrix (ECM) of all animals with tissue organization [37–41]. They can be distributed into three groups, depending on their cellular localization: membrane HSPGs (as syndecans and glypicans), HSPGs secreted into the ECM (perlecan, collagen-type XVIII), and the HSPG serglycin that is located in cell vesicles [42, 43].

The biological functions of HSPGs are very varied, and there is no common denominator. Many of their functions depend on the interaction with the protein backbone, while others depend on sugar chains [44, 45]. Among many roles, the HSPGs are present in basement membranes, where they collaborate with other matrix components to define their structure and assist in cell migration [46]. They are also found in secretory vesicles (serglycin) participating in the granular content packaging, activation of proteases, and regulating activities after secretion such as coagulation and wound healing [47].

At the cell surface, the HSPGs may bind to cytokines, chemokines, and growth factors; in this way, these PGs protect themselves from proteolysis or act as coreceptors [48]. These interactions provide a deposit of regulatory factors that can be released by selective degradation of HS chains. Acting as receptors for proteases or protease inhibitors, HSPGs regulate their spatial distribution and activity [49]. Membrane HSPGs may cooperate with different cell adhesion receptors such as integrins and facilitate cell-ECM adhesion, cell-cell interactions, and cell motility [50, 51].

Therefore, several cellular mechanisms regulated by HSPG are critically involved in cancer. There is an abundance of evidence relating HSPG fine structures to cancer growth, invasion, and metastasis. Through the aberrant modulation of HS biosynthetic enzymes, the specific HS fine structure enables cancer cells to spread by the breakdown of ECM, to receive nutrients through angiogenesis, to proliferate via disruption of signaling pathways, and to escape immune

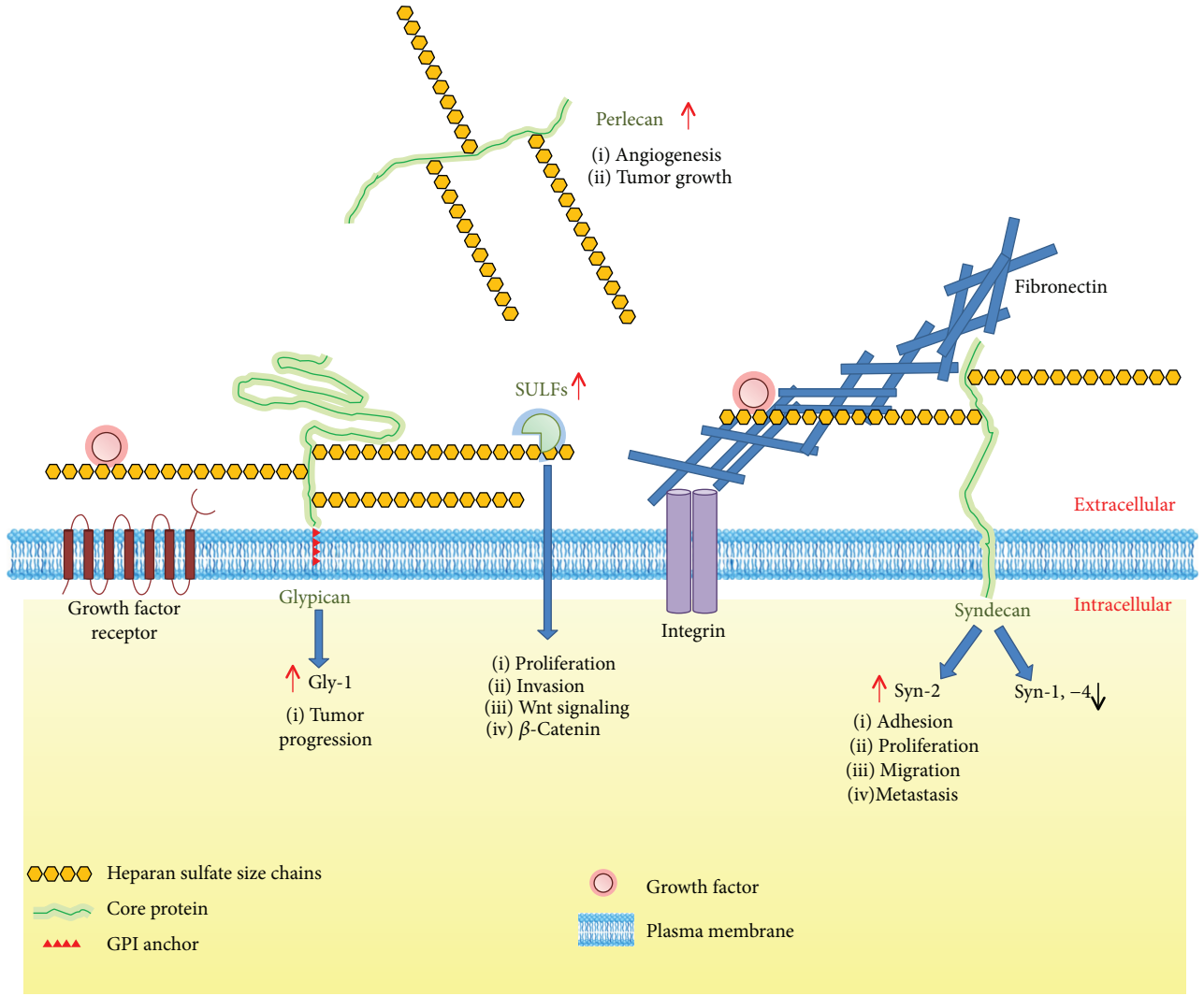

Figure 1: Putative model of the functions of HSPGs in CRC cells. The cell surface HSPG syndecan-2 (Syn-2) is upregulated and promotes cancer cell adhesion, proliferation, migration, and metastasis. Syndecan-1 and syndecan-4 (Syn-1; Syn-4), generally antitumor molecules, are reduced in colon carcinoma cells. The cell surface HSPG glypican-1 (Gly-1) is increased in CRC and is involved in tumor progression. The augmentation of matrix HSPG perlecan favors angiogenesis and tumor growth. The SULF enzymes are upregulated, and the edition of HS chains promotes proliferation and invasion of CRC cells. In addition, SULFs release growth factors that were bound to HS, stimulating the Wnt signaling pathway and the activation of β-catenin.

cells. In addition, different levels of HSPG core proteins are involved in several tumor-promoting processes [26, 52].

2.1. Cell Surface HSPG

2.1.1. Syndecans. The syndecans are a family of four transmembrane proteoglycans that bear predominantly heparan sulfate glycosaminoglycan chains [28]. The core proteins consist of a short intracellular domain, a highly conserved transmembrane domain, and an ectodomain that is divergent in amino acid sequence among the four syndecan family members [41].

The syndecans regulate cell adhesion, migration, cytoskeleton organization, and gene expression through the binding of ECM molecules and soluble ligands [40]. Since cancer cells exhibit less adhesive and more migratory characteristics in comparison to normal cells, syndecans are candidate molecules to be differently regulated in cancer cells. Therefore, it is probable that syndecans may influence cell morphology, adhesion to the ECM, and tumorigenic activity.

According to the literature, syndecan-2 is the most involved in CRC. Syndecan-2 regulates cell adhesion in several cell lines including epithelial cells [53], neuronal cells [54], and mesenchymal cells [55]. Moreover, different reports indicate that syndecan-2 positively regulates cell migration, since it is highly expressed in cells under migratory conditions [56]. Park et al. [57] demonstrated that syndecan-2 mRNA levels were increased in CRC cell lines compared with a normal colon cell line. Our results corroborate with these data (Figure 2). The addition of purified recombinant extracellular domain of syndecan-2 to the cell medium completely blocked the adhesion of colon cancer cells on the ECM.

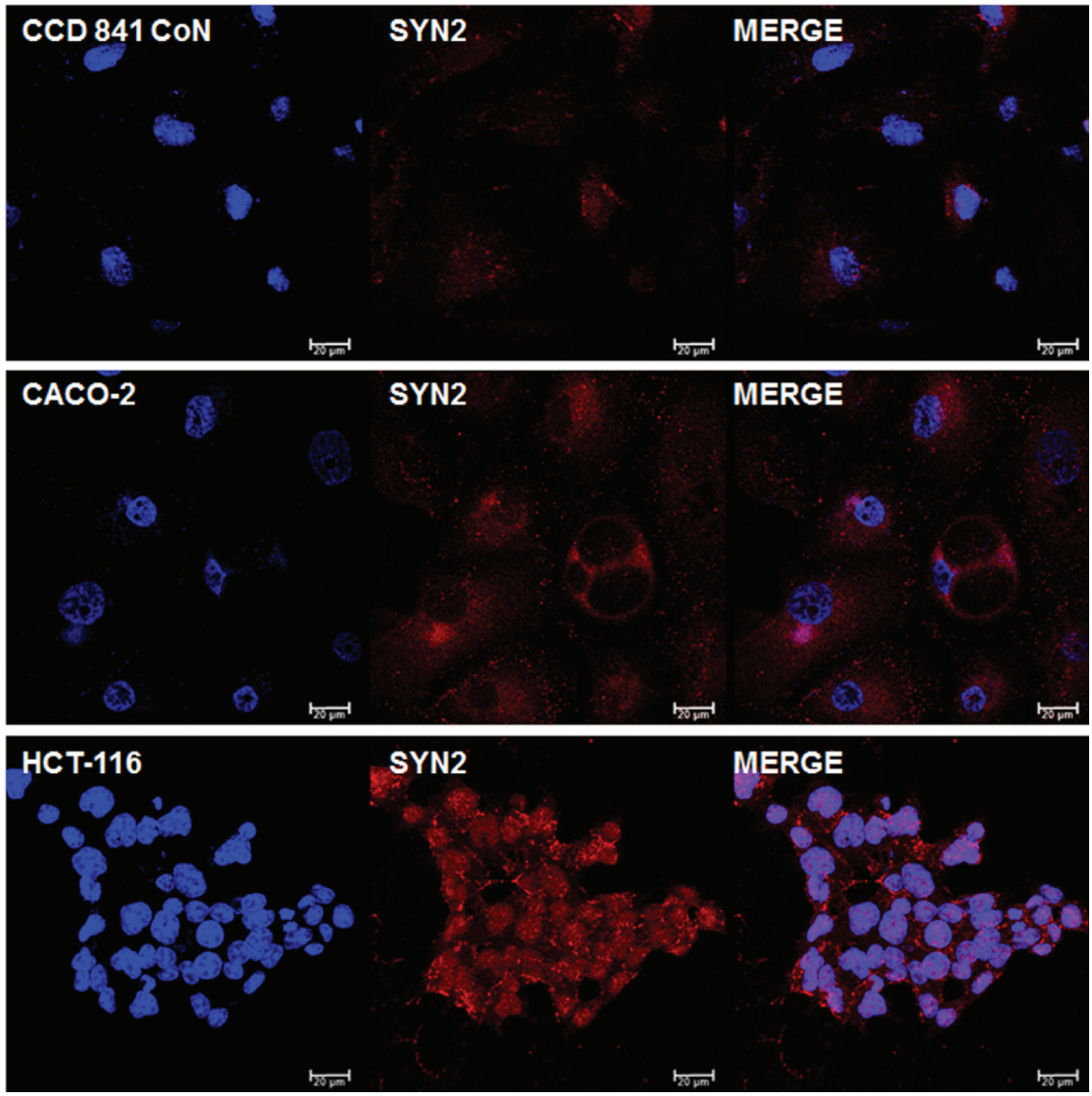

Figure 2: Expression of syndecan-2 (Syn-2) in normal colorectal cell line (CCD 841 CoN), in nonmetastatic CRC cell line CACO-2, and in high metastatic CRC cell line HCT-116. Immunostaining (red) was detected using an antibody specific for syndecan-2 (Santa Cruz) and an Alexa Fluor 594-labeled secondary antibody. Cell nuclei were stained with DAPI (blue). Images were obtained using a confocal a microscope Leica Microsystems TCS SP8 and analyzed by software LAS-AF.

Moreover, it induced G0/G1 cell cycle arrest with concomitant increase in p21, p27, and p53 expressions. Therefore, in CRC, syndecan-2 plays a critical role in adhesion of colon carcinoma cells onto the ECM, regulating the proliferation and tumorigenic activity in colon carcinoma cells [57].

It has been well established that the extracellular domain of syndecan-2 interacts with fibronectin [58]. In CRC, the contact between cancer cells with fibronectin enhances syndecan-2 expression, promoting a migratory behavior of highly metastatic tumor cells [29]. In addition, HCT116 transfected with syndecan-2 presented increased cell migration, which was diminished by the knockdown of integrin alpha2 using a specific siRNA [59]. Therefore, this dynamic interaction, including syndecan-2, fibronectin, and integrin, might be a possible mechanism underlying the metastatic characteristics of colon cancer cells. In addition, Choi et al. [60] reported that the overexpression of syndecan-2 enhanced migration and invasion of Caco-2 and HCT116 cells through Tiam1-mediated activation of Rac, a GTPase family member involved in cell contact regulation.

Finally, it has been recently reported that in HT29 cells, syndecan-2 overexpression promotes E-cadherin shedding to the conditioned medium [61]. Consistently, the overexpression of syndecan-2 in HT29 cells increased the expression and secretion of MMP-7 whereas siRNA-mediated knockdown of MMP-7 in these same cells significantly increased E-cadherin levels. The shedding of E-cadherin disrupts cell-cell adhesion and induces cells to undergo morphological changes toward a fibroblast-like phenotype, inducing the epithelial-mesenchymal transition in CRC cells.

On the other hand, syndecan-1 has been associated with a tumor suppressor function [62]. Similarly, syndecan-4,

which is mainly involved in cytoskeletal and membrane reorganization and formation of focal adhesions, inhibits cell migration and tumor activity [63]. Consistently, mRNA expression of syndecan-1 and syndecan-4 is significantly reduced in colon carcinoma cells [40]. However, in different types of cancers, syndecan-1 and syndecan-4 may present the opposite effect, promoting the tumor progression [64, 65]. In addition, it has already been demonstrated that the shed of syndecan-1 is associated with chemotherapy resistance in castration-resistant prostate cancer [66]. These data evidence that the function of cell surface HSPGs can be altered by extracellular ectodomain shedding by proteases, converting them into soluble paracrine effector molecules. It is worth mentioning that the shedding of HSPGs is a controlled mechanism that can occur constitutively and can be substantially enhanced by exogenous stimuli or by a pathogenic state, including cancer [67].

2.1.2. Glypicans. Glypicans (GPCs) constitute a family of HSPGs externally linked to the plasma membrane by a glycosylphosphatidylinositol (GPI) anchor [68]. In mammals, the glypican family comprises six members, GPC1 to GPC6. GPCs can modify cell signaling pathways including Wnts, hedgehogs, fibroblast growth factors, and bone morphogenetic proteins, which are mainly involved in cellular proliferation and tissue growth [68]. GPC functions may either be stimulatory or inhibitory through these different pathways.

GPC1 has been implicated in tumor progression events, such as growth, angiogenesis, and metastasis, and has been especially studied in pancreatic cancer, glioma, and breast cancer [69]. De Robertis et al. [70] found that the GPC1 gene was significantly upregulated in azoxymethane/dextran sodium sulfate (AOM/DSS) mouse model, which mimics human CRC. Results were confirmed by immunohistochemical analysis in 10 human tumor cases and 10 normal matched mucosa specimens, revealing a strong increase of membrane/cytoplasmic staining for GPC1 in 80% of tumors.

Several studies have demonstrated a correlation between GPC3 expression levels and various types of cancer. Downregulation of GPC3 has already been detected in ovarian carcinoma, breast cancer, and mesothelioma, suggesting that it may act as a tumor suppressor gene in these tissues [67]. In contrast, GPC3 is upregulated in hepatocellular carcinoma, germ cell tumor, and lung squamous cell carcinoma, suggesting that GPC3 may also behave as an oncofetal protein [68].

In CRC, downregulation of GPC3 mRNA levels was observed in all 10 tumor samples, compared to normal mucosa [70]. Moreover, a retrospective study involving 150 CRC cases reported that nonmucinous carcinoma (NMA) showed a higher expression of GPC3 than did mucinous carcinoma (MA), which is associated with worse prognosis [71]. Interestingly, GPC3 immunohistochemistry analysis demonstrated a strong staining in normal mucosa and a cytoplasmic staining in tumor cells.

2.2. Matrix HSPG

2.2.1. Perlecan. Having a large multidomain, perlecan is a proteoglycan of five domains secreted to the extracellular matrix. It has homology to growth factors, immunoglobulin, and adhesion molecules [69]. Perlecan is able not only to bind but also to cross-link many ECM components and cell-surface molecules. By collaborating with other matrix components, perlecan defines the basement membrane structure and provides a matrix for cell migration [72]. Moreover, it was discovered that perlecan exhibits high-affinity binding of fibroblast growth factor- (FGF-) 2, a proangiogenic factor, to cells lacking heparan sulfate and to the FGF receptor [69].

Perlecan is an important component of the vascular ECM. Different studies have suggested that perlecan could function as an initial scaffold upon which endothelial cells would migrate and deposit an appropriate vascular basement membrane [38, 39]. Several independent studies using antisense RNA strategies in various tumor cells have confirmed the central role of perlecan in angiogenesis, with both *in vitro* and *in vivo* models [38].

Perlecan suppression caused significant tumor reduction and inhibition of angiogenesis in human CRC tumor xenografts [73]. Proliferation of HCT116 human CRC cells was markedly reduced upon obliteration of perlecan gene expression by an antisense cDNA, and these effects correlated with reduced responsiveness to FGF-7.

Interestingly, perlecan was more expressed in the AG2 colon cancer-initiating cell line, compared to the carcinoma cells HCT116. However, the gene expression of perlecan was downregulated 2-fold in colon tumors from 12 patients, using the surrounding tissue as control [74]. Therefore, the function of perlecan in CRC requires to be better clarified.

3. HSPG Biosynthetic Enzymes

In general terms, the initial HS chain is synthesized by the alternating action of different glycosyltransferases, which add D-glucuronic acid (GlcA) and N-acetyl-D-glucosamine (GlcNAc) residues. Subsequently, the chain undergoes a series of reactions of polymer modifications: N-deacetylation/N-sulfation, epimerization of β-D-glucuronic acid residue to α-L-iduronic acid, and O-sulfation in different positions [75]. Each product of one reaction is a substrate for the next enzyme [76], and $3'$-phosphoadenosine-$5'$-phosphosulfate (PAPS) is used as a sulfate donor by sulfotransferases [77]. The length of the HS chain, as well as its degree of sulfation, may vary depending on the protein skeleton and the cell type [76].

On the cell surface or ECM, two endosulfatases (SULF1 and SULF2) can further modify the HS chains by removing specific C6-located sulfate groups from the glucosamine units or by the action of extracellular heparanase or proteases [77].

3.1. SULFs. Being located on the cell surface or released into the ECM, SULFs represent a family of secreted enzymes that selectively remove 6-O-sulfate groups from HS, with preference for those present in trisulfated disaccharides [78].

After cloning the human SULF cDNA, analyses of SAGE databases provided the first indication that these genes are relevant for cancer. SULF1 and SULF2 occur with a higher frequency in three types of human tumors (breast,

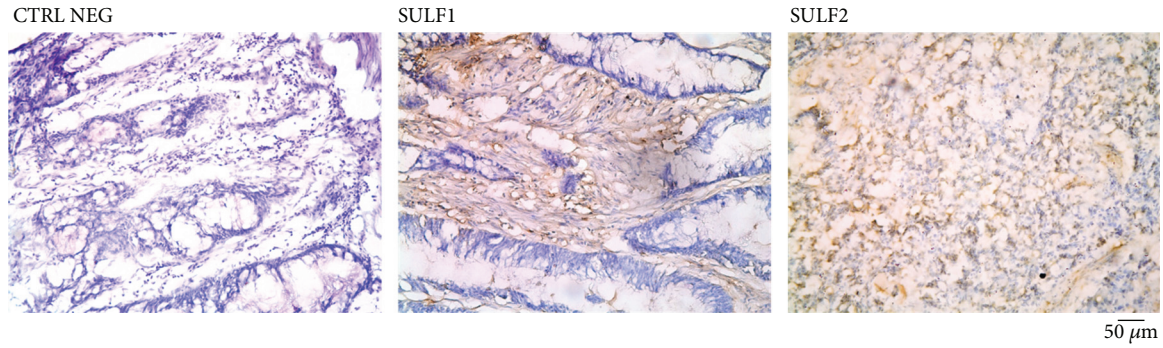

Figure 3: Expression of SULF1 and SULF2 in CRC tissue sample. Immunostaining was detected using an antibody specific for SULF1 or SULF2 (Santa Cruz) and HRP peroxidase/DAB reaction. Tissue samples were stained after with hematoxylin. Images were obtained using a Nikon Eclipse microscope.

central nervous system, and colon) compared to normal tissues [79, 80].

In more recent studies, the overexpression of SULFs in a wide range of tumors has been reported through quantitative PCR or gene microarray: SULF1 is upregulated in hepatocellular carcinoma [81], gastric cancer [82], head and neck carcinoma [83], pancreatic cancer [84], and lung adenocarcinoma [85], and SULF2 is highly expressed in hepatocellular carcinomas [86] and lung carcinoma [85], among others.

Stable overexpression of SULFs in the CRC cells, Caco-2, and HCT-116 induced an increase in cell viability and proliferation and augmented cell migration [33]. These effects were reversed by shRNA-mediated knockdown of SULF1 or SULF2 and by the addition of unfractionated heparin to the cell medium. Moreover, CRC cell lines overexpressing SULFs presented increased Wnt signaling, represented by the accumulation of active nonphosphorylated beta-catenin in the cells. Ai et al. [87] proposed a model by which SULFs could promote Wnt signaling. The model suggests that the action of SULFs weakens the association of Wnt ligands with HSPGs on the cell surface, which allows ligands to activate signal transduction receptors (frizzled).

In addition, the gene expression of SULFs in human CRC tissue samples revealed a significant increase of those sulfatases, which argues for a possible distortion of HS sulfation patterns in colon tumors [74] (Figure 3). Therefore, these studies reveal that SULFs have oncogenic effects in CRC, suggesting an important role for these enzymes in cancer progression.

4. Conclusions and Clinical Relevance

Dysregulated expression of HSPGs, as well as of enzymes involved in their biosynthesis and degradation, has been reported to affect all stages of tumorigenesis [88]. As extracellular proteins, HSPGs and the extracellular enzymes that modify them, such as SULFs, are amenable to therapeutic targeting [89]. Heparan sulfate mimetics, highly sulfated oligosaccharides, inhibit SULF functions and sequester HS-binding ligands, making them attractive candidates for cancer therapy [90, 91]. It is noteworthy that an inhibitor of SULFs has already been identified, named PI-88 [92]. This agent consists of a mixture of chemically sulfated yeast oligosaccharides with a molecular weight range of 1400–3100 Da. This compound has been tested in clinical trials for advanced melanoma (phase II), liver cancer, lung cancer, and prostate cancer. However, these studies have demonstrated recurring problems of immune-mediated thrombocytopenia in a significant number of patients associated with the use of PI-88 [93]. Therefore, both the detection and the inhibition of SULFs can present clinical value for CRC treatment.

As demonstrated, syndecan-2 is a candidate for CRC diagnosis. Shed or secreted proteoglycans and their extracellular modifying enzymes can often be detected in the blood [94]. As these are often altered in cancer, changes in their blood levels may be useful as biomarkers of disease. Moreover, the inhibition of syndecan-2 could reduce tumor cell migration, protecting CRC patients from metastasis.

In addition to potential direct antitumor effects, therapeutic targeting of HSPGs in CRC could also modulate angiogenesis. The inhibition of perlecan in early stages of CRC could contribute to preventing tumor development. Therefore, these studies illustrate the critical importance of HSPGs in all stages of CRC and reinforce the relevance of conducting preclinical studies to test the therapeutic efficacy and safety of potential targeting agents.

Based on these important functions, the question arises as to whether HSPGs can be utilized as potential candidate molecules for CRC diagnosis and treatment. First, as mainly extracellular molecules, they can be easily achieved by different mechanisms, being interest targets for cancer therapy, which could include the usage of specific antibodies targeting HSPGs. In addition, the detection of the HSPG ectodomain or SULF levels in the serum or stool samples emerge as promising diagnostic tools for CRC patients.

Furthermore, HSPGs are involved in all tumor stages, including cell proliferation and migration, metastasis, and angiogenesis. Therefore, it is worth exploring the still unknown complex molecular events involving HSPGs. However, appropriate studies are crucial to deciphering the paradoxes of the involvement of different isoforms of HSPGs in CRC. Finally, a highly promising next step will be the development of precise inhibitors for specific types of HSPG, which would contribute to a better comprehension of the roles of HSPGs in CRC. This may represent the greatest

challenge since HSPGs have different isoforms and possess ambiguous roles. However, the development of these molecules could represent an important step towards the application of HSPGs in clinical trials.

Abbreviations

PAPS: 3′-Phosphoadenosine-5′-phosphosulfate
APC: Adenomatous polyposis coli
CRC: Colorectal cancers
GlcA: D-Glucuronic acid
ECM: Extracellular matrix
FAP: Family adenomatous polyposis
FOBT: Fecal occult blood test
(FGF)-2: Fibroblast growth factor
GPI: Glycosylphosphatidylinositol
GPCs: Glypicans
HS: Heparan sulfate
HNPCC: Hereditary nonpolyposis colorectal cancer
MMP: Metalloproteinase
MA: Mucinous carcinoma
GlcNAc: N-Acetyl-D-glucosamine
NMA: Nonmucinous carcinoma
PCR: Polymerase chain reaction
PG: Proteoglycans
SULF: Endosulfatase
TGF-beta: Transforming growth factor
VEGF: Vascular endothelial growth factor.

Ethical Approval

The procedures were performed based on the guidelines of the National Institutes of Health (NIH) regarding the use of human tissues and with permission from the Institutional Ethical Board of Federal University of São Paulo, Brazil (Protocol no. 34986214.1.0000.5505).

Consent

Terms of consent were obtained from adult patients after a brief explanation of the study. The authors were given the consent for publication.

Conflicts of Interest

The authors declare that they have no competing interests.

Authors' Contributions

Nora Manoukian Forones and Leny Toma provided direction and guidance throughout the preparation of this manuscript. Carolina Meloni Vicente conducted the literature review and drafted the manuscript. Helena Bonciani Nader and Daiana Aparecida da Silva reviewed the manuscript and made significant revisions on the drafts. Daiana Aparecida da Silva, Priscila Veronica Sartorio, Tiago Donizetti Silva, and Sarhan Sydney Saad contributed to the figures. All authors read and approved the final manuscript.

Acknowledgments

This work is supported by grants from FAPESP (Projects 2016/18066-6 and 2015/03964-6).

References

[1] T. D. Silva, V. M. Vidigal, A. V. Felipe et al., "DNA methylation as an epigenetic biomarker in colorectal cancer," *Oncology Letters*, vol. 6, no. 6, pp. 1687–1692, 2013.

[2] Y. Teixeira, J. M. Lima, M. L. A. P. O. Souza, P. Aguiar Jr., T. D. Silva, and N. M. Forones, "Human DNA quantification in the stools of patients with colorectal cancer," *Arquivos de Gastroenterologia*, vol. 52, no. 4, pp. 293–298, 2015.

[3] M. Riihimäki, A. Hemminki, J. Sundquist, and K. Hemminki, "Patterns of metastasis in colon and rectal cancer," *Scientific Reports*, vol. 6, no. 1, article 29765, 2016.

[4] M. Riedy, "Preventing colorectal cancer," *Advance for NPs & PAs*, vol. 4, no. 6, pp. 18–21; quiz 22, 2013.

[5] R. M. Winkels, L. van Lee, S. Beijer et al., "Adherence to the World Cancer Research Fund/American Institute for Cancer Research lifestyle recommendations in colorectal cancer survivors: results of the PROFILES registry," *Cancer Medicine*, vol. 5, no. 9, pp. 2587–2595, 2016.

[6] M. Mengual-Ballester, E. Pellicer-Franco, G. Valero-Navarro, V. Soria-Aledo, J. A. García-Marín, and J. L. Aguayo-Albasini, "Increased survival and decreased recurrence in colorectal cancer patients diagnosed in a screening programme," *Cancer Epidemiology*, vol. 43, pp. 70–75, 2016.

[7] I. Laake, I. K. Larsen, R. Selmer, I. Thune, and M. B. Veierød, "Pre-diagnostic body mass index and weight change in relation to colorectal cancer survival among incident cases from a population-based cohort study," *BMC Cancer*, vol. 16, no. 1, p. 402, 2016.

[8] T. Niedermaier, K. Weigl, M. Hoffmeister, and H. Brenner, "Flexible sigmoidoscopy in colorectal cancer screening: implications of different colonoscopy referral strategies," *European Journal of Epidemiology*, vol. 33, no. 5, pp. 473–484, 2018.

[9] C. Mansfield, D. U. Ekwueme, F. K. L. Tangka et al., "Colorectal cancer screening: preferences, past behavior, and future intentions," *The Patient - Patient-Centered Outcomes Research*, 2018.

[10] M. P. Pignone and C. L. Lewis, "Using quality improvement techniques to increase colon cancer screening," *The American Journal of Medicine*, vol. 122, no. 5, pp. 419-420, 2009.

[11] M. Diop, E. C. Strumpf, and G. D. Datta, "Measuring colorectal cancer incidence: the performance of an algorithm using administrative health data," *BMC Medical Research Methodology*, vol. 18, no. 1, p. 38, 2018.

[12] T. F. Imperiale, D. F. Ransohoff, S. H. Itzkowitz, B. A. Turnbull, M. E. Ross, and Colorectal Cancer Study Group, "Fecal DNA versus fecal occult blood for colorectal-cancer screening in an average-risk population," *The New England Journal of Medicine*, vol. 351, no. 26, pp. 2704–2714, 2004.

[13] S. Winawer, R. Fletcher, D. Rex et al., "Colorectal cancer screening and surveillance: clinical guidelines and rationale—update based on new evidence," *Gastroenterology*, vol. 124, no. 2, pp. 544–560, 2003.

[14] P. E. Daly, S. Samiee, M. Cino et al., "High prevalence of adenomatous colorectal polyps in young cancer survivors treated with abdominal radiation therapy: results of a prospective trial," *Gut*, vol. 66, no. 10, pp. 1797–1801, 2016.

[15] E. R. Fearon and B. Vogelstein, "A genetic model for colorectal tumorigenesis," *Cell*, vol. 61, no. 5, pp. 759–767, 1990.

[16] B. C. Kim, K. S. Han, C. W. Hong et al., "Clinical outcomes of palliative self-expanding metallic stents in patients with malignant colorectal obstruction," *Journal of Digestive Diseases*, vol. 13, no. 5, pp. 258–266, 2012.

[17] F. Coppedè, A. Lopomo, R. Spisni, and L. Migliore, "Genetic and epigenetic biomarkers for diagnosis, prognosis and treatment of colorectal cancer," *World Journal of Gastroenterology*, vol. 20, no. 4, pp. 943–956, 2014.

[18] J. Liang, C. Lin, F. Hu et al., "APC polymorphisms and the risk of colorectal neoplasia: a HuGE review and meta-analysis," *American Journal of Epidemiology*, vol. 177, no. 11, pp. 1169–1179, 2013.

[19] C.-C. Chang, C.-C. Lin, C.-H. Wang et al., "miR-211 regulates the expression of RRM2 in tumoral metastasis and recurrence in colorectal cancer patients with a k-ras gene mutation," *Oncology Letters*, vol. 15, no. 5, pp. 8107–8117, 2018.

[20] H. Y. Lu, R. T. Lin, G. X. Zhou, T. M. Yu, and Z. J. Liu, "Critical role of p 53 and K-ras in the diagnosis of early colorectal cancer: a one-year, single-center analysis," *International Journal of Medical Sciences*, vol. 14, no. 11, pp. 1154–1162, 2017.

[21] J. N. Nojadeh, S. Behrouz Sharif, and E. Sakhinia, "Microsatellite instability in colorectal cancer," *EXCLI Journal*, vol. 17, pp. 159–168, 2018.

[22] W. M. Grady and J. M. Carethers, "Genomic and epigenetic instability in colorectal cancer pathogenesis," *Gastroenterology*, vol. 135, no. 4, pp. 1079–1099, 2008.

[23] A. P. Feinberg and B. Vogelstein, "Hypomethylation distinguishes genes of some human cancers from their normal counterparts," *Nature*, vol. 301, no. 5895, pp. 89–92, 1983.

[24] F. Coppedè, "Epigenetic biomarkers of colorectal cancer: focus on DNA methylation," *Cancer Letters*, vol. 342, no. 2, pp. 238–247, 2014.

[25] A. Goel and C. R. Boland, "Epigenetics of colorectal cancer," *Gastroenterology*, vol. 143, no. 6, pp. 1442–1460.e1, 2012.

[26] K. Raman and B. Kuberan, "Chemical tumor biology of heparan sulfate proteoglycans," *Current Chemical Biology*, vol. 4, no. 1, pp. 20–31, 2010.

[27] R. J. Giordano, "Heparanase-2 and syndecan-1 in colon cancer: the ugly ducklings or the beautiful swans?," *European Journal of Gastroenterology & Hepatology*, vol. 20, no. 8, pp. 716–718, 2008.

[28] S. Choi, Y. Choi, E. Jun et al., "Shed syndecan-2 enhances tumorigenic activities of colon cancer cells," *Oncotarget*, vol. 28, no. 6, pp. 3874–3886, 2015.

[29] C. M. Vicente, R. Ricci, H. B. Nader, and L. Toma, "Syndecan-2 is upregulated in colorectal cancer cells through interactions with extracellular matrix produced by stromal fibroblasts," *BMC Cell Biology*, vol. 14, no. 1, p. 25, 2013.

[30] A. Seko, K. Nagata, S. Yonezawa, and K. Yamashita, "Ectopic expression of a GlcNAc 6-*O*-sulfotransferase, GlcNAc6ST-2, in colonic mucinous adenocarcinoma," *Glycobiology*, vol. 12, no. 6, pp. 379–388, 2002.

[31] E. Hermano, I. Lerner, and M. Elkin, "Heparanase enzyme in chronic inflammatory bowel disease and colon cancer," *Cellular and Molecular Life Sciences*, vol. 69, no. 15, pp. 2501–2513, 2012.

[32] C. Bret, J. Moreaux, J. F. Schved, D. Hose, and B. Klein, "SULFs in human neoplasia: implication as progression and prognosis factors," *Journal of Translational Medicine*, vol. 9, no. 1, p. 72, 2011.

[33] C. M. Vicente, M. A. Lima, E. A. Yates, H. B. Nader, and L. Toma, "Enhanced tumorigenic potential of colorectal cancer cells by extracellular sulfatases," *Molecular Cancer Research*, vol. 13, no. 3, pp. 510–523, 2015.

[34] I. Fernández-Vega, O. García-Suárez, B. García, A. Crespo, A. Astudillo, and L. M. Quirós, "Heparan sulfate proteoglycans undergo differential expression alterations in right sided colorectal cancer, depending on their metastatic character," *BMC Cancer*, vol. 15, no. 1, p. 742, 2015.

[35] M. Capurro, T. Martin, W. Shi, and J. Filmus, "Glypican-3 binds to frizzled and plays a direct role in the stimulation of canonical Wnt signaling," *Journal of Cell Science*, vol. 127, no. 7, pp. 1565–1575, 2014.

[36] J. D. Esko, K. Kimata, and U. Lindahl, "Proteoglycans and sulfated glycosaminoglycans," in *Essentials of Glycobiology*, A. Varki, R. D. Cummings, J. D. Esko, H. H. Freeze, P. Stanley, C. R. Bertozzi, G. W. Hart, and M. E. Etzler, Eds., pp. 229–248, Cold Spring Harbor Laboratory Press, 2009.

[37] L. M. Jenkins, B. Horst, C. L. Lancaster, and K. Mythreye, "Dually modified transmembrane proteoglycans in development and disease," *Cytokine & Growth Factor Reviews*, vol. 39, pp. 124–136, 2018.

[38] D. M. Gardiner, "Regulation of regeneration by heparan sulfate proteoglycans in the extracellular matrix," *Regenerative Engineering and Translational Medicine*, vol. 3, no. 3, pp. 192–198, 2017.

[39] V. H. Pomin and B. Mulloy, "Glycosaminoglycans and proteoglycans," *Pharmaceuticals*, vol. 11, no. 1, 2018.

[40] P. W. Park, "Isolation and functional analysis of syndecans," *Methods in Cell Biology*, vol. 143, pp. 317–333, 2018.

[41] A. D. Theocharis and N. K. Karamanos, "Proteoglycans remodeling in cancer: underlying molecular mechanisms," *Matrix Biology*, 2017.

[42] S. Sarrazin, W. C. Lamanna, and J. D. Esko, "Heparan sulfate proteoglycans," *Cold Spring Harbor Perspectives in Biology*, vol. 3, no. 7, article a004952, 2011.

[43] J. L. Dreyfuss, C. V. Regatieri, T. R. Jarrouge, R. P. Cavalheiro, L. O. Sampaio, and H. B. Nader, "Heparan sulfate proteoglycans: structure, protein interactions and cell signaling," *Anais da Academia Brasileira de Ciências*, vol. 81, no. 3, pp. 409–429, 2009.

[44] J. Kreuger, D. Spillmann, J.-p. Li, and U. Lindahl, "Interactions between heparan sulfate and proteins: the concept of specificity," *Journal of Cell Biology*, vol. 174, no. 3, pp. 323–327, 2006.

[45] A. N. Alexopoulou, H. A. B. Multhaupt, and J. R. Couchman, "Syndecans in wound healing, inflammation and vascular biology," *The International Journal of Biochemistry & Cell Biology*, vol. 39, no. 3, pp. 505–528, 2007.

[46] J. Kruegel and N. Miosge, "Basement membrane components are key players in specialized extracellular matrices," *Cellular and Molecular Life Sciences*, vol. 67, no. 17, pp. 2879–2895, 2010.

[47] O. J. Scully, P. J. Chua, K. S. Harve, B. H. Bay, and G. W. Yip, "Serglycin in health and diseases," *The Anatomical Record: Advances in Integrative Anatomy and Evolutionary Biology*, vol. 295, no. 9, pp. 1415–1420, 2012.

[48] M. A. Nugent, J. Zaia, and J. L. Spencer, "Heparan sulfate-protein binding specificity," *Biochemistry*, vol. 78, no. 7, pp. 726–735, 2013.

[49] I. Capila and R. J. Linhardt, "Heparin-protein interactions," *Angewandte Chemie International Edition*, vol. 41, no. 3, pp. 391–412, 2002.

[50] S. H. Kim, J. Turnbull, and S. Guimond, "Extracellular matrix and cell signalling: the dynamic cooperation of integrin, proteoglycan and growth factor receptor," *The Journal of Endocrinology*, vol. 209, no. 2, pp. 139–151, 2011.

[51] U. Lindahl and L. Kjellén, "Pathophysiology of heparan sulphate: many diseases, few drugs," *Journal of Internal Medicine*, vol. 273, no. 6, pp. 555–571, 2013.

[52] F. H. Blackhall, C. L. Merry, E. J. Davies, and G. C. Jayson, "Heparan sulfate proteoglycans and cancer," *British Journal of Cancer*, vol. 85, no. 8, pp. 1094–1098, 2001.

[53] A. Utani, M. Nomizu, H. Matsuura et al., "A unique sequence of the laminin α3 G domain binds to heparin and promotes cell adhesion through syndecan-2 and -4," *Journal of Biological Chemistry*, vol. 276, no. 31, pp. 28779–28788, 2001.

[54] I. M. Ethell, K. Hagihara, Y. Miura, F. Irie, and Y. Yamaguchi, "Synbindin, a novel syndecan-2-binding protein in neuronal dendritic spines," *Journal of Cell Biology*, vol. 151, no. 1, pp. 53–68, 2000.

[55] D. Modrowski, M. Baslé, A. Lomri, and P. J. Marie, "Syndecan-2 is involved in the mitogenic activity and signaling of granulocyte-macrophage colony-stimulating factor in osteoblasts," *Journal of Biological Chemistry*, vol. 275, no. 13, pp. 9178–9185, 2000.

[56] B. Jang, H. Jung, S. Choi, Y. H. Lee, S. T. Lee, and E. S. Oh, "Syndecan-2 cytoplasmic domain up-regulates matrix metalloproteinase-7 expression via the protein kinase Cγ–mediated FAK/ERK signaling pathway in colon cancer," *Journal of Biological Chemistry*, vol. 292, no. 39, pp. 16321–16332, 2017.

[57] H. Park, Y. Kim, Y. Lim, I. Han, and E. S. Oh, "Syndecan-2 mediates adhesion and proliferation of colon carcinoma cells," *Journal of Biological Chemistry*, vol. 277, no. 33, pp. 29730–29736, 2002.

[58] M. J. Kwon, Y. Kim, Y. Choi et al., "The extracellular domain of syndecan-2 regulates the interaction of HCT116 human colon carcinoma cells with fibronectin," *Biochemical and Biophysical Research Communications*, vol. 431, no. 3, pp. 415–420, 2013.

[59] S. Choi, Y. Kim, H. Park et al., "Syndecan-2 overexpression regulates adhesion and migration through cooperation with integrin α2," *Biochemical and Biophysical Research Communications*, vol. 384, no. 2, pp. 231–235, 2009.

[60] Y. Choi, H. Kim, H. Chung et al., "Syndecan-2 regulates cell migration in colon cancer cells through Tiam1-mediated Rac activation," *Biochemical and Biophysical Research Communications*, vol. 391, no. 1, pp. 921–925, 2010.

[61] B. Jang, H. Jung, H. Chung, B. I. Moon, and E. S. Oh, "Syndecan-2 enhances E-cadherin shedding and fibroblast-like morphological changes by inducing MMP-7 expression in colon cancer cells," *Biochemical and Biophysical Research Communications*, vol. 477, no. 1, pp. 47–53, 2016.

[62] M. Fujiya, J. Watari, T. Ashida et al., "Reduced expression of syndecan-1 affects metastatic potential and clinical outcome in patients with colorectal cancer," *Japanese Journal of Cancer Research*, vol. 92, no. 10, pp. 1074–1081, 2001.

[63] R. P. Cavalheiro, M. A. Lima, T. R. Jarrouge-Bouças et al., "Coupling of vinculin to F-actin demands syndecan-4 proteoglycan," *Matrix Biology*, vol. 63, pp. 23–37, 2017.

[64] Z. Ren, H. van Andel, W. de Lau et al., "Syndecan-1 promotes Wnt/β-catenin signaling in multiple myeloma by presenting Wnts and R-spondins," *Blood*, vol. 131, no. 9, pp. 982–994, 2018.

[65] S. Takashima, Y. Oka, F. Fujiki et al., "Syndecan-4 as a biomarker to predict clinical outcome for glioblastoma multiforme treated with WT1 peptide vaccine," *Future Science OA*, vol. 2, no. 4, article FSO96, 2016.

[66] T. Szarvas, S. Sevcenco, O. Módos et al., "Circulating syndecan-1 is associated with chemotherapy-resistance in castration-resistant prostate cancer," *Urologic Oncology: Seminars and Original Investigations*, vol. 36, no. 6, pp. 312.e9–312.e15, 2018.

[67] Z. Piperigkou, B. Mohr, N. Karamanos, and M. Götte, "Shed proteoglycans in tumor stroma," *Cell and Tissue Research*, vol. 365, no. 3, pp. 643–655, 2016.

[68] J. Filmus, M. Capurro, and J. Rast, "Glypicans," *Genome Biology*, vol. 9, no. 5, p. 224, 2008.

[69] R. V. Iozzo and R. D. Sanderson, "Proteoglycans in cancer biology, tumour microenvironment and angiogenesis," *Journal of Cellular and Molecular Medicine*, vol. 15, no. 5, pp. 1013–1031, 2011.

[70] M. De Robertis, M. Arigoni, L. Loiacono et al., "Novel insights into notum and glypicans regulation in colorectal cancer," *Oncotarget*, vol. 6, no. 38, pp. 41237–41257, 2015.

[71] A. A.-R. M. Foda, M. A. Mohammad, A. Abdel-Aziz, and A. K. El-Hawary, "Relation of glypican-3 and E-cadherin expressions to clinicopathological features and prognosis of mucinous and non-mucinous colorectal adenocarcinoma," *Tumour Biology*, vol. 36, no. 6, pp. 4671–4679, 2015.

[72] R. Nakamura, F. Nakamura, and S. Fukunaga, "Perlecan Diversely Regulates the Migration and Proliferation of Distinct Cell Types in vitro," *Cells Tissues Organs*, vol. 200, no. 6, pp. 374–393, 2015.

[73] J. Rnjak-Kovacina, F. Tang, X. Lin, J. M. Whitelock, and M. S. Lord, "Recombinant domain V of human perlecan is a bioactive vascular proteoglycan," *Biotechnology Journal*, vol. 12, no. 12, 2017.

[74] A. V. Suhovskih, S. V. Aidagulova, V. I. Kashuba, and E. V. Grigorieva, "Proteoglycans as potential microenvironmental biomarkers for colon cancer," *Cell and Tissue Research*, vol. 361, no. 3, pp. 833–844, 2015.

[75] M. C. Z. Meneghetti, T. Gesteira Ferreira, A. K. Tashima et al., "Insights into the role of 3-*O*-sulfotransferase in heparan sulfate biosynthesis," *Organic & Biomolecular Chemistry*, vol. 15, no. 32, pp. 6792–6799, 2017.

[76] T. N. Wight, "A role for proteoglycans in vascular disease," *Matrix Biology*, 2018.

[77] M. Lima, T. Rudd, and E. Yates, "New applications of heparin and other glycosaminoglycans," *Molecules*, vol. 22, no. 5, 2017.

[78] Y. Dai, Y. Yang, V. MacLeod et al., "HSulf-1 and HSulf-2 are potent inhibitors of myeloma tumor growth in vivo," *The Journal of Biological Chemistry*, vol. 280, no. 48, pp. 40066–40073, 2005.

[79] M. Morimoto-Tomita, K. Uchimura, Z. Werb, S. Hemmerich, and S. D. Rosen, "Cloning and characterization of two extracellular heparin-degrading endosulfatases in mice and humans," *Journal of Biological Chemistry*, vol. 277, no. 51, pp. 49175–49185, 2002.

[80] M. Morimoto-Tomita, K. Uchimura, and S. D. Rosen, "Novel extracellular sulfatases: potential roles in cancer," *Trends in*

Glycoscience and Glycotechnology, vol. 15, no. 83, pp. 159–164, 2003.

[81] J. P. Lai, J. R. Chien, D. R. Moser et al., "hSulf1 sulfatase promotes apoptosis of hepatocellular cancer cells by decreasing heparin-binding growth factor signaling," *Gastroenterology*, vol. 126, no. 1, pp. 231–248, 2004.

[82] S. Junnila, A. Kokkola, T. Mizuguchi et al., "Gene expression analysis identifies over-expression of CXCL1, SPARC, SPP1, and SULF1 in gastric cancer," *Genes, Chromosomes & Cancer*, vol. 49, no. 1, pp. 28–39, 2010.

[83] Y. Kudo, I. Ogawa, S. Kitajima et al., "Periostin promotes invasion and anchorage-independent growth in the metastatic process of head and neck cancer," *Cancer Research*, vol. 66, no. 14, pp. 6928–6935, 2006.

[84] J. Li, J. Kleeff, I. Abiatari et al., "Enhanced levels of Hsulf-1 interfere with heparin-binding growth factor signaling in pancreatic cancer," *Molecular Cancer*, vol. 4, no. 1, p. 14, 2005.

[85] H. Lemjabbar-Alaoui, A. van Zante, M. S. Singer et al., "Sulf-2, a heparan sulfate endosulfatase, promotes human lung carcinogenesis," *Oncogene*, vol. 29, no. 5, pp. 635–646, 2010.

[86] J. P. Lai, D. S. Sandhu, C. Yu et al., "Sulfatase 2 up-regulates glypican 3, promotes fibroblast growth factor signaling, and decreases survival in hepatocellular carcinoma," *Hepatology*, vol. 47, no. 4, pp. 1211–1222, 2008.

[87] X. Ai, A.-T. Do, O. Lozynska, M. Kusche-Gullberg, U. Lindahl, and C. P. Emerson Jr., "QSulf1 remodels the 6-O sulfation states of cell surface heparan sulfate proteoglycans to promote Wnt signaling," *Journal of Cell Biology*, vol. 162, no. 2, pp. 341–351, 2003.

[88] G. W. Yip, M. Smollich, and M. Götte, "Therapeutic value of glycosaminoglycans in cancer," *Molecular Cancer Therapeutics*, vol. 5, no. 9, pp. 2139–2148, 2006.

[89] A. Wade, A. E. Robinson, J. R. Engler, C. Petritsch, C. D. James, and J. J. Phillips, "Proteoglycans and their roles in brain cancer," *The FEBS Journal*, vol. 280, no. 10, pp. 2399–2417, 2013.

[90] K. Dredge, E. Hammond, P. Handley et al., "PG545, a dual heparanase and angiogenesis inhibitor, induces potent anti-tumour and anti-metastatic efficacy in preclinical models," *British Journal of Cancer*, vol. 104, no. 4, pp. 635–642, 2011.

[91] K. D. Johnstone, T. Karoli, L. Liu et al., "Synthesis and biological evaluation of polysulfated oligosaccharide glycosides as inhibitors of angiogenesis and tumor growth," *Journal of Medicinal Chemistry*, vol. 53, no. 4, pp. 1686–1699, 2010.

[92] S. D. Rosen and H. Lemjabbar-Alaoui, "Sulf-2: an extracellular modulator of cell signaling and a cancer target candidate," *Expert Opinion on Therapeutic Targets*, vol. 14, no. 9, pp. 935–949, 2010.

[93] M. M. Hossain, T. Hosono-Fukao, R. Tang et al., "Direct detection of HSulf-1 and HSulf-2 activities on extracellular heparan sulfate and their inhibition by PI-88," *Glycobiology*, vol. 20, no. 2, pp. 175–186, 2010.

[94] H. Joensuu, A. Anttonen, M. Eriksson et al., "Soluble syndecan-1 and serum basic fibroblast growth factor are new prognostic factors in lung cancer," *Cancer Research*, vol. 62, no. 18, pp. 5210–5217, 2002.